جمهورية العراق
وزارة التعليم العالي والبحث العلمي
جامعة بابل
كلية الهندسة
قسم الهندسة الكهربائية

تقييم أداء تعدد الإرسال بتقسيم التردد العمومي القطبي المرمز باستخدام تقنيات الذكاء الاصطناعي

اطروحة
مقدمة إلى كلية الهندسة في جامعة بابل
وهي جزء من متطلبات الحصول على درجة الدكتوراة
فلسفة في هندسة الالكترونيك والاتصالات

من قبل

امير حسين محمد علي

بإشراف
الاستاذ الدكتور

سعد سفاح حسون حريشي

٢٠٢٣م ١٤٤٥ هـ

Republic of Iraq
Ministry of Higher Education and Scientific Research
University of Babylon
College of Engineering
Department of Electrical Engineering

Performance Evaluation of Polar-Coded Generalized Frequency Division Multiplexing Using Artificial Intelligent Techniques

A Dissertation

Submitted to the College of Engineering / University of Babylon in Partial Fulfillment of the Requirements for the Degree of Doctor of Philosophy in Electrical Engineering / Electronic and Communications

By

Ameer Hussein Mohammed Ali

(B.Sc. 2013)

(M.Sc. 2015)

Supervised by

Prof. Dr. Saad S. Hreshee

2023 A.D ***1445 A.H***

بِسْمِ اللَّهِ الرَّحْمَنِ الرَّحِيمِ

﴿ نَرْفَعُ دَرَجَاتٍ مَنْ نشَاءُ وَفَوْقَ كُلِّ ذِي عِلْمٍ عَلِيمٌ ﴾

صَدَقَ اللَّهُ الْعَلِيّ الْعَظِيم

الآية 76 من سورة يوسف

Dedication

To my family

Asst. Prof. Ameer Hussein Mohammed Ali

2023

Supervisor Certification

I certify that this dissertation entitled **(Performance Evaluation of Polar-Coded Generalized Frequency Division Multiplexing Using Artificial Intelligent Techniques)** and submitted by student **(Ameer Hussein Mohammed Ali)** was prepared under my supervision at the Department of Electrical Engineering, College of Engineering, University of Babylon, as a part of requirement for the degree of Doctor of Philosophy in Electrical Engineering \ Electronic and Communications.

Signature:

Name: ***Prof. Dr. Saad S. Hreshee***

Date: / / 2023

I certify that this dissertation mentioned above has been completed in Electronic and Communications Engineering in the college of Engineering\ University of Babylon.

Signature:

Name: ***Prof. Dr. Qais Kareem Omran***

(Head of Electrical Engineering Dept.)

Date: / / 2023

Examining Committee Certificate

We certify that we have read this dissertation entitled (**Performance Evaluation of Polar-Coded Generalized Frequency Division Multiplexing Using Artificial Intelligent Techniques)**, and as an examining committee, examined that student **(Ameer Hussein Mohammed Ali)** in its contents and that, in our opinion it meets the standard of a dissertation for the degree of Doctor of Philosophy in Electrical Engineering\Electronic and Communication.

Signature:
Name: ***Prof. Dr. Samir J. Al-Muraab*** (Chairman)
Date: / / 2023

Signature:
Name***: Prof. Dr. Hikmat N. Abdullah*** (Member)
Date: / / 2023

Signature:
Name: ***Prof. Dr. Adheed H. Sallomi*** (Member)
Date: / / 2023

Signature:
Name: ***Prof. Dr. Ahmed A. Hamad*** (Member)
Date: / / 2023

Signature:
Name: ***Asst. Prof. Dr. Hilal Al-Libawy*** (Member)
Date: / / 2023

Signature:
Name: ***Prof. Dr. Saad S. Hreshee*** (Supervisor)
Date: / / 2023

Approval of Head of Department

Signature:
Name: ***Prof. Dr. Qais Kareem Omran*** (Head of Electrical Engineering Dept.)
Date: / / 2023

Approval of the Dean of College

Signature:
Name: ***Prof. Dr. Laith A. Abdul-Rahaim*** (Dean of College of Engineering)
Date: / / 2023

Acknowledgments

In the name of **ALLAH**, the Most Gracious and the Most Merciful for giving me the determination and will to complete this research work.

I appreciate the inspirations and guidelines that I have received from my supervisors Prof. Dr. Saad S. Hreshee, for his advice, guidance and encouragement. Without their continuous support and interest, this work would not have been the same as presented here.

I would like to extend my indebtedness to the teaching staff members of the Department of Electrical Engineering, University of Babylon, for their continuing support and fruitful discussion throughout all steps of the research work presented in this dissertation.

Asst. Prof. Ameer Hussein Mohammed Ali

2023

Abstract

Due to the tremendous development in the wireless communication field and the wide requirements of current generations, such as high data rates, extremely low power consumption, and high performance, it is necessary to think about techniques and methods that present the improvement to meet the growing requirements. The introduction of the Generalized Frequency Division Multiplexing (GFDM) technique was one of the proposed methods; it is one of the candidate schemes for the current generations and beyond. Its multicarrier modulation scheme and structure are independent blocks, and each block contains K sub-carriers and M sub-symbols; K is filtered with a prototype Pulse Shaping Filter (PSF) that shifts by time and frequency domain. GFDM was presented as an improved method over other Multiplexing technique, as it provided an improvement in the field of Out Of Band (OOB) and Peak To Average Power Ratio (PAPR). Still, at the same time, it provided a lower performance in BER with respect to SNR. In this dissertation, several scenarios were presented based Matlab to improve the performance of the GFDM system, as two structures were presented, K16 M15 and K20 M16, where the first structure had better performance compared to the second structure, where it was improved by adding a coding system based on Polar Coding (PC) and interleaving based using three types, random, matrix and helical. In comparison, the second structure gave a worse performance to give way for improvement methods based on artificial intelligence.

A method is presented to improve the performance of GFDM by using the Genetic Algorithm (GA) to improve the performance of the PSF in GFDM. The channel estimation is accomplished by means of LS method, and the Artificial Neural Network (ANN) based on feed-forward back propagation is used to enhance the estimation process. Scenarios Polar Code

Interleaver GFDM (PI-GFDM), Least Square Polar Code-GFDM (LP-GFDM), Least Square Polar Code Interleaver-GFDM (LPI-GFDM), Genetic Algorithm-GFDM (G-GFDM), Genetic Algorithm Artificial Neural Network-GFDM (GN-GFDM), Genetic Algorithm Artificial Neural Network Polar Code-GFDM (GNP-GFDM) and Genetic Algorithm Artificial Neural Network Polar Code Interleaver GFDM (GNPI-GFDM) were presented. A comparison was made between the types of proposed scenarios in terms of the amount of improvement. The proposed GNPI-GFDM presents an enhancement over the traditional GFDM of more than 3.5dB at BER=10^{-4} over Rayleigh fading channel. The PI-GFDM presents an enhancement over the traditional GFDM about 5 dB at BER=10^{-5} over the AWGN channel.

List of Contents

List of Abbreviations

2-Sided SIC	Double-Sided Serial Interference Cancellation
3G	Third Generation
4G	Fourth Generation
5G	Fifth Generation
ANN	Artificial Neural Network
AWGN	Additive White Gaussian Noise
BER	Bit Error Rate
BICM	Bit-Interleaved Coded Modulation
BR	Bayesian Regularization
CBBO-SLM	Chaotic Biogeography Based Optimization-Selective Level Mapping
CP	Cyclic Prefix
DFT	Discrete Fourier Transform
Eb/No	Energy Per Bit to Noise Power Spectral Density Ratio
FFT	Fast Fourier Transforms
GA	Genetic Algorithm
GFDM	Generalized Frequency Division Multiplexing
G-GFDM	Genetic Algorithm-GFDM
GL-GFDM	Genetic Algorithm Least square-GFDM
GLP-GFDM	Genetic Algorithm Least Square Polar Code-GFDM
GLPI-GFDM	Genetic Algorithm Least Square Polar Code Interleaver-GFDM
GN-GFDM	Genetic Algorithm Artificial Neural Network-GFDM

GNP-GFDM	Genetic Algorithm Artificial Neural Network Polar Code-GFDM
GNPI-GFDM	Genetic Algorithm Artificial Neural Network Polar Code Interleaver-GFDM
IFFT	Inverse Fast Fourier Transforms
ISI	Inter-Symbol Interference
itr	Iteration (number of send blocks)
LDPC	Low-Density Parity-Check Code
LLR	Logarithmic Likelihood Ratio
LM	Levenberg Marquardt
LP-GFDM	Least Square Polar Code-GFDM
LPI-GFDM	Least Square Polar Code Interleaver-GFDM
LS	Least Square
MIMO	Multiple Input Multiple Output
MLC	Multi-Level Coding
MMSE	Minimum Mean Square Error
Mu	Modulation order of the QAM symbol
ne	Number of neurons in hidden layer
NI	National Instruments
NLMS	Normalized Least Mean Squares
NP	Number of paths
obs	observations
O-GFDM	Orthogonality-GFDM
OOB	Out Of Band
Op-PSF	Optimized-Pulse Shaping Filter
P/S	Parallel to serial converter
PAPR	Peak-To-Average Power Ratio

PC	Polar Code
PI-GFDM	PC-Interleaver-GFDM
PR	PC-Rate
PSD	Power Spectral Density
PSF	Pulse Shaping Filter
QAM	Quadrature amplitude modulation
S/P	Serial to Parallel converter
SCG	Scaled Conjugate Gradient
SDR	Software-Defined Radio
SIC	Serial Interference Cancellation
SIC	Serial Inter- Carrier Interference Cancellation
SIM-CP	Subcarrier Index Modulation and Constellation Precoding
SLM	Selective Mapping
SNR	Signal-To-Noise Ratio
St-PSF	Standard-Pulse shaping Filter
USRP	Universal Software Radio Peripheral
Wi-Fi	Wireless-Fidelity
WLAN	Wireless Local Area Network
ZF	Zero Forcing

List of Symbols

$+$	The XOR operation
π and β	The parameters of cost function
$*$	The convolution operation
$[n]$	The sampling index
$\otimes$	Kronecker product operation
α	The step size
a	constant value
D	The output desired
$d_{k,m}$	Data Symbols
e	A vector of network errors
E_D	The sum of errors
e_{NLMS}	The error
E_W	The sum of squared weights
F	Generator matrix
$f()$	The activation functions
$F(w)$	The cost function
g	The gradient
$g_{m,}[n]$	Prototype PSF
$h(n)$	The channel effect
H_{LS}	The channel estimation
h_{NLMS}	The NLMS estimation for channel
H_{NLMS}	The channel estimation
J	The Jacobian matrix
K	Sub-carriers
LS_{es}	The LS estimation
LLR	Logarithmic Likelihood Ratio
ln	Natural logarithm
M	Sub-symbols
min	The minimum sum between two receivers
MSE	The Mean Square Error
mu	Modulation order of the QAM symbol
N	The data block
n	The number of inputs to neurons
net	the input to activation function
o	The actual output

P	The length of data bit
$\mathrm{pr}(\mathrm{bit}=0)$	The probability of 0 bit
$\mathrm{pr}(\mathrm{bit}=1)$	The probability of 1 bit
q	The PC stage
r	Roll off factor of the PSF
S	The searching direction vector
sgn	Sign function
ζ	Combination coefficient
u	The input data
V	The input data to PC encoder
w	The weight
$w(n)$	The AWGN
Y_{es}	The estimation of received signal
w_{NLMS}	Output of NLMS
w_{t+1}	The new weight vector
x	The input
$x(n)$	The transmitted signal.
x_p	The transmitted pilot
XOR	Exclusive OR operation
y	The output
$y(n)$	The received signal
Y_{NLMS}	The received estimation
Y_p	The received pilot
$\partial()$	The derivation operation.

List of Figures

List of Tables

CHAPTER ONE

Introduction

Chapter One

Introduction

1.1 General View

Generalized Frequency Division Multiplexing (GFDM) is a technique used in modern communication systems such as wireless systems. It is a generalization of the traditional Frequency Division Multiplexing technique, which is used to share a communication channel among users by dividing the frequency spectrum into separate sub-carriers. It can achieve high spectral efficiency, transmitting more data in a given frequency band than other multiplexing techniques. Its structure is based on the block of multicarrier containing several sub-carriers, sub-symbols, and prototype Pulse Shaping Filter (PSF). The GFDM block is created by time and frequency shifting of prototype PSF with the multiplication of finite time windows. The GFDM presents preference motivation based on efficient multicarrier filter bank utilization [1].

1.2 Generalized Frequency Division Multiplexing

GFDM has several advantages over other schemes based on multicarrier techniques, it has a minimum Out-Of-Band (OOB), which allows it to transmit a higher power signal without causing interference to other systems. It also has an efficient Peak-To-Average Power Ratio (PAPR), which makes it more power-efficient. Additionally, GFDM has a flexible sub-carrier spacing, allowing it to adapt to the channel conditions and improve the system's spectral efficiency. GFDM is a relatively new technology that is still being researched and developed. It might be utilized in several communication systems, including, satellite systems, Wireless Local Area Network (WLAN) and different generations of communication

systems. However, it has some challenges, such as the high computational complexity, which can make efficient by advanced techniques [2]. Moreover, the degradation can be enhanced by various methods, such as Artificial intelligence, which will present some of them in this dissertation.

1.3 Channel Estimation

Wireless communication systems face various challenges, such as interference, noise, fading, and limited bandwidth. These challenges can be mitigated using multiple techniques, such as channel estimation, error correction codes, and multiplexing techniques [3].

Channel estimation is estimating the characteristics of the communication channel in a wireless communication system to the compensation in the receiver. In the mobile strategy, stations move and the received signal strength and phase change rapidly. Moreover, the signal transmitted over the channel is reflected by buildings and other obstacles in the ground, which leads to different paths to the receiver, which leads to different time delays, phases, amplitudes, and additional noise. It will cause severe fading. The estimated perform based known signal for the transmitter and receiver signal called pilot insert in each data frame with various forms depending on practical cases. It is an essential aspect of wireless communication, as the channel's characteristics can affect the system's performance, such as the Signal-To-Noise Ratio (SNR) and the error-correction capabilities. A transmission signal's channel characteristics show how the environment in which it is being sent affects it. This includes signal-weakening factors including fading, interference, and noise when transformed between the transmitter and receiver [4]. The channel performance estimation process performs based on the traditional method such as Least Squares (LS) and Normalized Least Mean Squares

(NLMS) or by innovative approaches such as Artificial Neural Network (ANN).

Channel estimation-based LS is one method for estimating the channel response. It is a low-complexity method because it does not require prior knowledge of environmental statistics. It involves an estimate based on a divided pilot of the received over the transmitter to find the channel response estimate. NLMS channel estimation differs from LS channel estimation, designed based on the adaptive filter, reducing errors iteratively [5].

1.4 Artificial Neural Networks

The human biological neural network simulation is called ANN. It is a computational network used to perform a wide range of tasks and controls based on the working of nerve cells of the central nervous system, which contains neurons that is simple and highly interconnected units. The neurons are the processing unit of the network that work in parallel and distributed form and belong with weighted links to adjacent neurons, and this weight is the memory unit of ANN. The weight can be changed according to the application by the training process [6].

The famous type of ANN is the feed-forward back-propagating network presented in public by David Parker in 1985 and Le Cun in 1986, and it gives an efficient structure of the network. Their presentation was as modeling and simulation and did not take up real space due to the high complexity and weakness of processors at that time. After the tremendous development in the field of processors and computers and their capabilities in processing vast and complex data, ANN has taken an excellent position in advanced applications. It is currently a widespread and developed field [7].

1.5 Genetic Algorithm

A Genetic Algorithm (GA) is a heuristic optimization search algorithm inspired by natural selection and evolution principles. It involves generating a population of possible solutions to a problem, evaluating their fitness, and selecting the best solutions for the next generation. This procedure is iterative until a solution or a predetermined number of iterations has been reached. GA is often used to solve complex optimization problems that are difficult to solve using traditional algorithms. GA is an evolutionary operation combining the random search containing the crossover and mutation and goal-oriented searches-based fitness functions. Its investigations are simultaneously in parallel form because it includes several chromosomes. The basic principle of the work is to find the definition of all the variables and find the optimal value. GA is an efficient method to solve the problem optimally based on natural selection. It continuously modified the population solutions values. The procedure of GA is based on randomly choosing individuals of the existing population to act as parents and bear the next generation's offspring. Over consecutive generations, the population develops across the best solution. GA is appropriate for specific optimization problems that standard optimization cannot solve when the issue is random, discontinuous, and indistinguishable [8].

1.6 Interleaver

An interleaver is a method that rearranges the order of a set of data elements systematically. It is used in digital communication systems to improve the system's performance by reducing the impact of errors on the transmitted data. There are many numbers of types depending on the arrangement of data. Interleavers are commonly used with the coding

algorithm, such as Polar Code (PC) or other, to improve further the transmitted data's reliability [9].

1.7 Coding System

The coding system corrects the error caused by interference, noise, or poor signal strength; the digital system encodes the transmitter device's information and decodes the receiver's signal, reducing the error and recovering the transmitted data. Various recent channel codes presented in the communication system are to be reliably sent in the 5th Generation, PC was chosen in the channel coding of the control signal [10]. PC is the constructive code representing the possibility of repair on memoryless channels, which Arıkan delivered in 2009[11]. It used the channel capacity technique in signal processing scenarios. PC is an error-correcting code designed to be highly efficient regarding its error-correction capabilities and computational complexity. They are based on channel polarization, separating the channel into several "good" and "bad" channels based on their reliability. The good channels transmit the data, while the bad channels are used for error correction. Polar codes are widely used in modern communication systems, including cellular and satellite communication systems [12].

1.8 Literature Survey

GFDM was first demonstrated by Gerhard Fettweis and his research team in 2009 with the Vodafone Chair in Mobile Communication Systems at the Dresden University of Technology, which presents some attractive features such as high degrees of spectrum fragmentation based on the efficient use of the cyclic prefix and the efficiency in the PAPR and OOB [13]. This research team continued to develop communication systems, especially those related to GFDM, in which Datta et al. 2011 presented the simple estimation method called Serial Inter-Carrier interference

cancellation (SIC). This method is applied under the effect of Additive White Gaussian Noise (AWGN) channel and gives an enhanced Bit Error Rate (BER) performance equal to 0.0009 at 16 dB and 0.00649 at 20dB [14].

Datta et al., in 2012 [15], present a technique to reduce the error-based Double-Sided Serial Interference Cancellation (2-Sided SIC). The serial interference cancellation technique is enhanced in the BER and OOB. The enhancement in BER is 0.0064 at 12dB.

Li et al. in 2016[16] proposed a new GFDM scheme by applying the Orthogonality-GFDM (O-GFDM) condition to eliminate the intrinsic interference of the conventional GFDM system. They used two prototype filters for odd and even sub-carriers. This proposed system presented enhancement over GFDM-based matched filter in performance at the muti-path given by 0.2×10^{-3} at 16dB.

Valluri and Mani 2018[17] used a Unique Word GFDM (UW-GFDM) to enhance the performance, which the BER reduced by using redundant sub-carriers that perform correlation in the frequency domain. The receiver used Weiner noise interpolation and sphere decoding. They use LABVIEW to simulate the GFDM transceiver with AWGN and multipath channels. And they have approved the National Instruments (NI) over other traditional receivers by 20×10^{-6} at 20dB.

Agrawal and Appaiah 2019[18] used a scattered pilot based then derived the Kalman filter as channel estimation for Multiple Input Multiple Output-GFDM (MIMO-GFDM) hence handling time-varying channels. The estimation-based Kalman filter gives enhancement in BER performance by 0.038 at 30 dB.

LI et al. in 2019 [19] present efficient GFDM system-based PC, turbo code, Multi-Level Coding (MLC), and Bit-Interleaved Coded Modulation (BICM). The enhancement is 0.0048 at 5dB.

Valluri et al., 2020[20] invested in the block circulant GFDM nature to reduce the error and complexity on the receiver side. The sum of permutation matrices represents the modulation matrix, which use the Discrete Fourier Transform with the theory of circular arrays. To reduce the complexity, it computes the inverse sum of permutation matrices. The transceiver system was built by LABVIEW as software and the hardware by using Universal Software Radio Peripheral 2953R, which presents enhancement in BER by 8×10^{-6} at 30 dB.

Kumar et al. in 2021[21] present an enhancement of GFDM system-based Sub-carrier Index Modulation and Constellation Precoding (SIM-CP). The enhancement is 0.00099 at 12dB.

Kumar et al. in 2022 [22] present an efficient method of reducing the PAPR and BER-based Chaotic Biogeography Based Optimization-Selective Level Mapping (CBBO-SLM) at lower computational complexity. The enhancement in BER is 0.0049 at 20dB.

Bouslam et al. in 2023[23] proposed an efficient reduction method for PAPR and BER-based intelligent swarm algorithm called JAYA and combined it with a Selective Mapping (SLM) scheme. The enhancement is 14×10^{-6} at 15 dB and 1 dB at BER $=10^{-6}$.

1.9Problem Statement

This dissertation deals with the problem of the BER performance of GFDM, which is considered the weak point despite its advantage of the minimum OOB and efficient PAPR, which presents scenarios for reducing the BER-based PC, interleaver, GA, and ANN methods.

1.10 Objectives

This dissertation will cover the following topics:

1. Present the background of GFDM, PC, interleaver, GA, and ANN.
2. Simulate the GFDM system-based PC and interleaver.
3. Develop the GFDM behavior by optimizing PSF based on GA.
4. Enhancing the channel estimation by ANN.
5. Investigate the BER performance in each scenario of proposed designs.

1.11 Main Contribution

1. Present enhancement scenarios in BER performance of GFDM system based on PC and interleaver.
2. Study the internal structure of GFDM and perform the enhancement by optimizing the performance by replacing the Standard PSF (St-PSF) with Optimized-PSF (Op-PSF); this optimizes the step-based assign the PSF by GA.
3. Perform the channel estimation based on LS and NLMS and use the data generated by this estimation to train different methods with the other numbers of neural in the hidden layer. Hence present enhancement of channel estimation-based ANN.

1.12 Outlines of Dissertation

This dissertation is organized into five chapters as follows:

1- Chapter one: introduces a general view of GFDM, channel estimation, ANN, GA, interleaver, and coding system. Then the literature survey of the last work is presented with objectives, main contribution and outlines of dissertation.

2- Chapter two: presents the theoretical background of the GFDM, wireless channel, channel estimation methods, PC, interleaver methods, ANN methods, and GA.

3- Chapter three: presents the proposed system's modeling details with different scenarios of GFDM, PC, interleaver, ANN, and GA.

4- Chapter Four: presents the simulation result of proposed systems with different scenarios and compares it with a literature survey of previous work.

5- Chapter Five: present the distinctive conclusions extracted from the proposed scenarios and suggest some work related to the proposed scenarios for the future.

CHAPTER Two

Theoretical background

Chapter Two

Theoretical Background

2.1Introduction

Due to the tremendous development in wireless communications and its rapid growth, the demand for frequency spectrum increased, making it a scarce commodity [24]. The multicarrier modulation technique spread in modern communication systems to ensure optimal use of the frequency spectrum and maximum throughput. This technique presents higher spectral efficiency when the high symbol rate wideband is split into a number of the narrowband lower rate and simulated simultaneously through a wireless channel [25].

Wireless communication systems can be optimized to improve their performance and efficiency. Some ways to optimize a wireless communication system include using suitable modulation and multiplexing techniques, different modulation and multiplexing techniques have different trade-offs regarding bandwidth efficiency, error correction capabilities, and complexity. Choosing the correct technique can improve the performance of the wireless system [26].

This chapter presented the theoretical background of GFDM, Channel estimation, Least Square (LS), Normalized Least Mean Squares (NLMS), Polar Code (PC), interleaver, Artificial Neural Network (ANN), and Genetic Algorithm (GA).

2.2Generalized Frequency Division Multiplexing

Generalized Frequency Division Multiplexing (GFDM) is a flexible multicarrier scheme proposed for the next-generation networks. GFDM is

a new optimization idea. It is a non-orthogonal frequency division multiplexing operating on Inverse Fast Fourier Transforms (IFFT)/Fast Fourier Transform (FFT), which perform tasks of reasonable complexity [27]. The waveform of GFDM is a Multicarrier, which divides the data stream over multiple lower data rate carriers. Each one is modulated individually. Present a suitable arrangement of boundaries over the requirements of the last generations. It does not require orthogonal verification between the sub-carriers and thus reduces the power loss to the lowest amount [28]. The structure is based on blocks built by sub-carriers (K) and sub-symbols (M) and modulated separately. Prototype Pulse Shaping Filter (PSF) designed in time and frequency shifting are applied for each K to reduce the Out Of Band (OOB) emission effect. The applied filtering on the K caused a loss of orthogonality [29].

Figure (2.1) present the blocks of data transmitted by each block divided by the spectrum into K in the frequency domain and M in the time domain. $d_{k,m}$ represents data send in GFDM blocks with k^{th} sub-carrier and m^{th} sub-symbol. Each symbol is filtered with a PSF. The behavior of PSF is present in Figure (2.2). Each block $N=K\times M$ that required to transmit. The spectral efficiency of GFDM is more efficient due to the single Cyclic Prefix (CP) of each block [30].

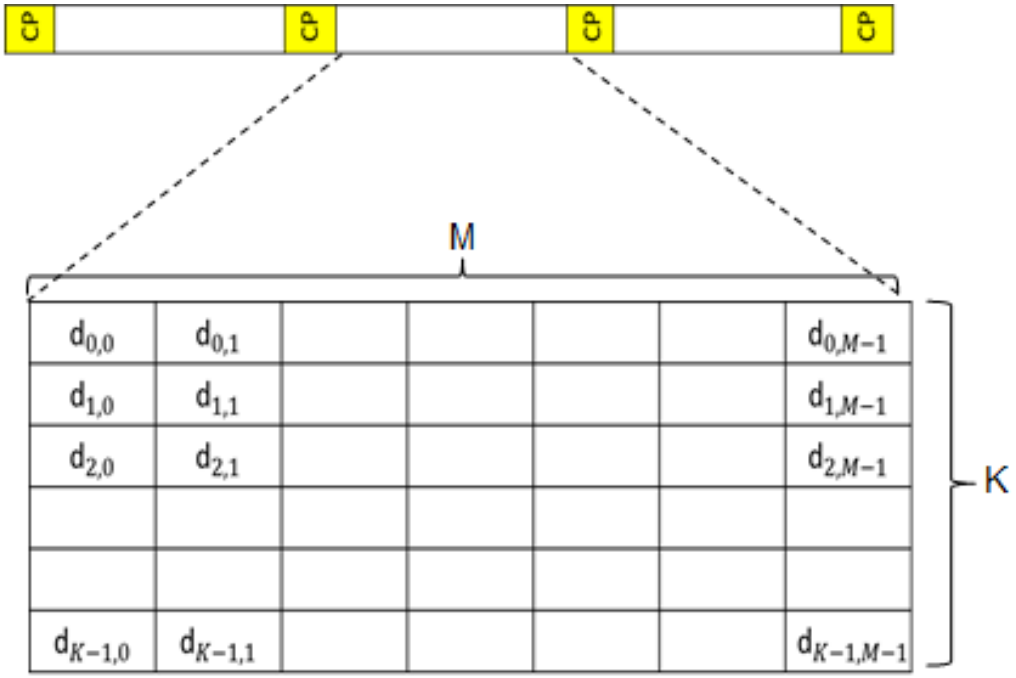

Figure (2.1): The structure of GFDM data block [31]

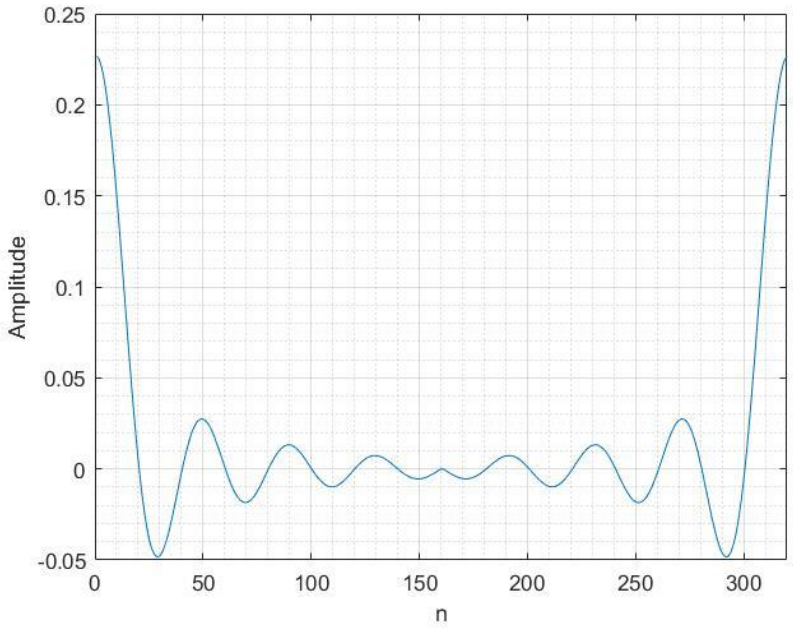

Figure (2.2): The impulse response of PSF [32].

The GFDM transmitted signal is presented in Equation (2.1), the filter circularly shifted in Equation (2.2), and the equation of PSF is given in Equation (2.3). The block diagram of modulation and demodulation of GFDM is present in Figure (2.3) and Figure (2.4) [34].

$$x[n] = \sum_{m=0}^{M-1} \sum_{k=0}^{K-1} d_{m,k} g_{m,}[n] \quad (2.1)$$

$$g_m[n] = g[(n - mk)_{mod\ N}] \exp\left(j2\pi\ \frac{kn}{K}\right) \quad (2.2)$$

$$g[n] = \frac{sinc(n) \times \cos(\pi \times_r \times n)}{1-(4 \times_r{}^2 \times n^2)} \quad (2.3)$$

Where $x[n]$ is the transmitted signal. $[n]$ is the sampling index $n = 0, \dots, N-1$. $d_{m,k}$ is the complex data. $g_{m,}[n]$ is prototype PSF, r is Roll off factor of the pulse shaping filter, N is K×M. k is constant value from 1 to K. m is constant value from 1 to M.

The main advantage of GFDM is summarized below [35]:

1- Presents lower OOB and PAPR due to the PSF.

2- Shows an efficient spectrum using one CP for each block.

3- present high flexibility in terms of setting up GFDM blocks.

Meanwhile, the disadvantages of GFDM are the complexity and the performance of Bit Error Rate (BER) [36].

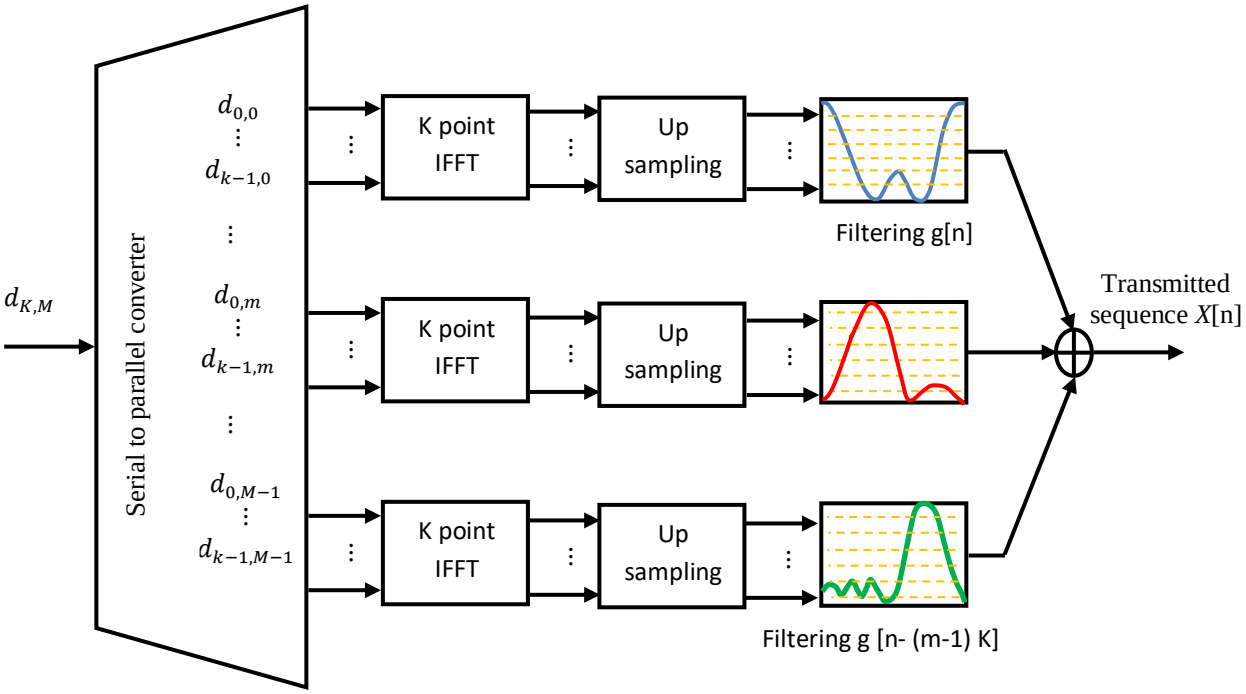

Figure (2.3): GFDM modulation [37].

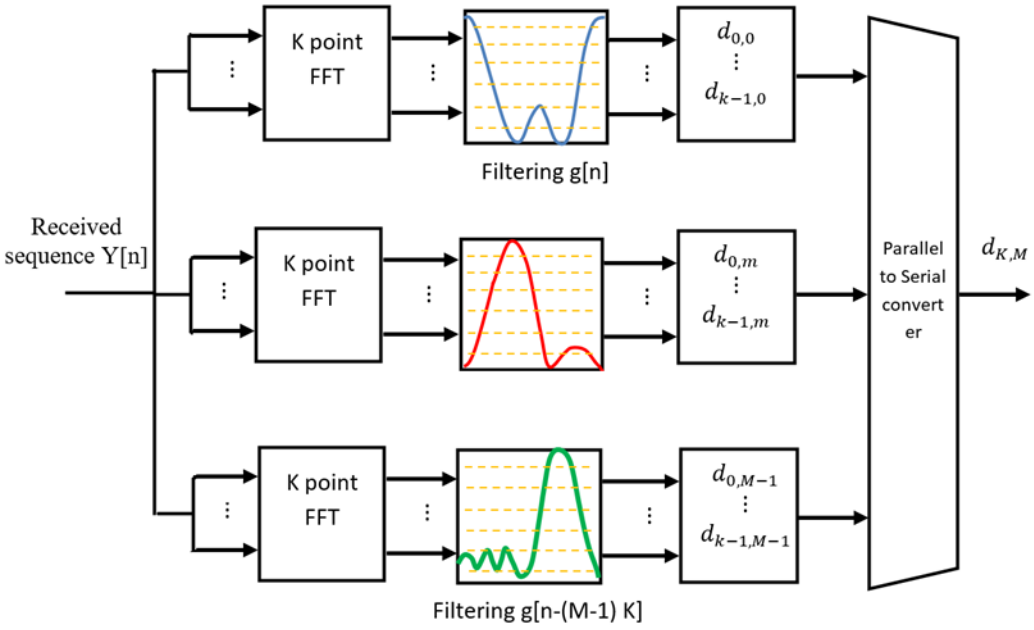

Figure (2.4): GFDM De-modulation [37].

The orthogonality between sub-carriers of GFDM was lost due to the PSF. Hence this leads to increasing the self-interference arising from BER. The self-interference between the neighboring sub-carrier present in Figure (2.5) [39].

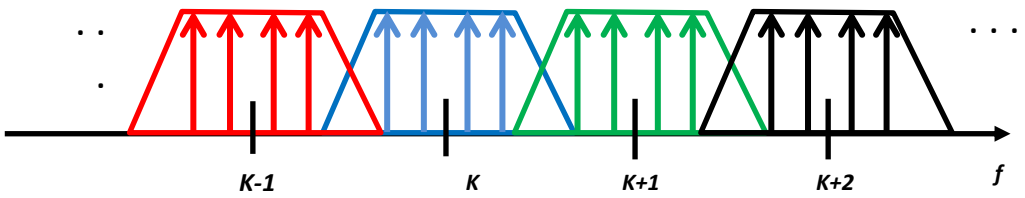

Figure (2.5): Self-interference between the neighboring sub-carrier [39].

2.3Wireless Channel

Typical mobile radio systems need the information transferred from a stationary base station to a mobile device in motion. The communication data is modulated and transmitted across a wireless channel as waveforms. As signals travel across the wireless channel to the receiver, objects such as automobiles, buildings, trees, mountains, and hills collide. Block the line-of-sight propagation route, causing unwanted effects on the propagating symbols. Due to the detrimental effects of these obstructions, the signals undergo reflection, diffraction, and scattering, causing them to arrive at the receiver via multiple reflective paths with varying time delays, amplitudes, and phases, a phenomenon known as multipath propagation [40].

When propagating, waves suffer from reflection, diffraction, and scattering. Reflection occurs when radio waves experience reflection caused by an obstacle with dimensions larger than the wavelength of the transmitted signal [41]. Diffraction occurs when a sharp object's surface blocks a wave, resulting in an apparent wave propagating toward the

receiver. Meanwhile, signal scattering occurs when objects with dimensions smaller than the wavelength of the transmitted signal block the signal. This signal scattering will then cause the signal to be reflected in all directions. For example, the signal is scattered by rainwater [42].

The transmitted data generally corrupted by noise through the channel propagation, which suffered from fading and multipath, the received signal present as Equation (2.4). This fading and multipath made detecting the transmitted data challenging, which required pinpoint methods to channel estimation [43].

$$y(n) = x(n) * h(n) + w(n) \quad (2.4)$$

Where: $y(n)$ is the received signal. $x(n)$ is the transmitted signal. * is the convolution operation. $h(n)$is the channel effect. $w(n)$ is the AWGN.

Rayleigh fading channel is one of the wireless channel simulations based on a Gaussian or normal distribution with more tapes, multiple indirect paths between transmitter and receiver, and no distinct dominant path. It means there is no line of sight. Rician fading channel differs with the applied direct line of sight in addition to the number of indirect multipath [44].

2.4Channel Estimation

The channel estimation process determines the characteristics of a communication channel in a wireless system, which helps the receiver to predict the approximation of the channel impulse response and understand the effects of the channel on the transmitted data, hence performing optimum reconstruction of the transmitted information. The precision of the channel estimate is essential to a wireless communication system's success since it directly impacts the quality of the recovered signal. The communication systems parameters, such as the modulation scheme,

channel type, and available resources, determine the channel estimate technique. There are various estimation types, one of which is the pilot-based channel estimation schemes [45].

The pilot-based channel estimate is a technique for assessing the parameters of a communication channel in a wireless communication system by introducing pilot symbols into the sent signal. The receiver then applies this information to estimate the channel response. In pilot-based channel estimation, the transmitter regularly broadcasts a known sequence of symbols throughout the data transmission. These symbols, known to the receiver, aim to offer a reference for the receiver to estimate the channel response. The receiver can estimate the channel response by comparing the known pilots to the received pilots. Pilot-based channel estimation is a straightforward and efficient technique, although it has limits. For example, it needs many pilot symbols in the transmission, limiting its capacity [46].

Additionally, the channel response varies across pilot symbols. In addition, a high-resolution channel assessment is necessary for the receiver to adjust correctly for channel-induced distortion. Pilot-based channel estimation is a simple and effective approach for channel estimate in wireless communication systems. However, it has significant drawbacks, mainly when dealing with high-resolution estimation is necessary [47]. The general block diagram related to channel estimation is presented in Figure (2.6).

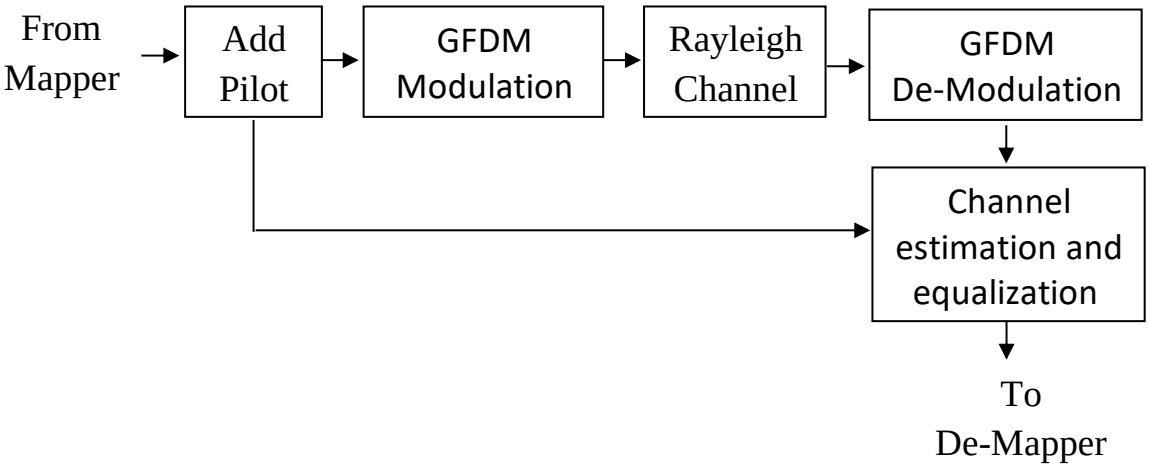

Figure (2.6): General channel estimation block diagram [48].

2.4.1 Least Square (LS)

The estimation-based LS is one of the channel estimation methods for wireless communication, which present how the channel affects the signal by the environment. This effect includes interference and noise, which always weaken the signal between sending and receiving. The LS estimation contains the training pilot signal inserted in the transmitted signal and used to estimate the signal in the receiver. LS reduces the sum square error between the transmitter and receiver pilot to find the best channel response estimate, the theoretical block diagram of LS present in Figure (2.7) [49].

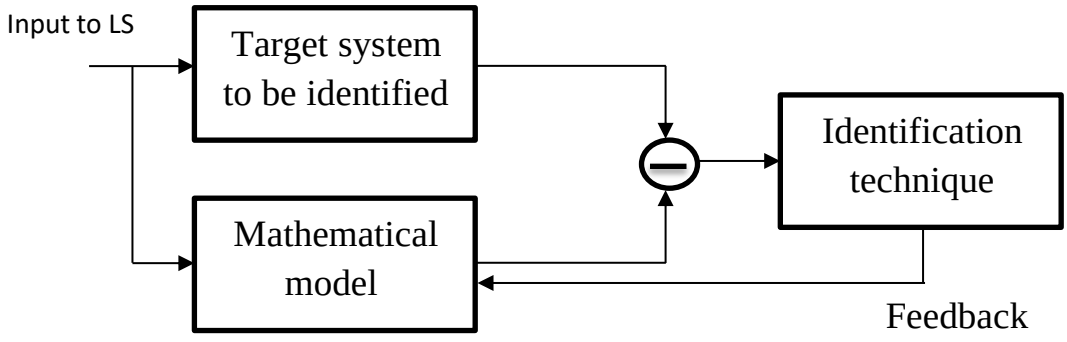

Figure (2.7): General block diagram of LS identification system [50].

After performing GFDM demodulation, LS steps were applied for each K. The received pilot extracted from the received signal (demodulated signal). Then the estimated LS is computed as Equation (2.5). Interpolation is applied to get the channel estimation H_{LS} as Equation (2.6). Finally, the transmitted signal was recovered by dividing the receiving signal over H_{LS} as Equation (2.7) [51].

$$LS_{es} = \frac{Y_p}{x_p} \tag{2.5}$$

$$H_{LS} = \text{interpolate } (LS_{es}) \tag{2.6}$$

$$Y_{es} = \frac{\text{Y}}{H_{LS}} \tag{2.7}$$

Where: LS_{es}: is the LS estimation. Y_p: is the received pilot. x_p : is the transmitted pilot. H_{LS}:is the channel estimation. Y_{es} :is the estimation of received signal.

2.4.2 Normalized Least Mean Square (NLMS)

One of the methods for channel estimation in wireless communication systems is the NLMS algorithm. The NLMS algorithm is a type of adaptive filter that is used to estimate the response of a wireless channel. The algorithm uses the adjustment of the filter coefficients to minimize the error between the desired signal and the filtered version of the received signal. In the NLMS algorithm, the filter coefficients are updated at each time step based on the current error, the current input signal, and a step size parameter. It is relatively simple to implement. However, it can be sensitive to the choice of step size, and the algorithm can sometimes converge to a suboptimal solution. It can join slowly when the channel is highly correlated [52]. The general block diagram of NLMS presented in Figure (2.8). Equation (2.8) to Equation (2.12) present the procedure of NLMS

which w_{NLMS} is the output of NLMS, h_{NLMS} is the NLMS estimation for channel. e_{NLMS} is the error. H_{NLMS} is the channel estimation. Y_{NLMS} is the received estimation [51].

$$w_{NLMS} = h_{NLMS} * x_p \tag{2.8}$$

$$e_{NLMS} = Y_p - w_{NLMS} \tag{2.9}$$

$$h_{NLMS} = h_{NLMS} + \frac{2*e_{NLMS}*x_p}{x_p{}^T * x_p} \tag{2.10}$$

$$H_{NLMS} = \text{interpolate}\ (h_{NLMS}) \tag{2.11}$$

$$Y_{NLMS} = \frac{\text{Y}}{H_{NLMS}} \tag{2.12}$$

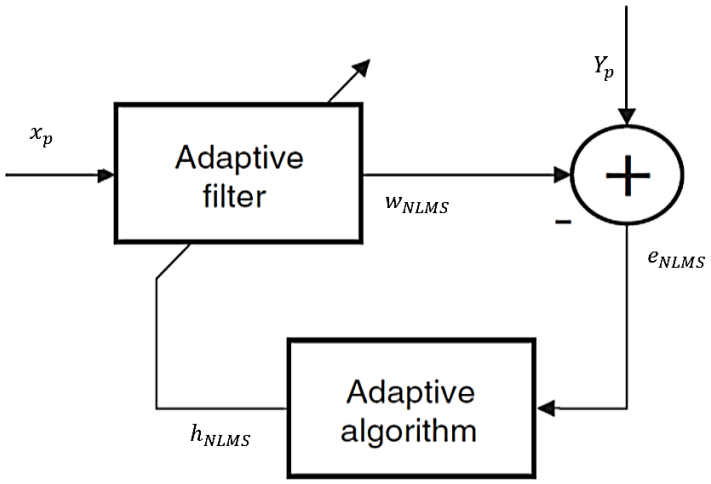

Figure (2.8): General block diagram of NLMS [51].

2.5 Polar Coding (PC)

Channel coding is used in mobile communication to protect the transmitted data from errors through the transmission, such as interference, noise, and drop strength of the signal, which encodes the data at the transmitter and decodes it at the receiver. Communication systems are continuously in development hence required to improve their performance and apply new services and applications [53]. PCs are one of the modern

types of coding systems. It is one kind of forward error correction; however, they have been used in 5G communication systems as channel coding of the control channel. PC performs well compared to Low-Density Parity-Check Code (LDPC) and turbo codes which give the lowest complexity [54].

PC generates virtual channels, which assign as proper channels and useless channels. The PC's encoding process is performed by kernel matrix or generator matrix (F) shown in Equation (2.13) and performs Kronecker product as in Equation (2.14). The Kronecker product contains the + character, which refers to the XOR operation. u refer to input bit data that length of P. The kernel matrix can expand to large number of bits as Equation (2.15). $\otimes$ is Kronecker product operation. The polar encoder of 2-bit present in Figure (2.9). The encoder can expand to a greater number of inputs as Figure (2.10). Which the stage compute based on $q = \log_2 P$. The input data to encoder is V bit and the output is P, P-V is the frozen bit often adjusts a value of 0 [55].

$$F_2 = \begin{bmatrix} 1 & 0 \\ 1 & 1 \end{bmatrix} \tag{2.13}$$

$$[u_1 \;\; u_2]F_2 = u^{(2)} = [u_1 + u_2 \;\; u_2] \tag{2.14}$$

$$G_{2^n} = \begin{bmatrix} 1 & 0 \\ 1 & 1 \end{bmatrix}^{\otimes \mathrm{q}} \tag{2.15}$$

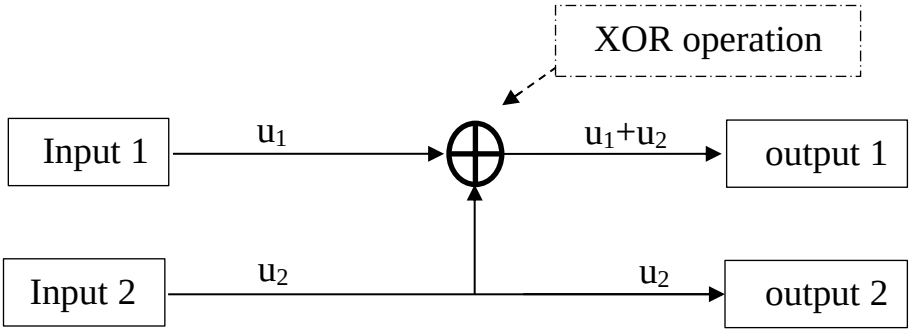

Figure (2.9): 2-bit PC encoder [56]

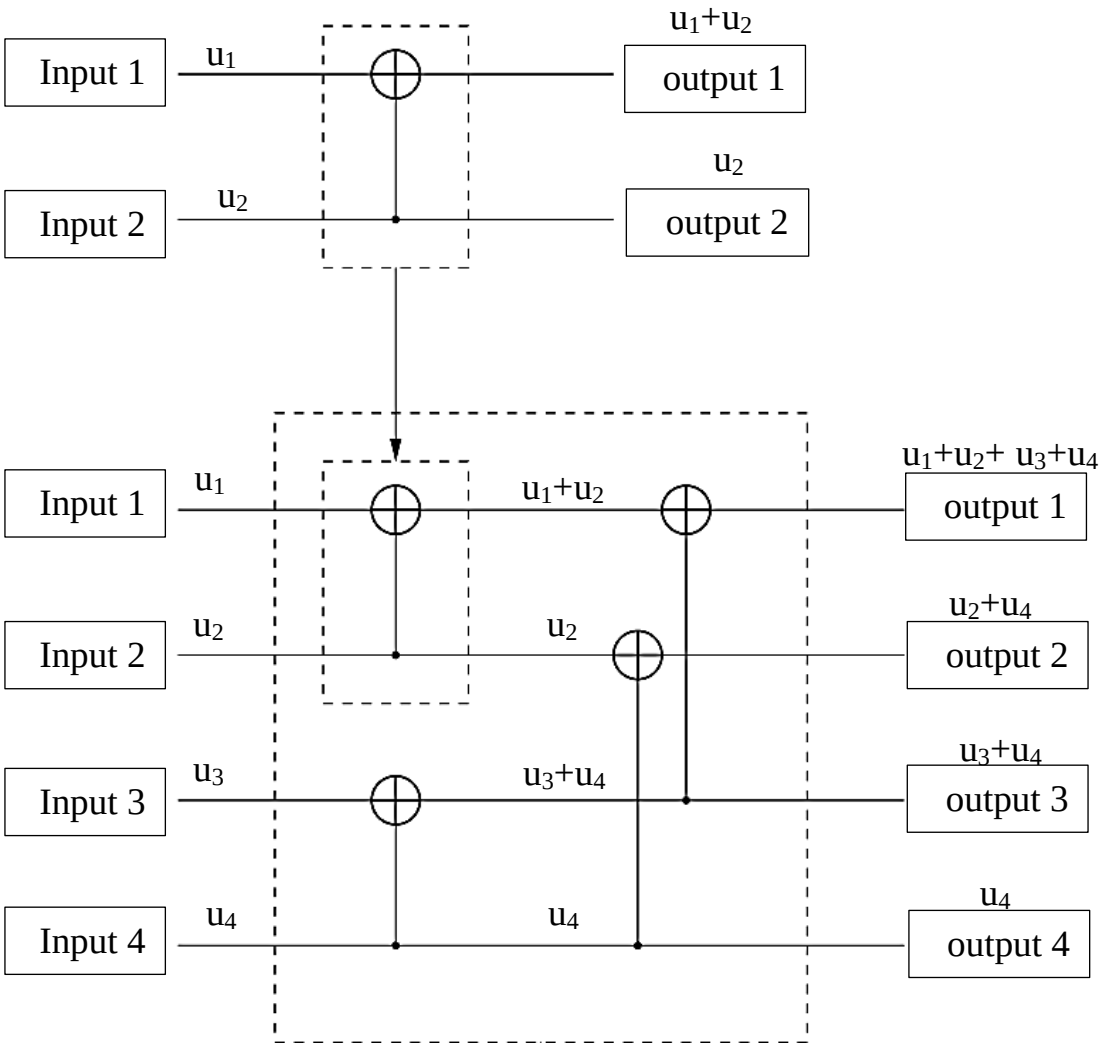

Figure (2.10): Extended PC encoder [57]

The information is recovered to the encoded data in the demodulator at the receiver based successive-cancellation list decoder method. In general,

the demodulator cannot get absolute confidence about the encoded block because of the unstable behavior of the noise in the communication channel. At the demodulator, give the confidence about of bit in the encoded by applying Logarithmic Likelihood Ratio (LLR) as in Equation (2.16). Then applied min-sum approximating as in Equation (2.17).

$$LLR = ln\left[\frac{pr(bit=0)}{pr(bit=1)}\right] \tag{2.16}$$

$$f(r_1, r_2) = sgn(r_1)sgn(r_2)\min(|r_1|, |r_2|) \tag{2.17}$$

The pr(bit=0) and pr(bit=1) in refer to the probability of 0 and 1 bit which the positive value of LLR indicates the possibility of 0 is high, and the negative value guide the likelihood of 1 being high. sgn is sign function that returns the positive number to +1 and negative number to -1. min is the minimum sum between two receivers r_1 and r_2.

2.6 Interleaver

The procedure of interleaving plays a crucial role in a modern communication system. Its present de-correlation through the neighboring bits in coding and decoding steps. Its method of arranging the data stream to become in nonadjacent locations without adding or losing anything. Different types depend on the behavior of change locations of a bit stream. The interleaved system is easy to build at the transmitter and receiver side and sometimes requires bit storage [58]. It converts burst errors to random errors and helps the error correction process by enhancing the coding algorithm, such as PC. On the transmitter side, it is used after the encoding of the PC, while the receiver is used before the PC decoding [59].

2.6.1 Random Interleaver

The Random type of interleaver performs the scrambling of data by different patterns. This permutation is present without a known pattern.

Despite its high efficiency, it requires a lot of memory space at the transmitter and receiver, which the data organized as a random set of the memory address. Figure (2.11) present random interleaver [60].

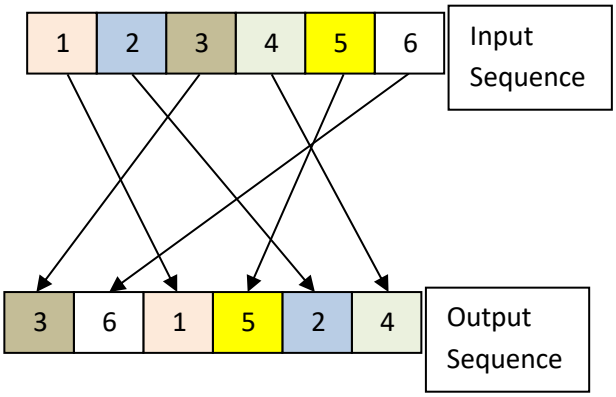

Figure (2.11): Random interleaver [61]

2.6.2 Helical Interleaver

Helical interleaver is one type of interleave that fil the block in deterministic order and reads it diagonal-wise (helical fashion) as in Figure (2.12) [62].

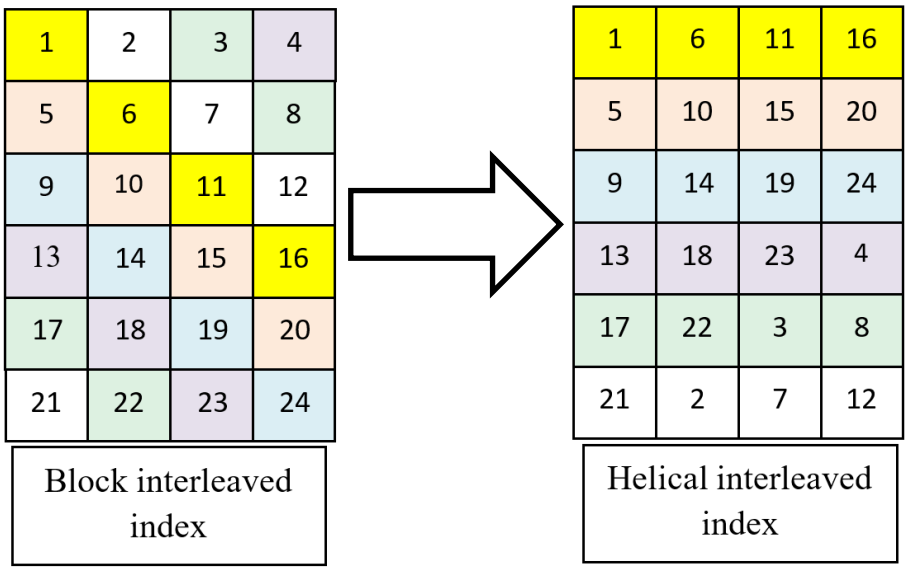

Figure (2.12): Helical interleaver [63]

2.6.3 Matrix Interleaver

Matrix interleaver is performed by writing the specific dimensions column by column until the matrix is complete, then for transmitting, read row by row as shown in Figure (2.13) [64].

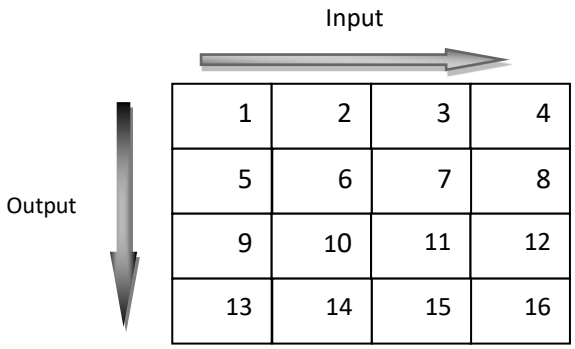

Figure (2.13): Matrix interleaver [62]

2.7Artificial Neural Network (ANN)

ANN is a method for processing information created to generalize a mathematical representation of people's brains. Inspired by the biological nervous system study. Understanding the biological nervous is restricted to medical details. The neuron is the brain's fundamental unit. Through input routes called dendrites, it is a complex metabolic and electrical signal processing unit that ingests and combines data from many other neurons. Figure (2.14) illustrates a neuron from the human brain [65].

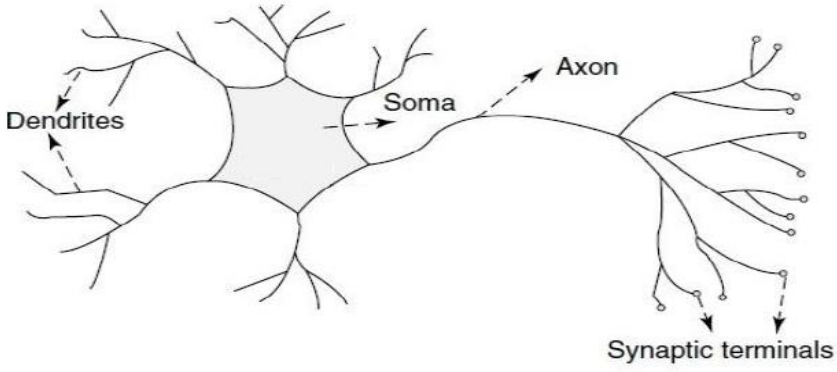

Figure (2.14): A biological neuron [65].

ANN is a grid of linked neurons. In other words, the neural network resembles the human brain in its operation. It aims to generate an output decision or pattern in response to the input [66]. The ANN process-based collecting data and prepared for training and testing to give its decision based on the error function. The general flow-chart of ANN is shown in Figure (2.15).

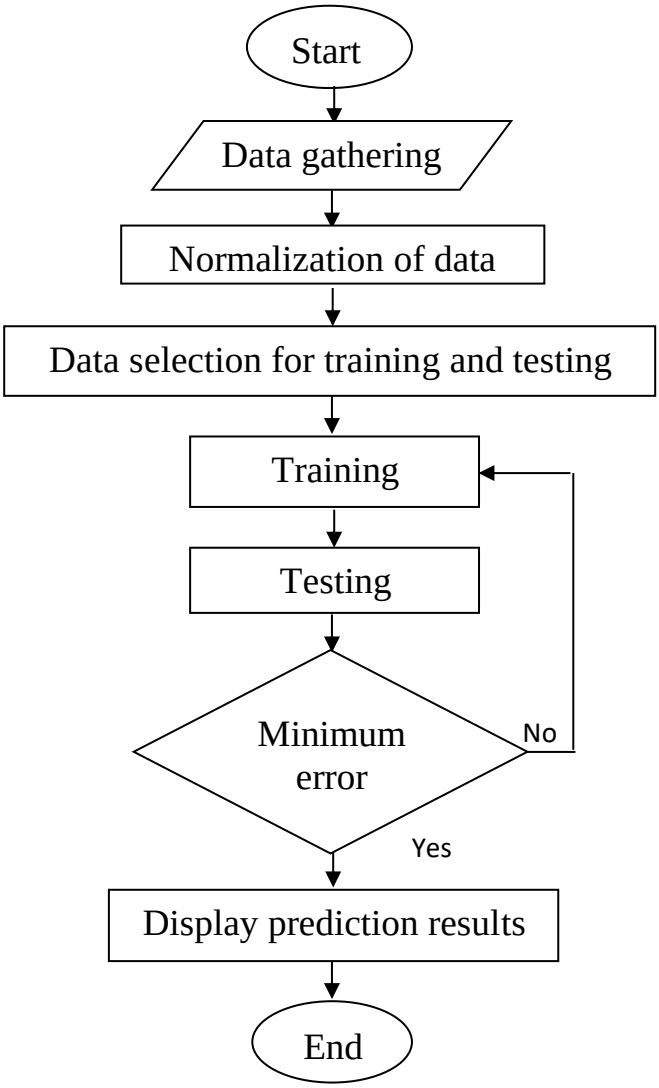

Figure (2.15): General flowchart of ANN [67].

The fundamental structure of single neurons is seen in Figure (2.17), and Equation (2.18) and Equation (2.19) present the mathematical model [68].

$$y = f(net) \tag{2.18}$$

$$net = w_1x_1 + w_2x_2 + w_3x_3 + \cdots + w_nx_n \tag{2.19}$$

where: y: The output of the neuron. $f()$: The activation functions. x: The input signals. w: The weight. n: The number of inputs to neurons, net is the input to activation function.

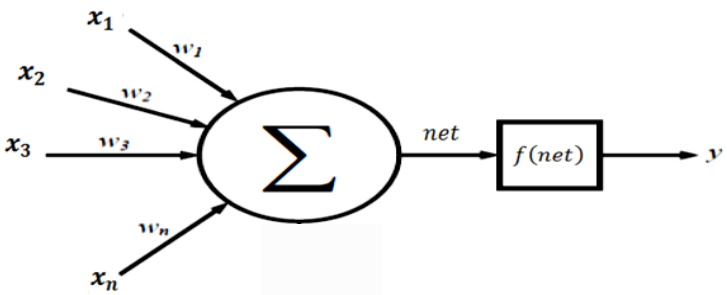

Figure (2.16): Single neuron [69].

The essential characteristic of ANN is the learning process, which is the ability to adjust the network parameters (synaptic weights) to generate the intended response. Learning is continuous until the output response converges with the expected output response. The training process finishes when the actual output response matches the desired output responses [70]. Back-propagation is a prominent form of supervised feed-forward multilayer networks [71]. Back-propagation is, fundamentally, compute the error based gradient descent approach. Several variants of the fundamental algorithm, including as Newton and conjugate gradient techniques, are used to optimize the network's performance. The training activity is terminated when the Mean Square Error (MSE) reaches its

minimal value [72]. For optimal training outcomes, the parameters must assign professionally, such as the training method, number of neurons, hidden layer and the activation function. In the back-propagation method, compute the MSE by the compute the actual output as Equation (2.20), then compute the gradient (g) as in Equation (2.21) Figure (2.17) depicts the procedure of supervised training [73-74].

$$\mathrm{MSE} = \frac{1}{2}\sum_{\mathrm{k}}(\mathrm{d}-\mathrm{y})^2 \tag{2.20}$$

$$\mathrm{g} = \frac{\partial(\mathrm{MSE})}{\partial \mathrm{w}} \tag{2.21}$$

where: MSE *:* The Mean Square Error. d: The output desired. g : The gradient of the MSE with respect to the weight. $\partial()$ is derivation operation.

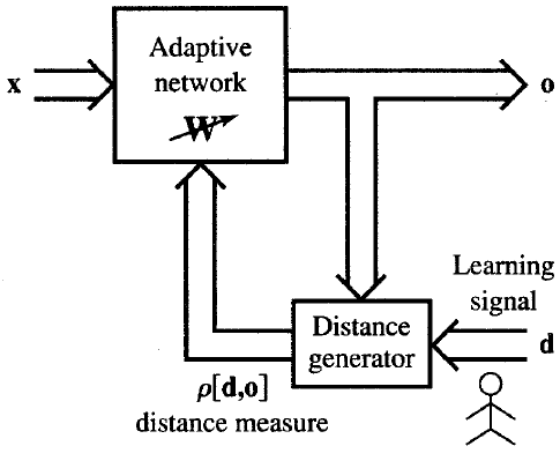

Figure (2.17): Block diagram of supervised training [75].

2.7.1.1 Levenberg–Marquardt (LM) Algorithm

Its efficient algorithm arrived at the optimum solution for solving the problem based on the Hessian matrix. LM combines the stability of the

steepest descent and the speed of the Gauss–Newton. The mathematical model of LM is present in Equation (2.22) [76].

$$w_{t+1} = w_t - [\,J^T J + \zeta\, I\,]^{-1} J^T e \tag{2.22}$$

where: w_{t+1} : The new weight vector. J : The Jacobian matrix. ζ : Combination coefficient. e: A vector of network errors.

2.7.1.2 Scaled Conjugate Gradient (SCG) Algorithm

SCG is a development of the method for steepest descent. In conjugate gradient, execute conjugate direction to provide quicker convergence, faster than at steepest descend, while preserving the low error rate established in the preceding phases. With each repetition, the step size is modified. As seen in Equation (2.23), the start directly with the negative of the gradient. Equation (2.24) present the weight updating. The direction of the steps is determined by Equation (2.25) and Equation (2.26) [77].

$$p_0 = -g_0 \tag{2.23}$$

$$w_{k+1} = w_k + \alpha_k\, g_k \tag{2.24}$$

$$\beta_K = \frac{(|g_{K+1}|^2 - g_{K+1}{}^T)}{g_K{}^T\, g_K} \tag{2.25}$$

$$P_{K+1} = -g_{K+1} + \beta_K S_K \tag{2.26}$$

Where: S is searching direction vector and g is gradient direction vector, w is the weight. α is the step size.

2.7.1.3 Bayesian Regularization (BR) Algorithm

In the classic algorithm, calculate the sum square error between actual and predicted data as Equation (2.27), then extended and enhanced by inserting regularization techniques which to measure the standard

deviation of the weights as Equation (2.28); hence the cost function becomes Equation (2.29) [78].

$$E_D = \sum_{K=1}^{n} {e_k}^2 \quad (2.27)$$

$$E_w = \sum_{i=1}^{n} {w_i}^2 \quad (2.28)$$

$$F(w) = \pi E_w + \beta E_D \quad (2.29)$$

Where: E_D is the sum of errors, E_w is the sum of squared weights. π and β are the parameters of cost function. $F(w)$ is the cost function.

2.8 Genetic Algorithm (GA)

Optimization is the primary purpose of using GA and any other evolutionary algorithm in all fields. Since optimization is the goal, it is also used in broad areas such as control, simulation, modelling and other. The conventional optimization methods start with a single factor of search performed iteratively to arrive at the optimal solution based on static heuristics. GAs represents the most representative, well-known, characterized, and widespread evolutionary computation; this was done by using the essential principles of biological evolution without the need to overcomplicate the biological mechanisms at the cell level. GA can be applied without restrictions related to the type of problem or method of optimization and requires a long time for execution which present a high number of iteration and hence has been categorized as an offline optimization algorithm [79].

GAs incorporates all the essential natural evolution items, making them exceptionally effective. It keeps simple and is hence easy to use for many problems. Generally, GA is used to search for an optimal solution or near-optimal under challenging issues. Their use is beneficial in nonsmoothed

optimization environments, while other algorithms present weak performance [80].

2.8.1 Basic GA Principles

GA used a group of candidates (population) to seek several paths or spaces together. GA operate based on the population of individuals; each can have a solution encoded as binary with fixed length string, similar to an actual chromosome. After generating the first population randomly, the algorithm develops the process through iterative and sequential selection, crossover, and mutation. New generations appear after the termination of each iteration. The population can merge previous knowledge with solutions. This process should not limit population variety; otherwise, convergence is accelerating. Selection is applied over the current population to generate an intermediate population, then crossover and mutation to develop the next generation's possible solutions [81].

2.8.2 Genetic Algorithm Block Diagram

GA is a powerful optimization technology that draws inspiration from the biological process of natural selection. Population initialization, crossover, mutations, and selection are the stages in GA. The block diagram of GA is present in Figure (2.18) [82].

Initialize Population: Creation of an initial set of people, commonly referred to as chromosomes, as the first stage in GA. It represents the potential solution to the current issue by the people. The user determines the population size and the starting values of the individuals, so it is important to choose a robust population initialization approach [83].

Crossovers: A crossover agent combines the genetic material of two individuals to create new individuals. New individuals represent new

potential solutions to the problem. The crossover factor is applied to a random selection of individuals from the population to generate new children [84].

Mutation: A mutation agent introduces small random changes to individuals to increase diversity in the population. The mutation factor is applied to a random selection of individuals from a population [84].

Selection: The selection factor chooses the individuals with the best performance. A selection factor is applied to the population to select the best individuals, which will be used to generate new offspring in the next iteration. This step is crucial in directing the search towards the optimal solution [84].

The process is repeated for a fixed number of generations or until the stopping criterion is met. The best individual in the final group is considered to be the optimal solution to the problem. It should be noted that different forms of GA may use different strategies for the above steps or even include additional steps such as elitism or other selection methods. The choice of strategy and GA criteria is critical to achieving optimal results [84].

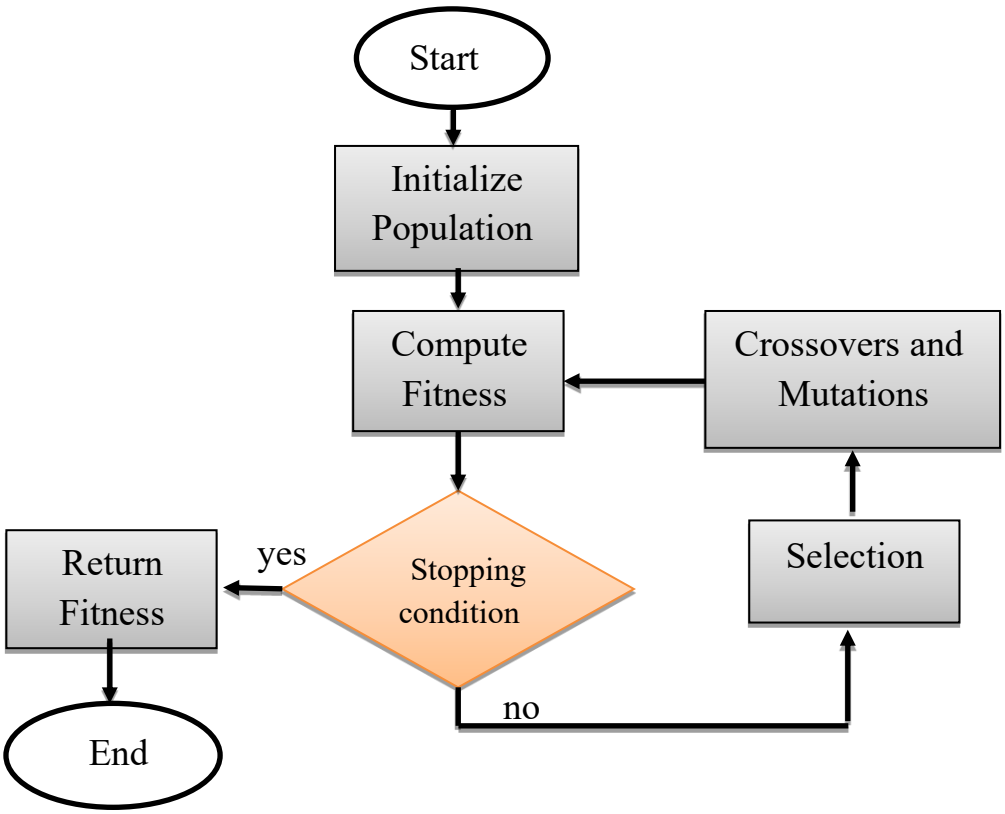

Figure (2.18): Block diagram of GA [85].

CHAPTER Three

The Proposed GFDM Scenarios

Chapter Three

The Proposed GFDM Scenarios

3.1Introduction

This chapter presents the proposed system's modeling details with different GFDM, PC, interleaver, ANN, and GA scenarios. The wireless communication system generally contains several steps. Each one belongs to the overall system and performs its function. The general block diagram of the transmitter and receiver system is shown in Figure (3.1).

- The first step is to generate data that would be sent over the channel and then received. This data is used to compute the performance by calculating the BER between the transmitted data and the received.
- The second step is the coding system used to detect and correct the error through the channel based on added redundancy bit, without the need to data re-transmit, which is considered a type of forward error correction.
- The third step is the interleaver, which almost belongs to the coding system to convert burst error to random error, enhancing the coding system's ability to detect and correct the error.
- The fourth step is the mapper, which gets a modulated signal.
- The fifth step is adding a pilot. It is considered bits of identifier for sending and receiving that can be used for channel estimation. It is used to know the channel effect on the transmitted signal and perform the estimation and equalization process.
- The sixth is the GFDM modulation step.

- The seventh step is adding CP, which cancels the effect of inter-symbol interference, and the multipath generates it through the channel.

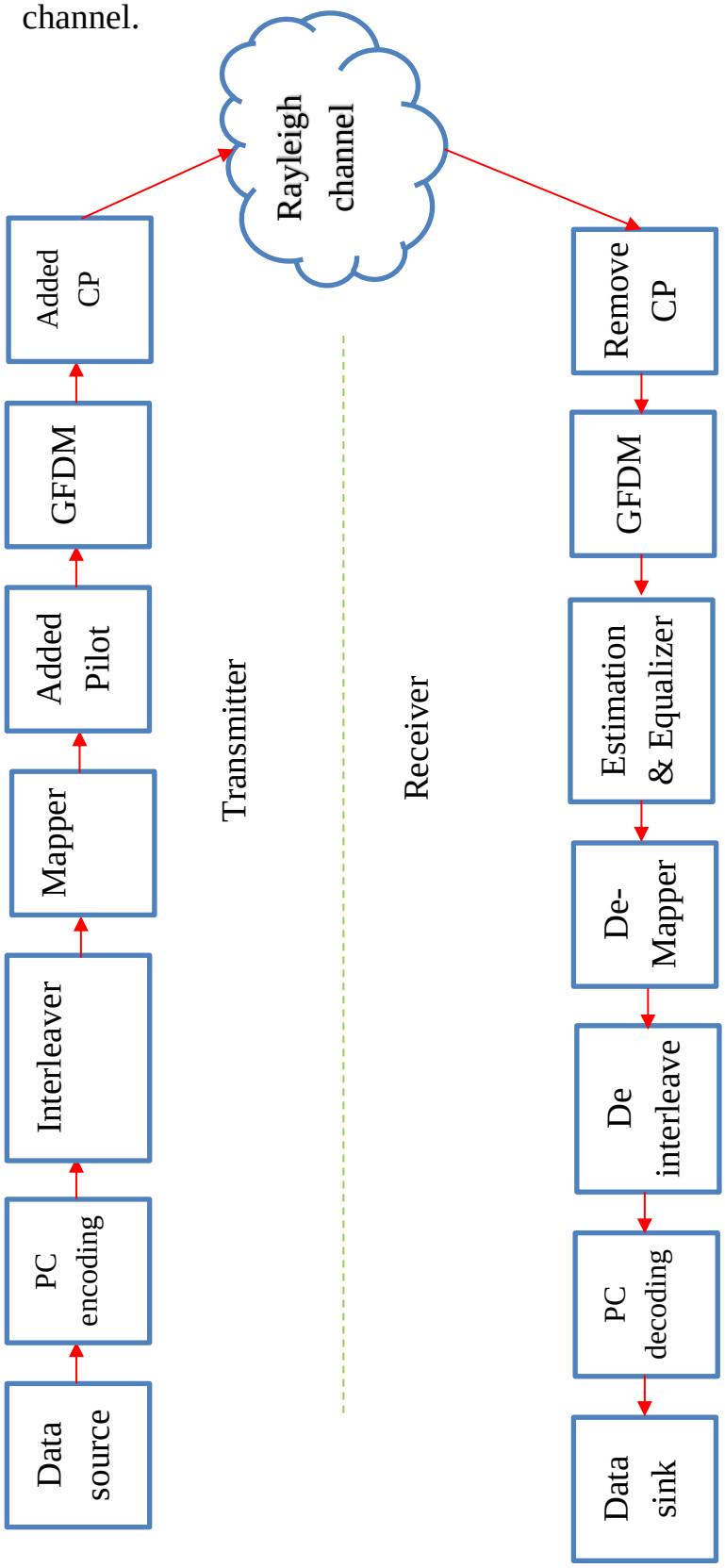

Figure (3.1) General block diagram of wireless communication

- The eighth step is the channel that transmits the signal through it. It is crucial due to its effect on the system's performance and various scenarios used to estimate its effect and equalize it to get the transmitted signal.

At the receiver, the signal entered the same transmitted step in reverse order with an additional step called the estimation and equalizer. In this step, estimate the channel effect over the transmitted signal, then equalize it to remove its effect.

In this dissertation the GFDM enhancement methods presented as in Table (3.1) which began with traditional methods then proposed scenario.

Table (3.1): Summary of the proposed work offer.

Type	Section
Traditional scenario	3.2 GFDM with AWGN
	3.3 GFDM Under Rayleigh Fading Channel
	3.4 GFDM with PC and AWGN
Proposed scenario	3.5 PI-GFDM
	3.6 LP-GFDM
	3.7 LPI-GFDM
	3.8 G-GFDM
	3.9 GN-GFDM
	3.10 GNP-GFDM
	3.11 GNPI-GFDM

3.2 Traditional GFDM with AWGN

In this traditional step, the GFDM system was built with an AWGN channel. The block diagram of this traditional step is shown in Figure (3.2), and the system is simulated based on parameters present in Table (3.2). This traditional step will give the effect of Roll Off Factor (r) on the Pulse Shaping Filter (PSF) behavior and performance. Several mapping orders will test and perform the BER performance. The transmitter and receiver GFDM's block diagrams are presented in Figures (3.3) and (3.4). The first step is to generate a random symbol with length K×M to generate Pseudorandom integers. QAM modulates the generated data with 16 modulation orders and then prepares for GFDM modulation. After that, add the AWGN channel. The receiver is in the same steps as the transmitter but in reverse order.

The general GFDM algorithm for the transmitter and receiver are presented below.

On the transmitter side:

Step one: Reshape the modulated symbol data to size K×M matrix.

Step two: Perform IFFT then Up sampling to N.

Step three: Create the shaping filter G_{N*1} and obtain the shift version

step four: Compute the GFDM modulation as in Equation (2.1).

On the receiver side:

Step one: Taking the FFT to the received signal

Step two: Multiply with the shifting PSF.

Step three: perform the down sampling then accumulate the samples of all sub-carriers.

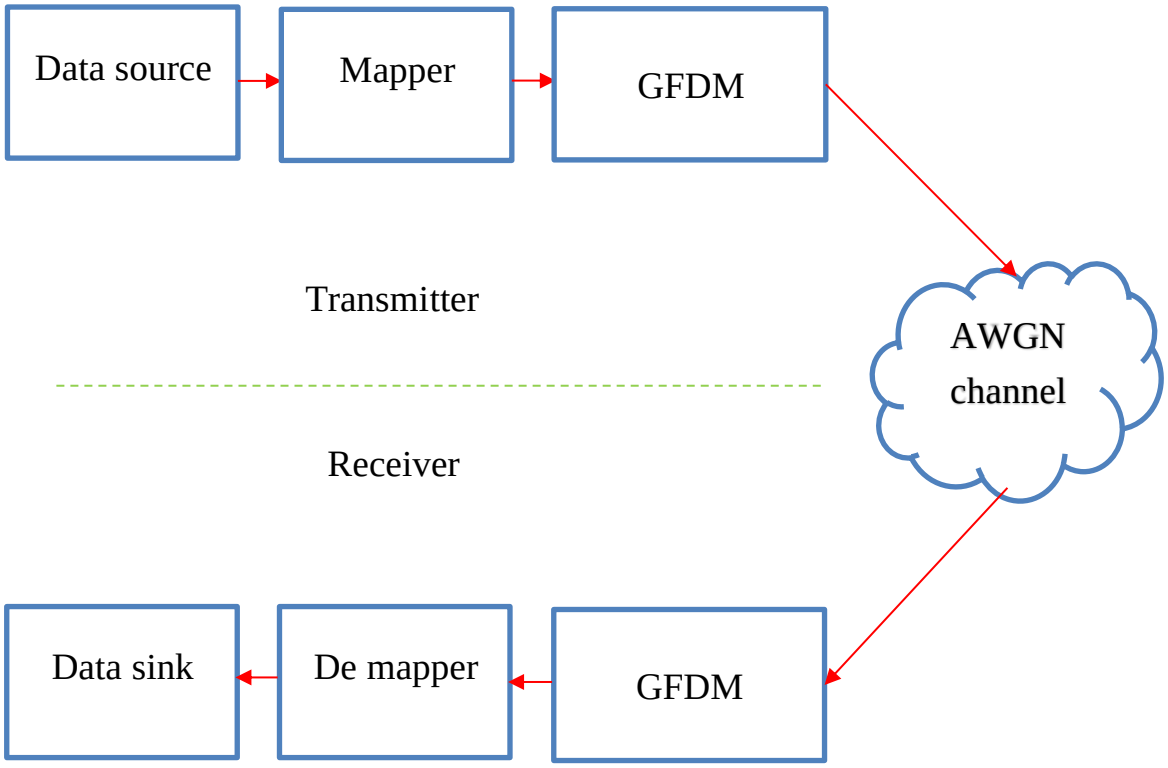

Figure (3.2): General block diagram of traditional GFDM with AWGN

Table (3.2): System parameters of traditional GFDM with AWGN

Symbols	**value**	**Description**
K	20,16	Number of sub-carriers
M	16,15	Number of sub-symbols
r	0.1	Roll off factor of the pulse shaping filter
mu	4	Modulation order of the QAM symbol = 16QAM
SNR	1:3:31	Signal-To-Noise Ratio range
itr	1000	Iteration (number of send blocks)
Channel	Random	AWGN

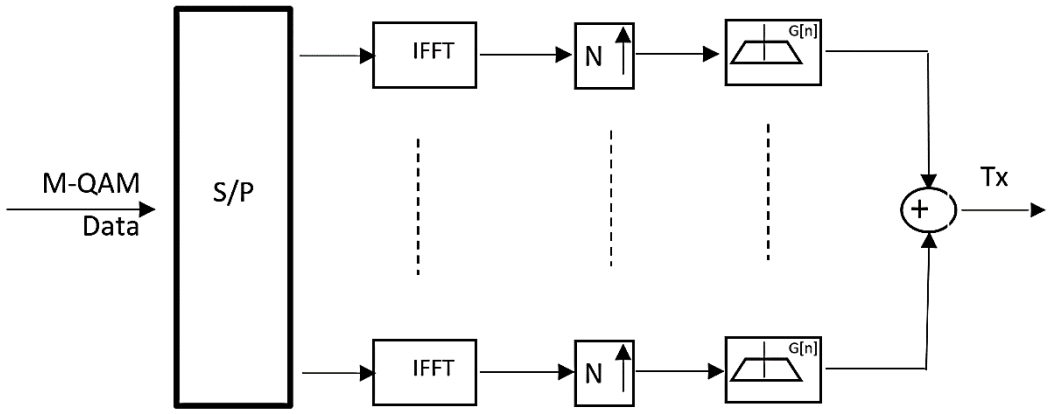

Figure (3.3): The block diagram of the transmitter GFDM.

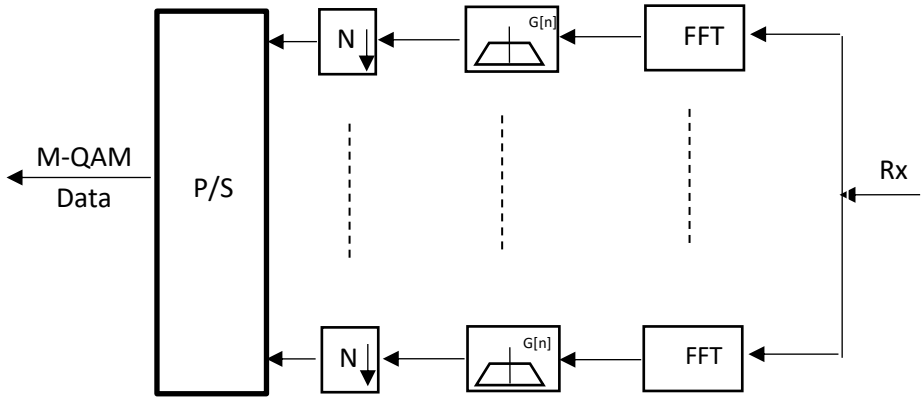

Figure (3.4): The block diagram of the receiver GFDM.

3.3 Traditional GFDM Under Rayleigh Fading Channel

This traditional step built the GFDM system with the number of paths and estimated the channel effect by LS and NLMS methods. The channel estimation is performed based on inserting a pilot signal at the transmitter side and used in the receiver to estimate the channel effect and then perform the equalization. The block diagram of this scenario is shown in Figure (3.5), and the parameters are present in Table (3.3).

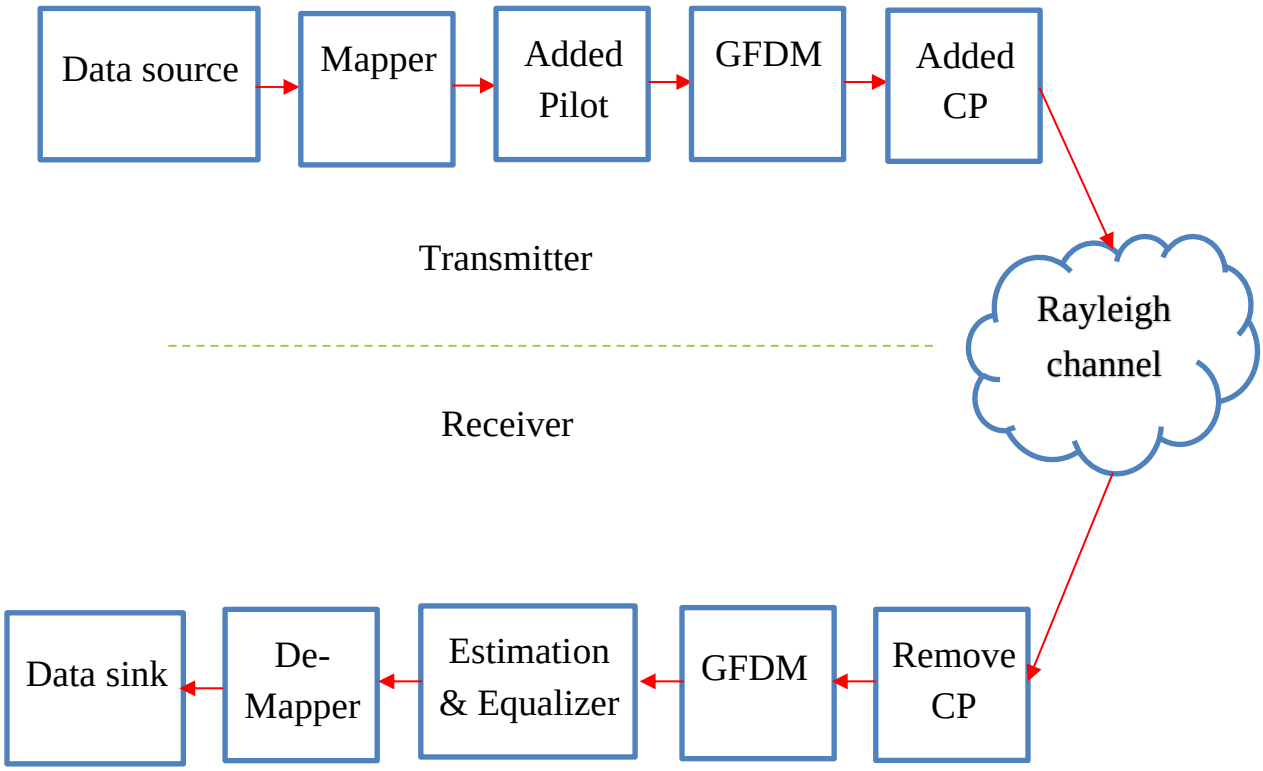

Figure (3.5): Block diagram of Traditional GFDM with multi path channel estimation

Table (3.3): System parameters of traditional GFDM with Rayleigh fading channel.

Symbols	**value**	**Description**
K	20,16	Number of sub-carriers
M	16,15	Number of sub-symbols
CP	0.1	Percentage of cyclic prefix
r	0.1	Roll off factor of the pulse shaping filter
pilot	20%	
Mu	4	Modulation order of the QAM symbol = 16QAM
SNR	1:3:31	SNR range
Channel	random	Rayleigh fading
NP	1,2,3,4	Number of paths (tapes)

3.4 Traditional GFDM with PC and AWGN

In this traditional step added, the PC as a coding system to the GFDM system-based AWGN channel. The block diagram of this traditional system is presented in Figure (3.6). The parameters of this system are shown in Table (3.4).

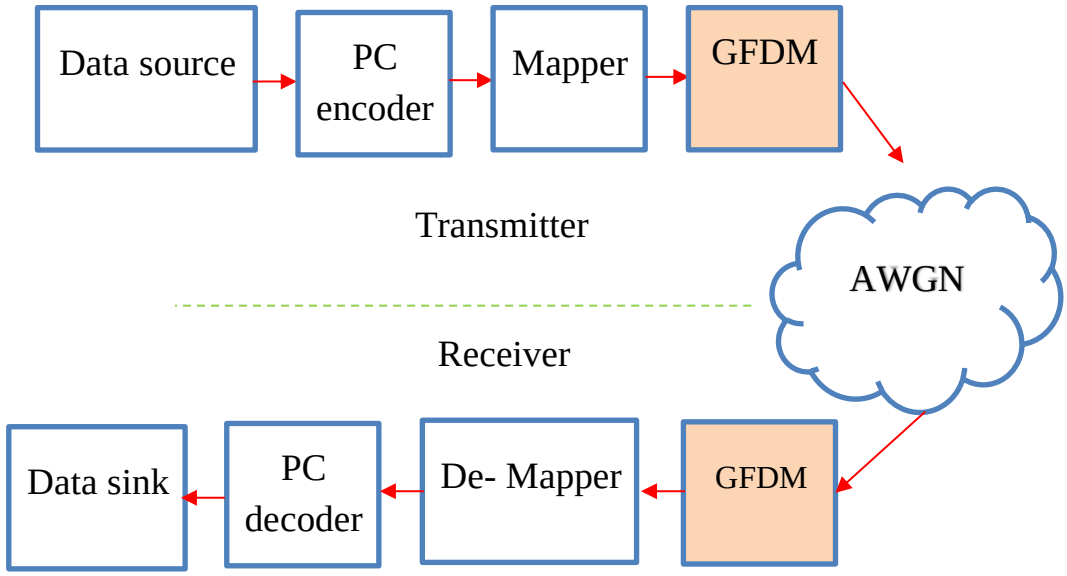

Figure (3.6): General block diagram of GFDM with PC and AWGN.

Table (3.4): System parameters of GFDM with PC and AWGN.

Symbols	value	Description
K	20,16	Number of sub-carriers
M	16,15	Number of sub-symbols
r	0.1	Roll off factor of the PSF
Mu	4	Modulation order of the QAM symbol = 16QAM
PR	$\approx\frac{1}{2}$	PC rate
SNR	1:3:31	SNR range
Channel	random	AWGN

3.5 PI-GFDM Scenario

This section presents scenario-based Polar Code Interleaver-GFDM (PI-GFDM) that combines the PC with the interleaver in one system to enhance the GFDM performance. The PC performs the coding system while the interleaver converts burst error to random error, supporting the PC's performance. The block diagram of PI-GFDM is shown in Figure (3.7). The parameters of this scenario are shown in Table (3.5).

Table (3.5): System parameters of PI-GFDM scenario.

Symbols	value	Description
K	20,16	Number of sub-carriers
M	16,15	Number of sub-symbols
r	0.1	Roll off factor of the pulse shaping filter
Mu	4	Modulation order of the QAM symbol = 16QAM
PR	$\approx\frac{1}{2}$	PC rate
SNR	1:3:31	SNR range
Channel	random	AWGN

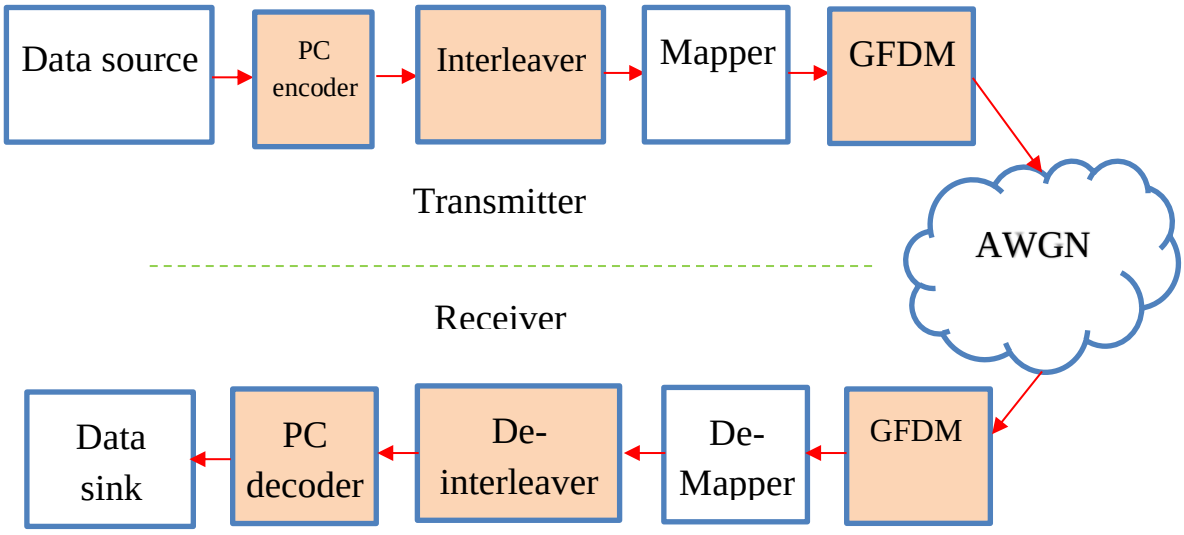

Figure (3.7): General block PI-GFDM scenario.

3.6 LP-GFDM Scenario

This scenario presents a method that uses PC as a coding system for GFDM with LS. Least Square Polar Code GFDM (LP-GFDM) is considered one of the new improvements introduced through several scenarios. Different PC Rate (PR) values are used and choose the best performance. PR the ratio of added redundancy bits to detect and correct the error. The proposed block diagram of this new scenario is shown in Figure (3.8). Table (3.6) presents the simulation parameters of this scenario.

Table (3.6): LP-GFDM scenario system parameters.

Symbols	Value	Description
K	20	Number of sub-carriers
M	16	Number of sub-symbols
CP	0.1	Percentage of cyclic prefix
r	0.1	Roll off factor of the pulse shaping filter
pilot	20%	
mu	4	Modulation order of the QAM symbol = 16QAM
SNR	1:3:31	SNR range
Channel	random	Rayleigh fading channel
NP	2	Number of paths (tapes)
PR	various	PC Rate

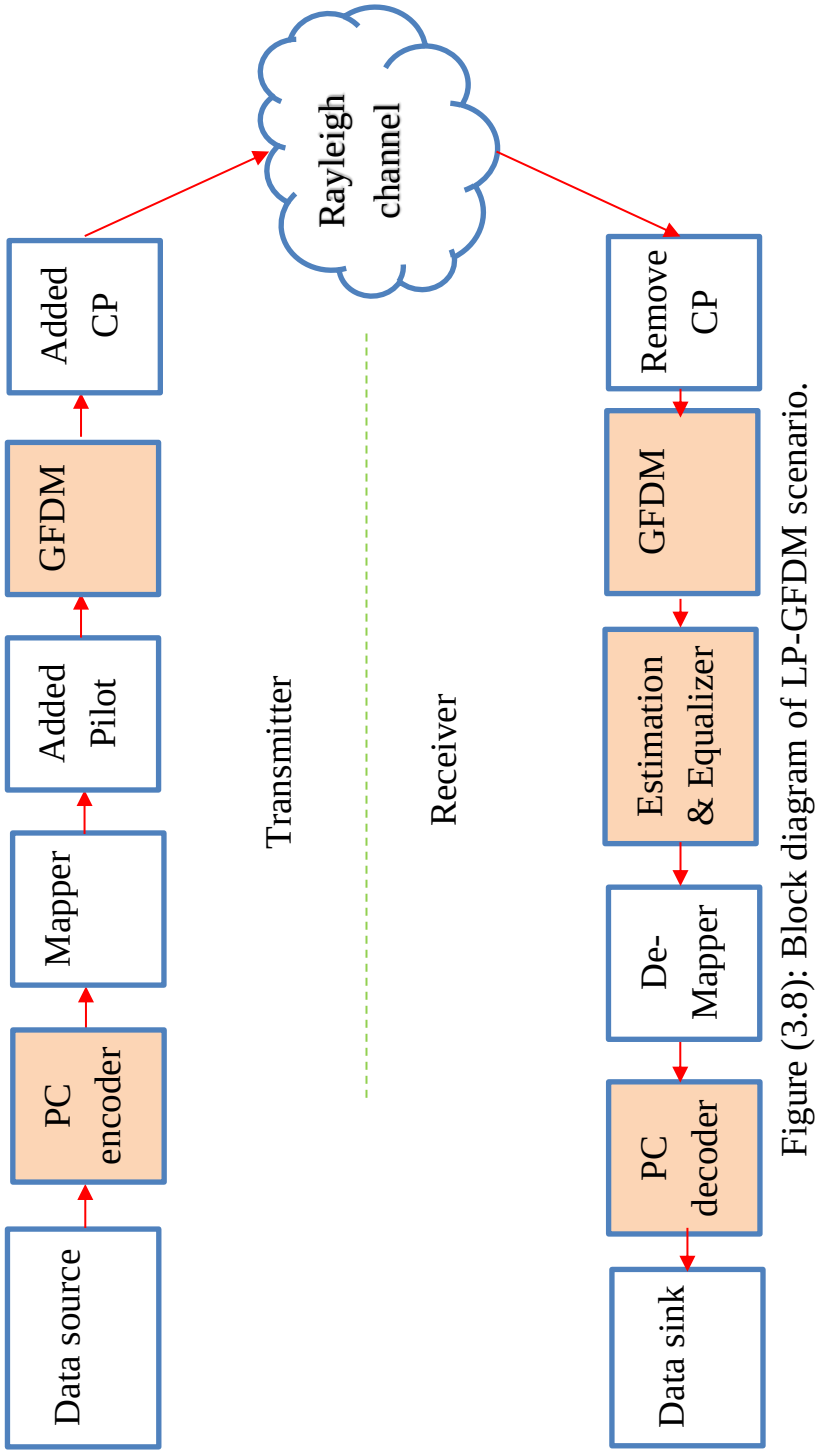

Figure (3.8): Block diagram of LP-GFDM scenario.

3.7LPI-GFDM Scenario

This scenario presents a improvement based adds PC as a coding system with interleaves that test three types: random, matrix, and helical**.** Least Square Polar Code Interleaver GFDM (LPI-GFDM) is a new scenario that compounds the ability to detect and correct the error of the PC and the ability to convert the burst error to a random error; hence reduce the BER of the system. The block diagram of this scenario is shown in Figure (3.9). Table (3.7) presents the simulation parameters of this scenario.

Table (3.7): LPI-GFDM scenario parameters.

Symbols	value	Description
K	20	Number of sub-carriers
M	16	Number of sub-symbols
CP	0.1	Percentage of cyclic prefix
r	0.1	Roll off factor of the pulse shaping filter
pilot	20%	
mu	4	Modulation order of the QAM symbol = 16QAM
SNR	1:3:31	SNR range
Channel	random	Rayleigh fading
NP	2	Number of paths (tapes)
PR	1/3	PC Rate

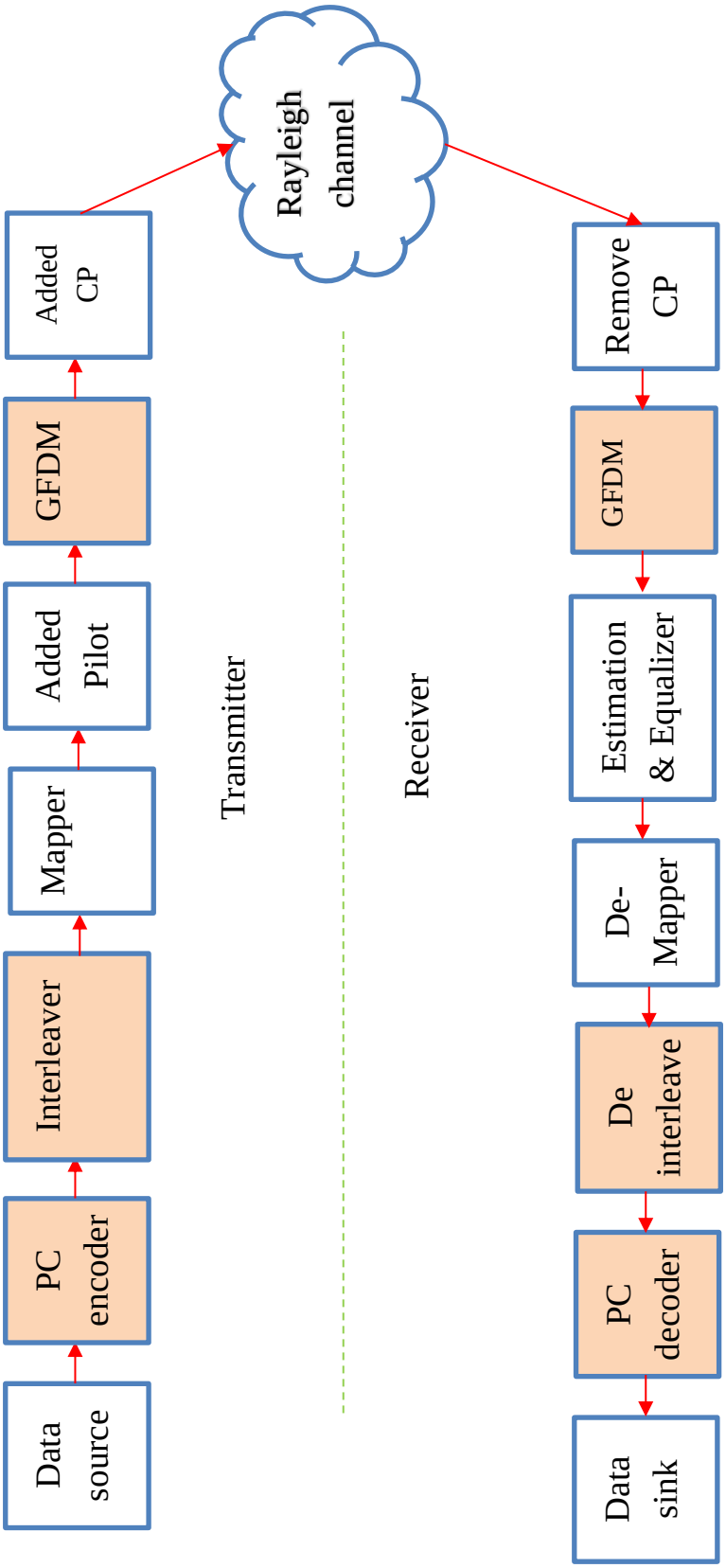

Figure (3.9): Block diagram of LPI-GFDM scenario

3.8G-GFDM Scenario

This scenario presents a new method of enhancing the performance of the GFDM system, its work-based Genetic Algorithm-GFDM (G-GFDM). Its target is the PSF, which is an important part, and considering this scenario is a new idea for enhancing the GFDM. GA performed the optimizing procedure to assign the PSF parameter and used the error between the transmitter and receiver as the cost function. The GA is a search for the best coefficient of PSF based on the initial value performed by a range of searches bounded by limiters values. The block diagram for Optimize-PSF (Op-PSF) is shown in Figure (3.10), which uses the GA used to optimize the PSF to present Op-PSF. Then, this optimized filter is used in the G-GFDM scenario. The block diagram of this scenario is shown in Figure (3.11). The parameters of this scenario are presented in Table (3.8).

Table (3.8): G-GFDM Scenario parameters.

Symbols	**Value**	**Description**
K	20	Number of sub-carriers
M	16	Number of sub-symbols
CP	0.1	Percentage of cyclic prefix
pilot	20%	
SNR	1:3:31	SNR range
Channel	Random	Rayleigh fading

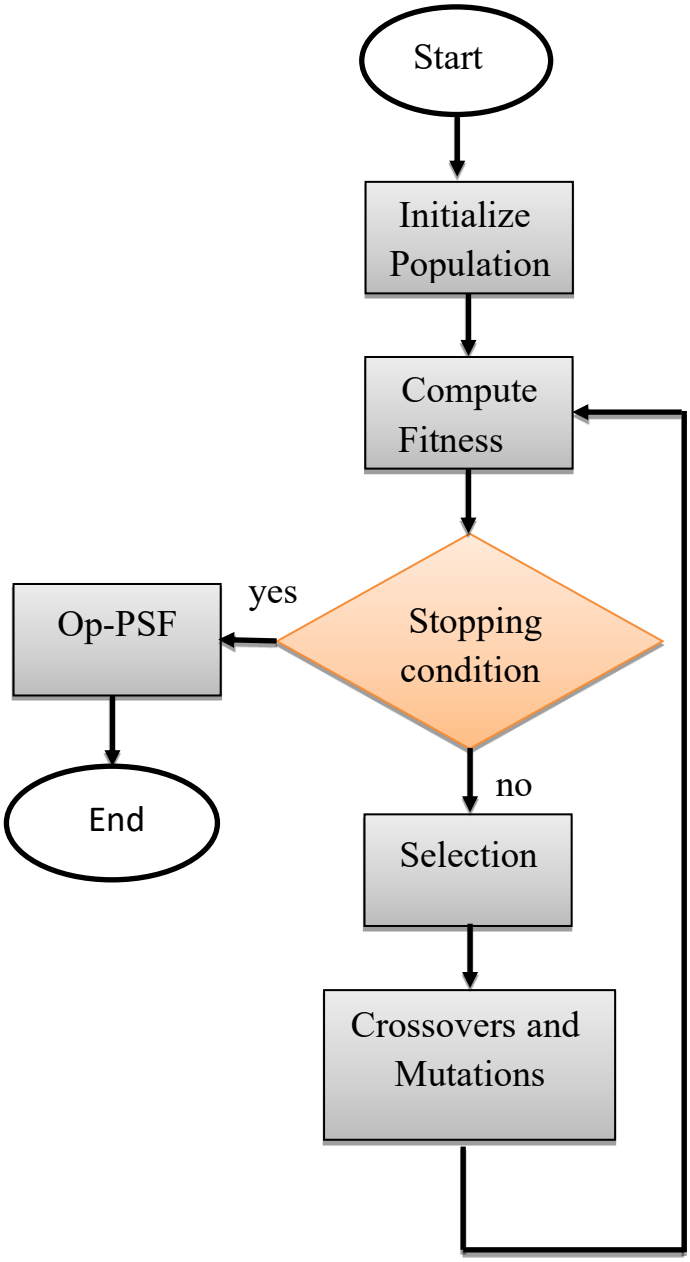

Figure (3.10): Block diagram of GA-PSF.

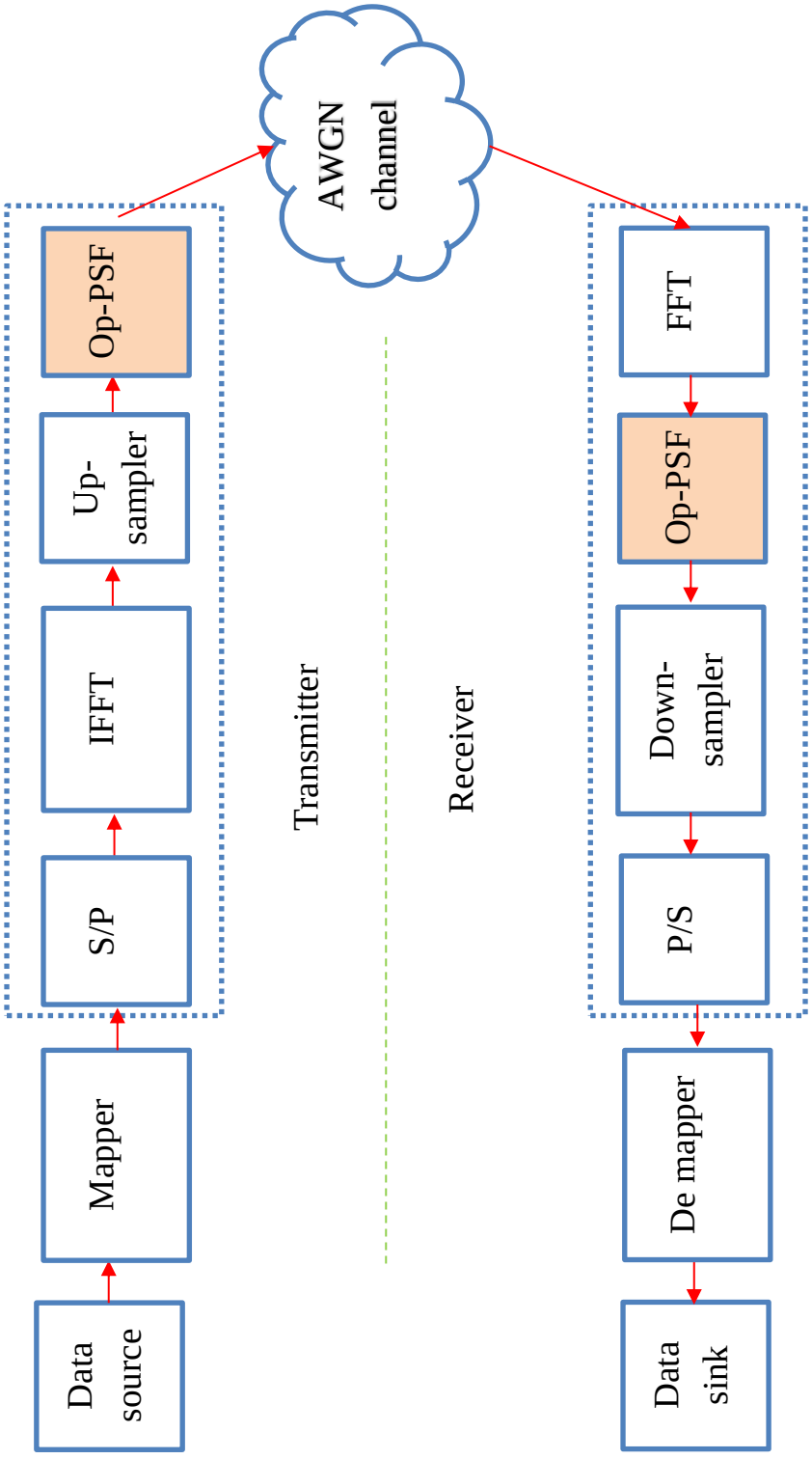

Figure (3.11): Block diagram of G-GFDM Scenario.

3.9GN-GFDM Scenario

This section presents a new scenario-based Genetic Algorithm Artificial Neural Network GFDM (GN-GFDM). It compares it with the Genetic Algorithm Least square GFDM (GL-GFDM), training the ANN as channel estimation with the Op-PSF for the GFDM system under the Rayleigh fading channel. The GA used to get Op-PSF as in Figure (3.10). The estimation-based ANN is performed by, at first, generating dataset-based LS, then using it to train the ANN network with different values of neurons in the hidden layer. The SNR values are assigned at infinity, and when running the system, extract the transmitted pilot, received pilot, and the channel estimation-based LS. These extraction data are used as a dataset to test ANN with different values of neurons and then perform the interpolate function to complete the estimation and equalization process. The block diagram of ANN channel estimation is shown in Figure (3.12). The block diagram of GN-GFDM is shown in Figure (3.13). The simulation parameters of this scenario are presented in Table (3.9).

Table (3.9): GN-GFDM scenario system parameters.

Symbols	value	Description
K	20	Number of sub-carriers
M	16	Number of sub-symbols
CP	0.1	Percentage of cyclic prefix
r	0.1	Roll off factor of the PSF
pilot	20%	
mu	4	Modulation order of the QAM symbol = 16QAM
SNR	1:3:31	SNR range
Channel	random	Rayleigh fading channel
NP	1	Number of paths (tapes)
itr	1000	Iteration (number of send blocks)
Ne	10-35	Number of neurons in hidden layer

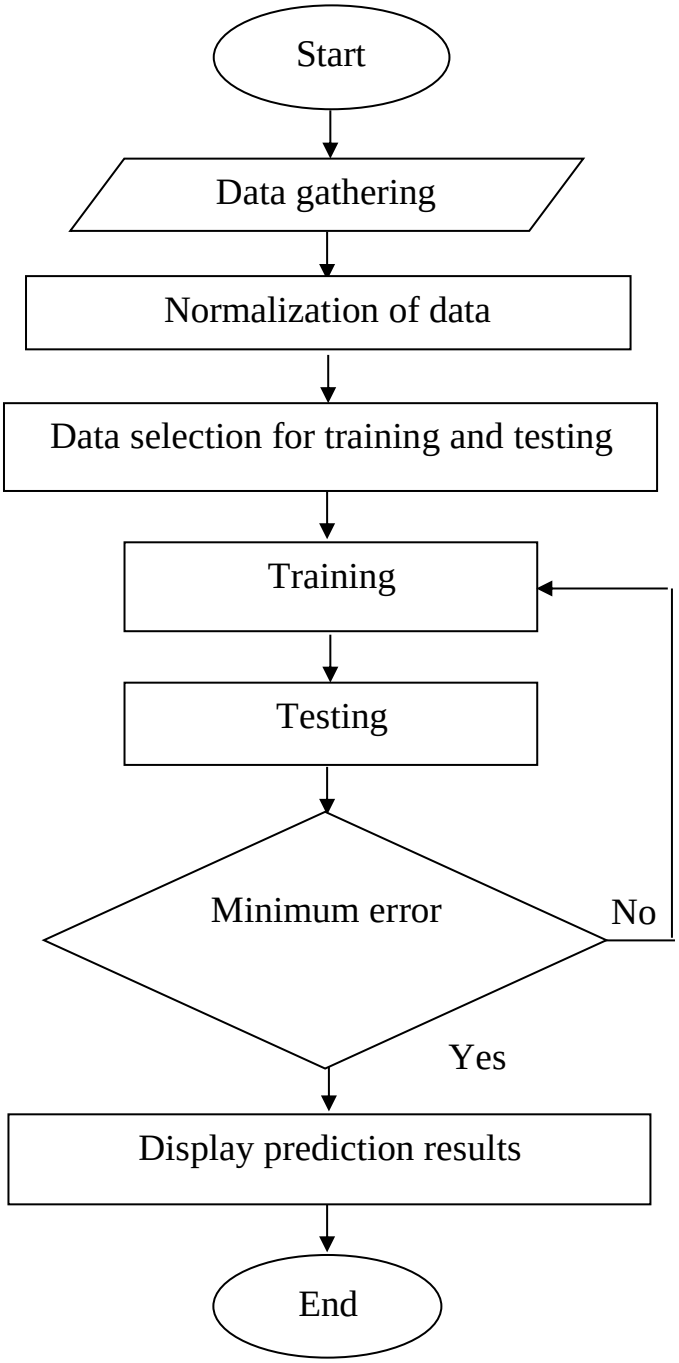

Figure (3.12): Block diagram of ANN channel estimation.

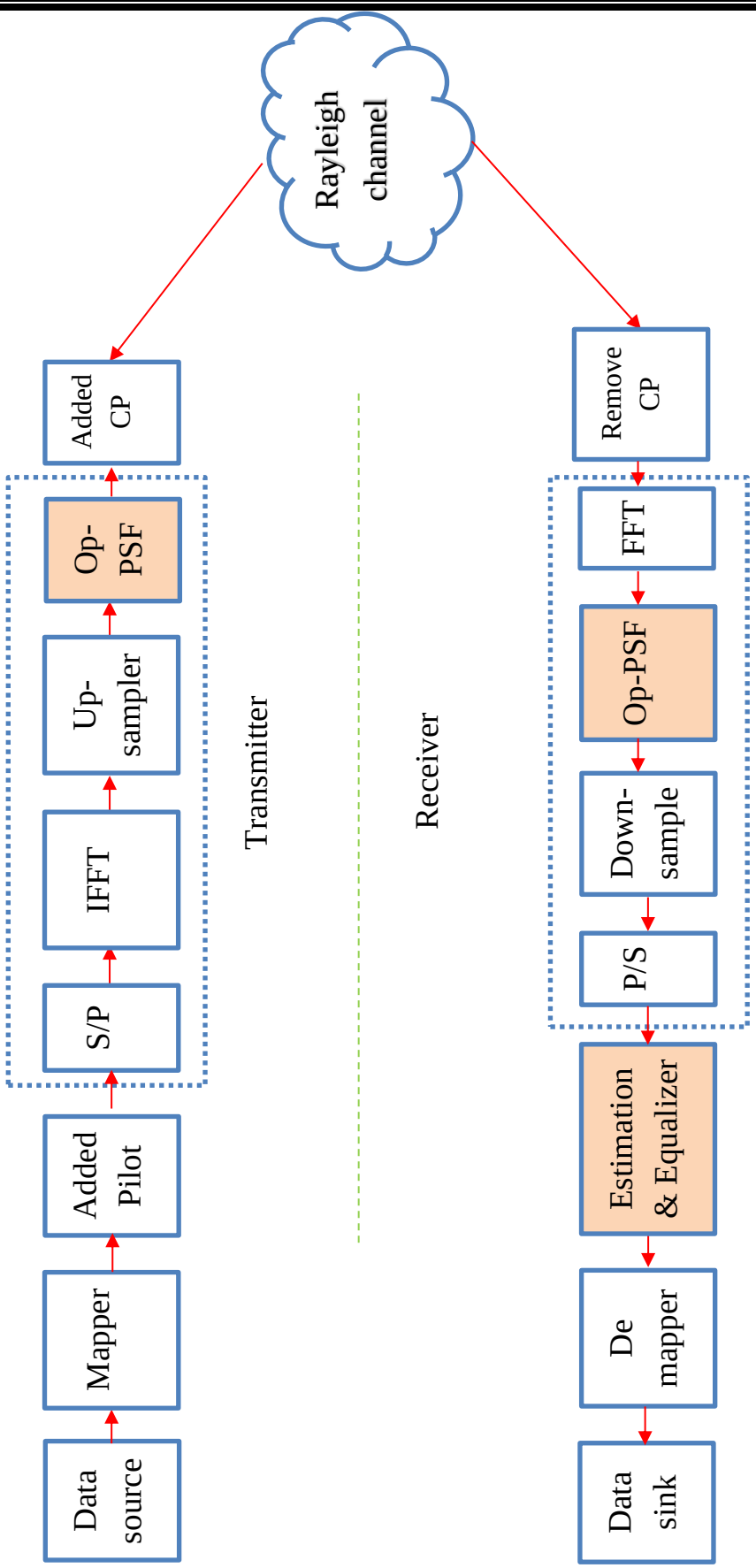

Figure (3.13): Block diagram GN-GFDM.

3.10 GNP-GFDM Scenario

This scenario combines the enhancement-based Genetic Algorithm Artificial Neural Network Polar Code-GFDM (GNP-GFDM) under the Rayleigh fading channel. It compares with the Genetic Algorithm Least Square Polar Code GFDM (GLP-GFDM). This scenario combines three new enhancement methods: the first one is optimizing the PSF by GA, the block diagram shown in Figure (3.10), estimation-based ANN performed by the second step, which is the block diagram shown in Figure (3.12), and applies enhancement-based GA and ANN over the GFDM system-based PC as a coding system. Figure (3.14) presents the block diagram of the GNP-GFDM scenario. Table (3.10) presents the system parameters of this scenario.

Table (3.10): GNP-GFDM scenario system parameters.

Symbols	Value	Description
K	20	Number of sub-carriers
M	16	Number of sub-symbols
CP	0.1	Percentage of cyclic prefix
r	0.1	Roll off factor of the pulse shaping filter
pilot	20%	
mu	4	Modulation order of the QAM symbol = 16QAM
SNR	1:3:31	SNR range
Channel	Random	AWGN
NP	1	Number of paths (tapes)
itr	1000	Iteration (number of send blocks)
Ne	10-35	Number of neurons in hidden layer

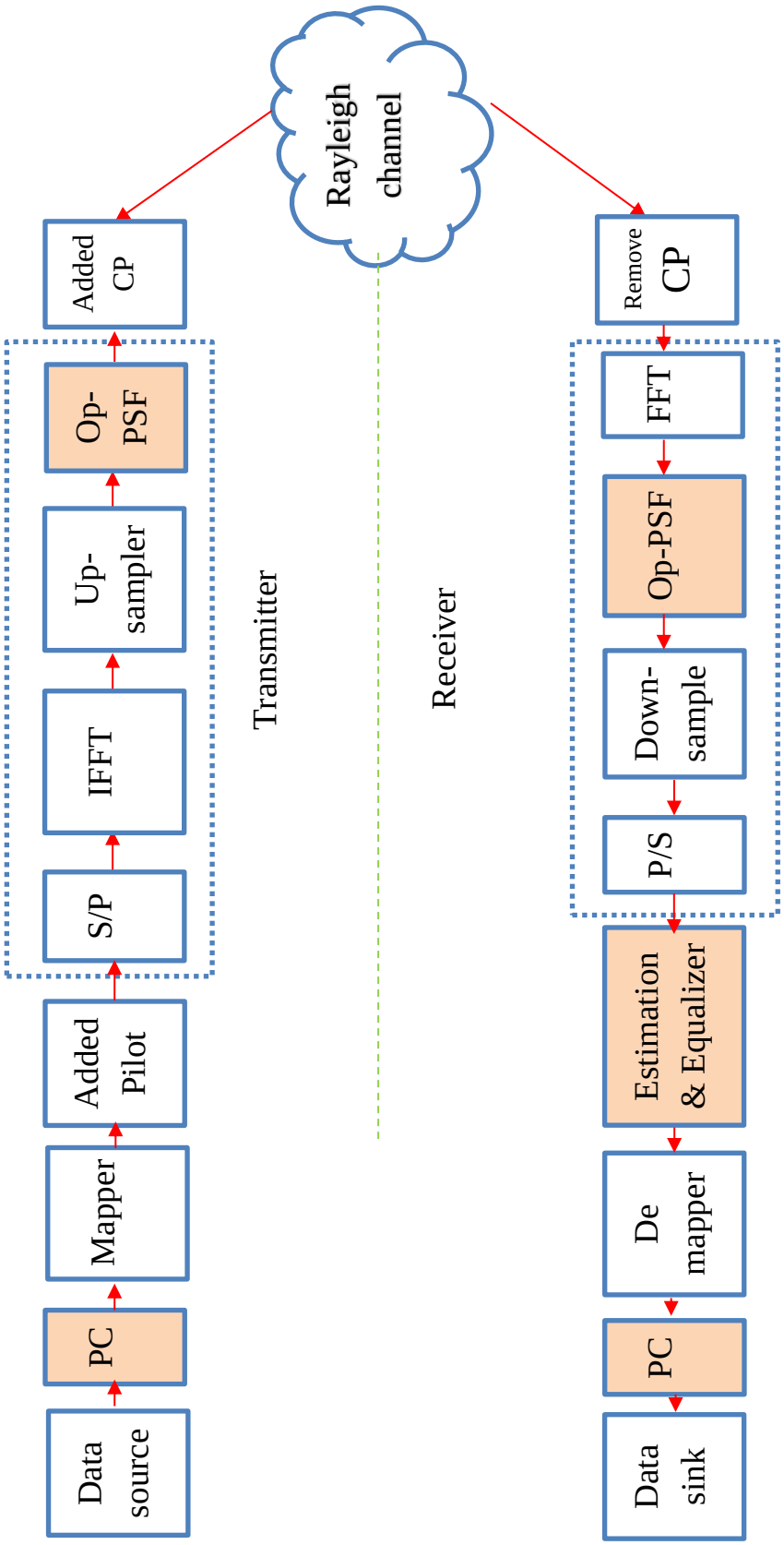

Figure (3.14) Block diagram GNP-GFDM

3.11 GNPI-GFDM Scenario

This section presents a new scenario-based Genetic Algorithm Artificial Neural Network Polar Code interleaver -GFDM (GNPI-GFDM) for developing the GFDM by combining new methods in one system and comparing with the Genetic Algorithm Least Square Polar Code interleaver -GFDM (GLPI-GFDM). This scenario generates Op-PSF by GA and uses ANN as channel estimation. PC and interleaver were added for the proposed system to complete the enhancement. This scenario combines all the last scenarios. The block diagram of Op-PSF is depicted in Figure (3.10), which is derived from the GA. The ANN block diagram is presented in Figure (3.12). The proposed GNPI-GFDM is shown in Figure (3.15). Table (2.11) presents the system parameters of this scenario.

Table (3.11): GNPI-GFDM scenario system parameters.

Symbols	value	Description
K	20	Number of sub-carriers
M	16	Number of sub-symbols
CP	0.1	Percentage of cyclic prefix
r	0.1	Roll off factor of the pulse shaping filter
pilot	20%	
mu	4	Modulation order of the QAM symbol = 16QAM
SNR	1:3:31	SNR range
Channel	random	AWGN
NP	1	Number of paths
Ne	10-35	Number of neurons in hidden layer

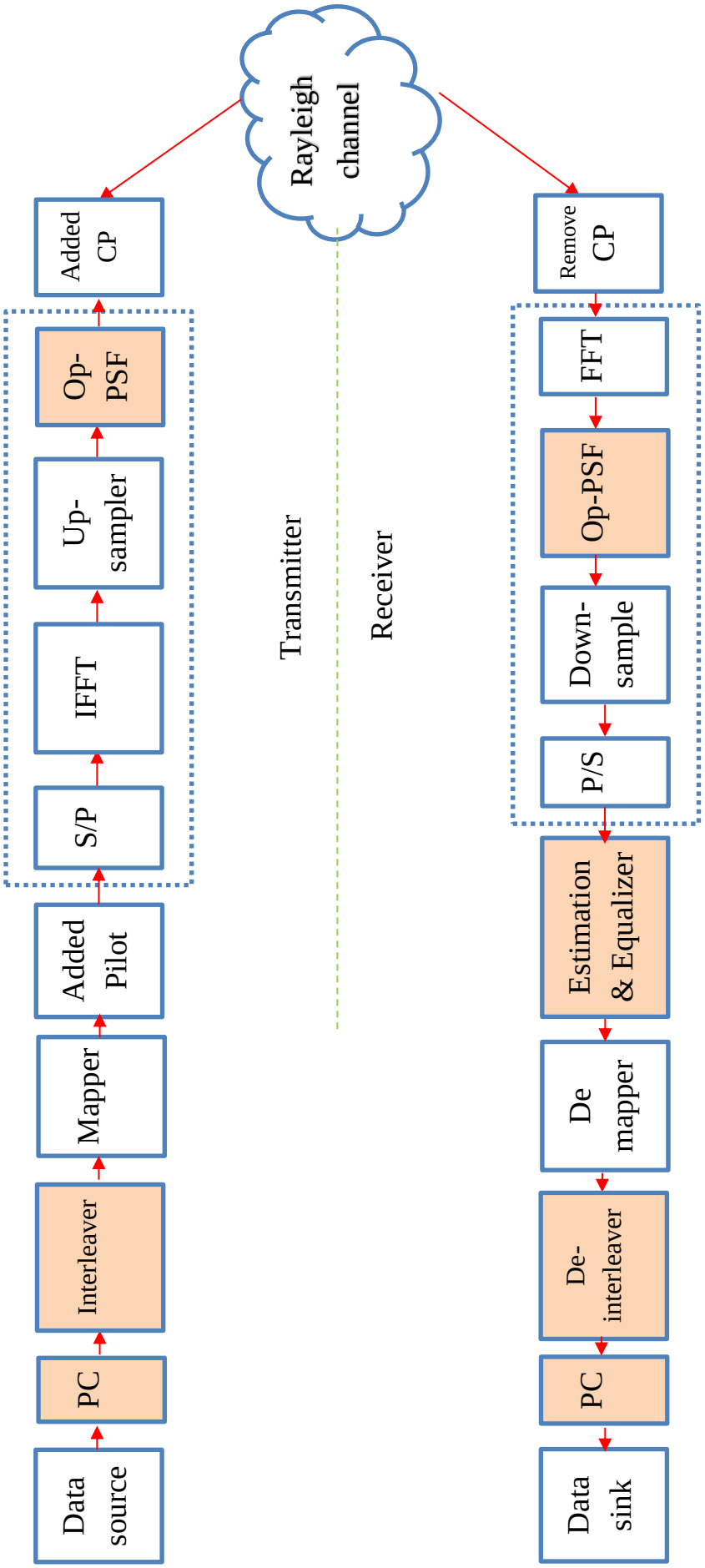

Figure (3.15) Block diagram GNPI-GFDM

CHAPTER Four

Simulation Result

Chapter Four

Simulation Result

4.1Introduction

This chapter presents the simulation result of proposed systems with different scenarios based on GFDM, PC, interleaver, ANN, and GA. as present in Table (3.1), the structure of this chapter first presents the traditional system based on GFDM, channel estimation-based Least Square (LS) and Normalized Least Mean Square (NLMS) and coding system. The seconds present the proposed GFDM system with PC, interleaver, GA, and ANN scenarios. The proposed scenarios present the enhancement of each part based on BER vs. Eb/N0. The enhancement computes based on the difference in BER between the traditional and the proposed cases at the assigned Eb/N0. The simulated result performs based on computer processor properties: 11th Generation, Core i7-11800H and 16GB RAM, using MATLAB 2021b. Some system structures such as the value of K and M were restricted based on these computer properties. The GFDM system is built based on two structures. The first one is K=20, M=16 and the second is K=16, M=15. These two structures are different in performance depending on the PSF behavior, which the second is best. The worst performance is based on the PSF behavior and used to apply proposed enhancement techniques.

4.2 Traditional GFDM with AWGN channel Results

The GFDM system with two structures (K=20, M=16 and K=16, M=15) was built in the AWGN channel. Figure (4.1) shows the impulse response of the PSF with a different value of Roll off factor (r). Figure (4.2) presents the performance under different value of r, which increased when its value

reduced the performance. At 22 dB and K=16, M=15, the BER is 3×10^{-6}, 0.0022, and 0.0026, when r equals 0.1,0.2 and 0.3, respectively. The 0.1 is assigned in all scenarios.

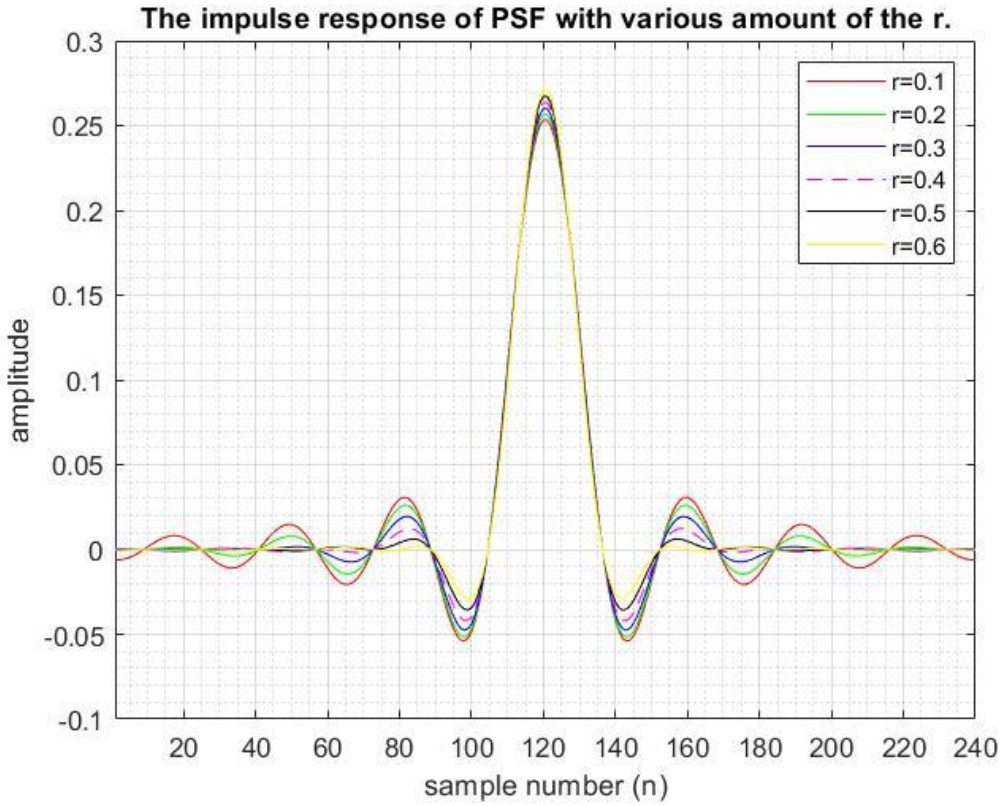

Figure (4.1): The behavior of PSF with various amount of the r.

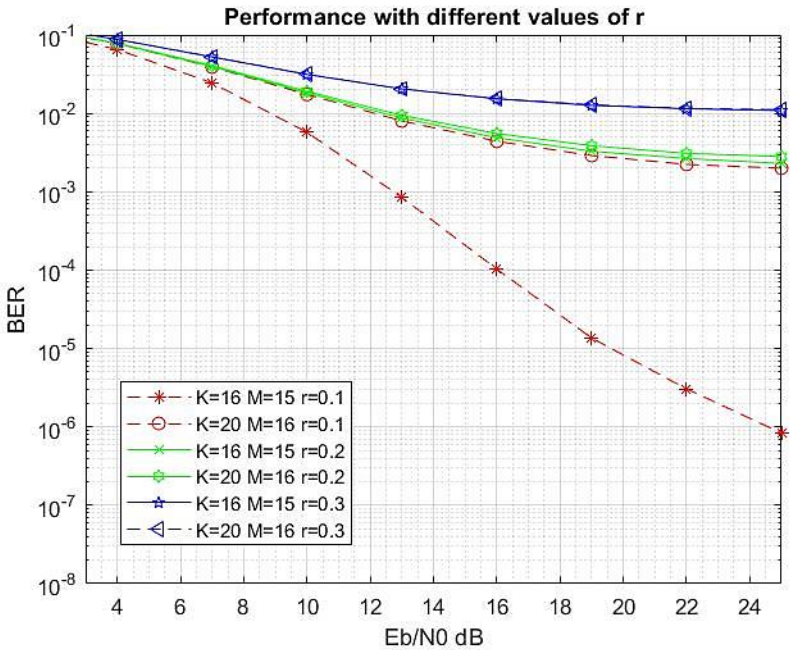

Figure (4.2) Performance with various amount of the r

Figure (4.3) shows the performance of GFDM with mapping order from 2 to 16. As with routine behavior, the performance decreases when increasing the mapping order. Figure (4.4) present the performance comparison between the GFDM and uncoded case. This comparison presents progress in the performance of uncoded over GFDM. At 13 dB, The BER of uncoded, GFDM K16 M15 and GFDM K20 M16 are 2.6×10^{-5}, 0.00084 and 0.0081, respectively.

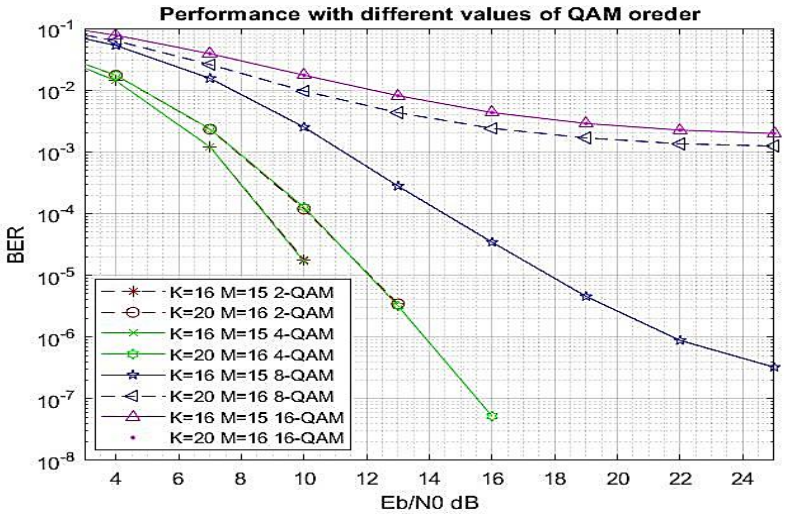

Figure (4.3) Performance with various amount of the QAM order

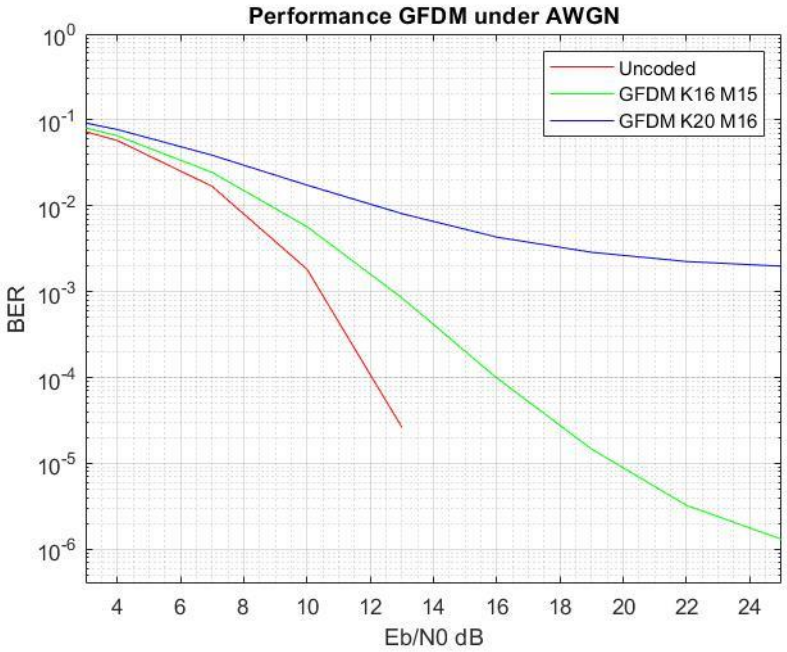

Figure (4.4): The GFDM Performance with 16 QAM.

4.3 Traditional GFDM Under Rayleigh Fading Channel Results

This part applied multipath Rayleigh fading channel and channel estimation for the GFDM system, which presents the LS and NLMS algorithm as channel estimation. Each presents an identical performance, as shown in Figure (4.5). Hence the LS is used in the following scenario. The GFDM test under different numbers of paths. Figure (4.6) present the performance when the number of paths is 1 to 4. When increasing the number of paths, increase the BER. The one path gives a suitable performance which is considered in the following scenarios.

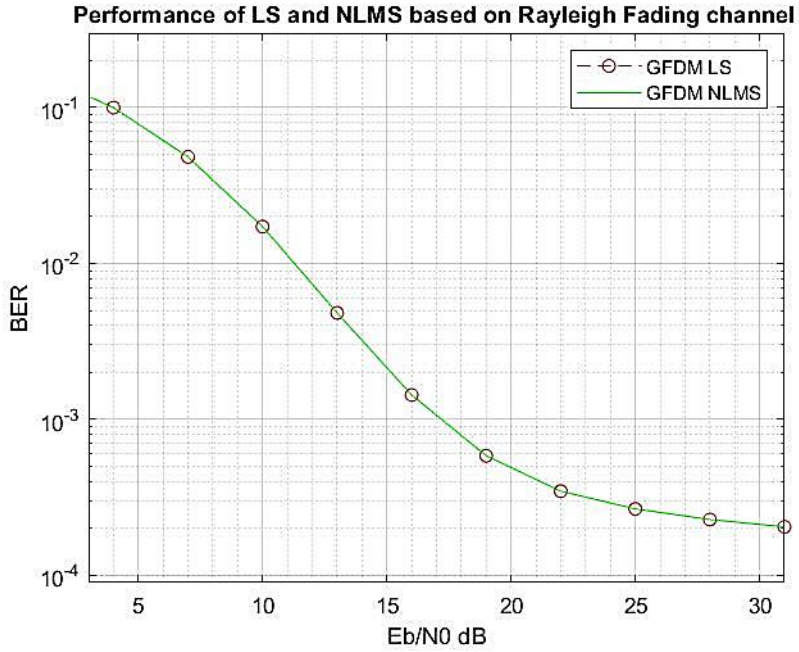

Figure (4.5): Performance of LS and NLMS with one path.

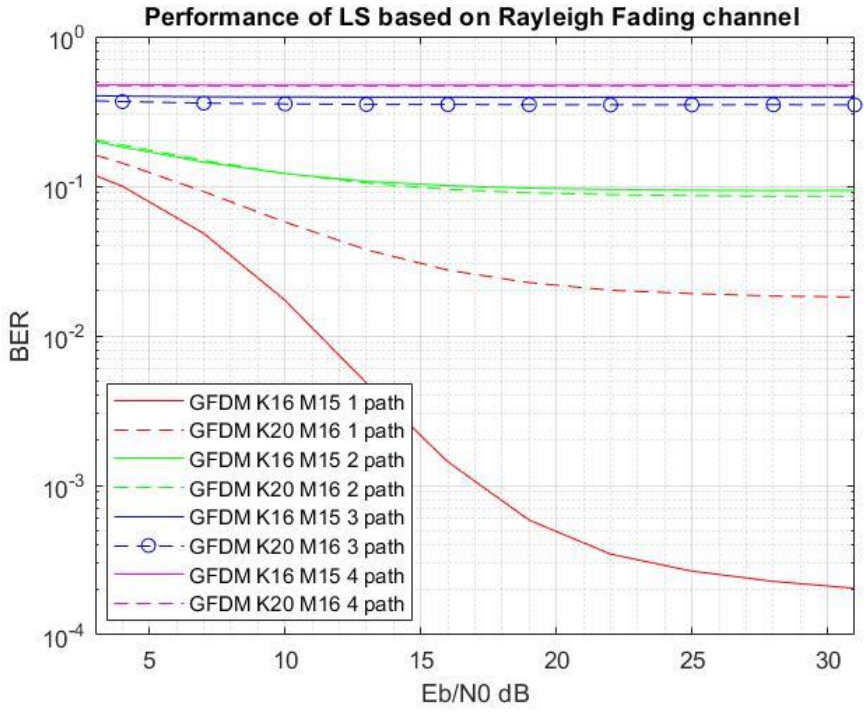

Figure (4.6): GFDM performance-based LS with different paths.

4.4Traditional GFDM with PC and AWGN

This section presented the traditional PC method as a coding system with GFDM. The two structures (K=20 M=16 and K=16 M=15) are used with the PC Rate (PR) approach to $\frac{1}{2}$. The enhancement of this system is present in Figure (4.7). At K=20 and M=16, the PC perform enhancement by 2.5 dB at BER equal 10^{-2}. When the structure the K=16 M=15, the PC present enhancement by 2 dB at 10^{-2} and 3.5 dB at 10^{-3}. Also, the performance of uncoded case present enhancement over GFDM with PC at PR=0.5.

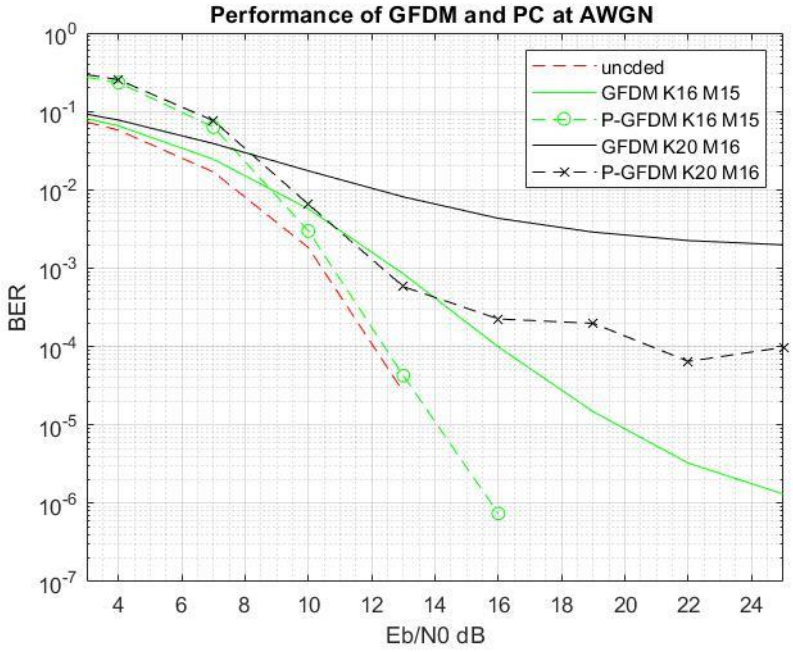

Figure (4.7) GFDM with PC.

4.5PI-GFDM Scenario Results

This section presents the Polar Code Interleaver GFDM (PI-GFDM), a enhancement scenario of the GFDM-based combined PC with interleaver methods. The scattering in bits location provided by the interleaver helped the coding system in enhancement and reduced the error. Figure (4.8) and Figure (4.9) present the effect of interleaver methods on two structures of GFDM.

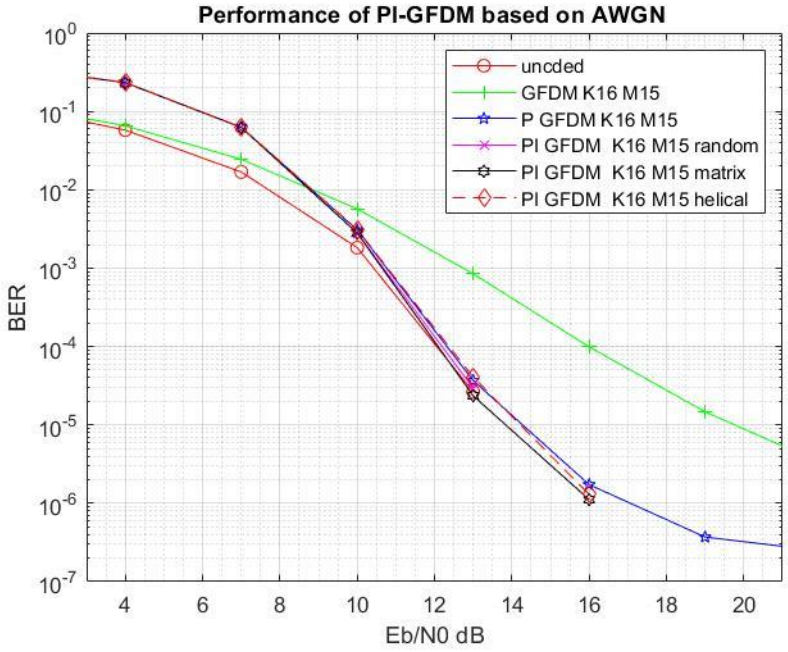

Figure (4.8): PI GFDM scenario based K16 M15.

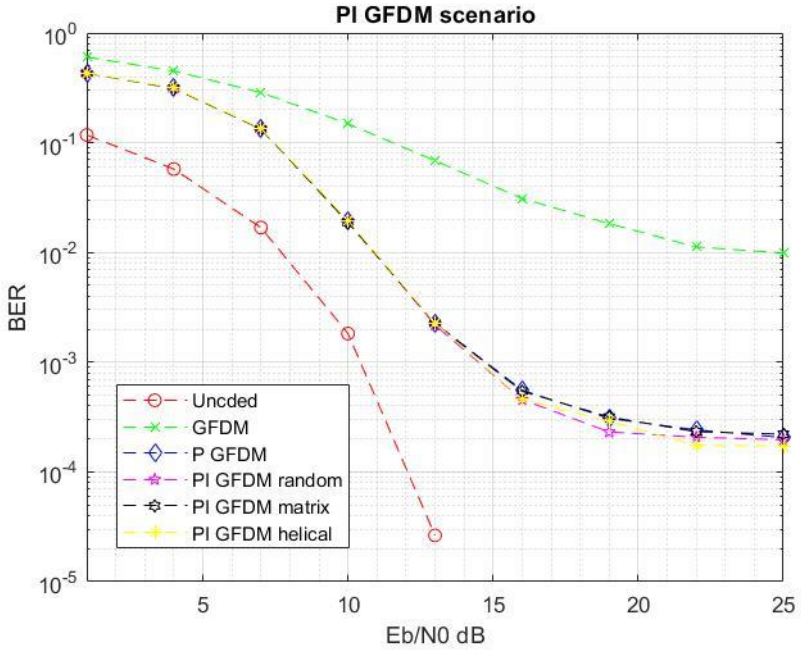

Figure (4.9): PI GFDM scenario based K20 M16.

Figure (4.8) presents the structure K16 M15; at 13 dB, the enhancement by adding PC is 2dB and 3.5 dB at BER 10^{-2} and 10^{-3} respectively. When adding the interleaves methods, its effect is neglect at AWGN due to not found burst error. Figure (4.9) presents the

performance at structure K=20, M=16. The PC presents enhancement by 4 dB at BER 10^{-1}. when used interleaver the enhancement is very little and therefore can be neglected.

4.6 LP-GFDM Scenario Results

The proposed Least Square Polar Code-GFDM (LP-GFDM) scenario performs based (K20, M16) and the addition of the PC as a coding system to the GFDM with LS as channel estimation. Figure (4.10) presents the performance with different PR values. The used PR is: $\frac{1}{3},\frac{1}{2},\frac{2}{3},\frac{3}{4}$. The enhanced performance gets when the PR approach of $\frac{1}{3}$. The PC effect with rate $\frac{1}{3}$ appears after 10.5 dB in enhancing BER. With PR =$\frac{1}{3}$ and BER= 0.03 the enhancement is 1.5 dB.

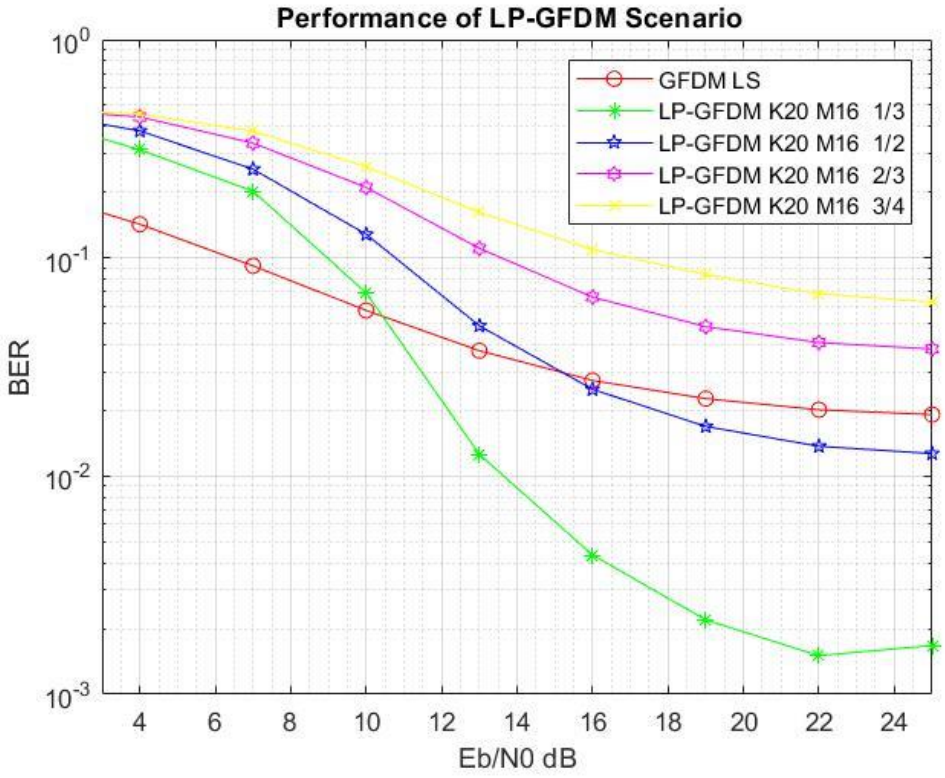

Figure (4.10) GFDM performance with PC.

4.7 LPI-GFDM Scenario Results

This proposed Least Square Polar Code Interleaver GFDM (LPI-GFDM) scenario that presents the effect of PC and interleaver on the GFDM system (K20, M16), shown in Figure (4.11). They use random, matrix, and helical interleaver to present the system's performance. All three types of interleaver present enhancement with different values. The random and helical interleaver overcome the matrix in all the range of Eb/No. the random helical interleaver present enhancement approach to 1.5 dB at 1×10^{-3}. The enhancement of matrix is very little and therefore can be neglected. Random interleaver has been assigned in the following scenarios based on the enhancement of random interleaver.

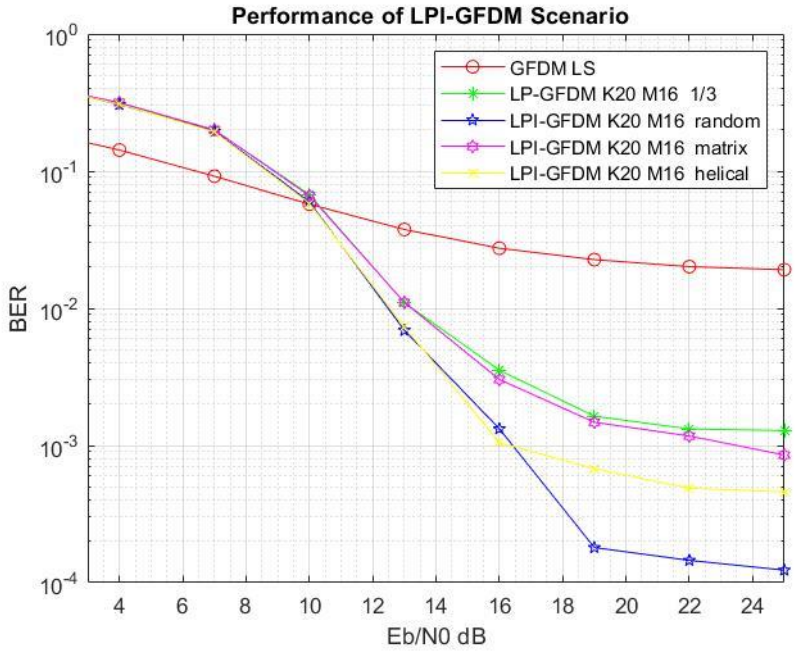

Figure (4.11): performance-based LPI-GFDM.

4.8 G-GFDM Scenario Results

This section added a scenario-based Genetic Algorithm-GFDM (G-GFDM) to optimize the GFDM-based internal improvement, which used the GA to optimize the PSF by searching about the based PSF coefficient, reducing the BER for SNR. The error is the cost function, and the GA worked based on optimizing the performance. The search range of GA is bounded by the upper and lower PSF presented in Equations (2.3). The Optimized PSF (Op-PSF) with St-PSF is shown in Figure (4.12). The Standard- PSF (St-PSF) and Op-PSF-based AWGN channel-based GFDM (K20, M16) are shown in Figure (4.13), while Figure (4.14) presents the behavior-based Rayleigh fading channel.

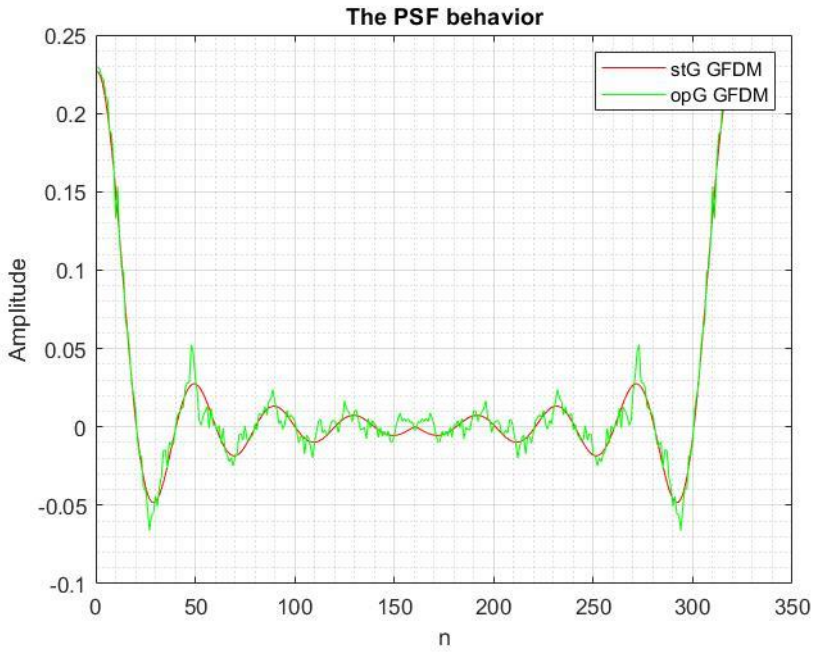

Figure (4.12): The impulse response of PSF.

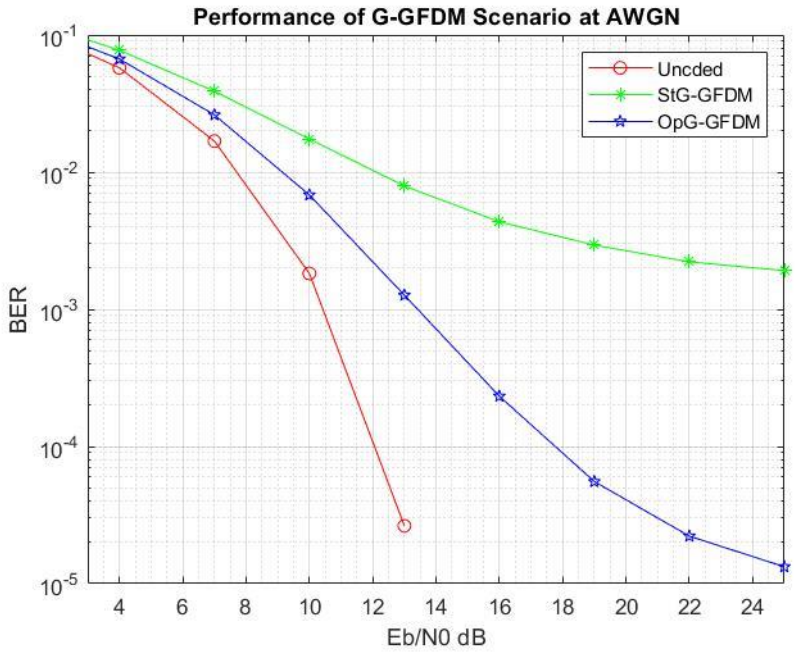

Figure (4.13) The performance of the G-GFDM scenario at the AWGN channel.

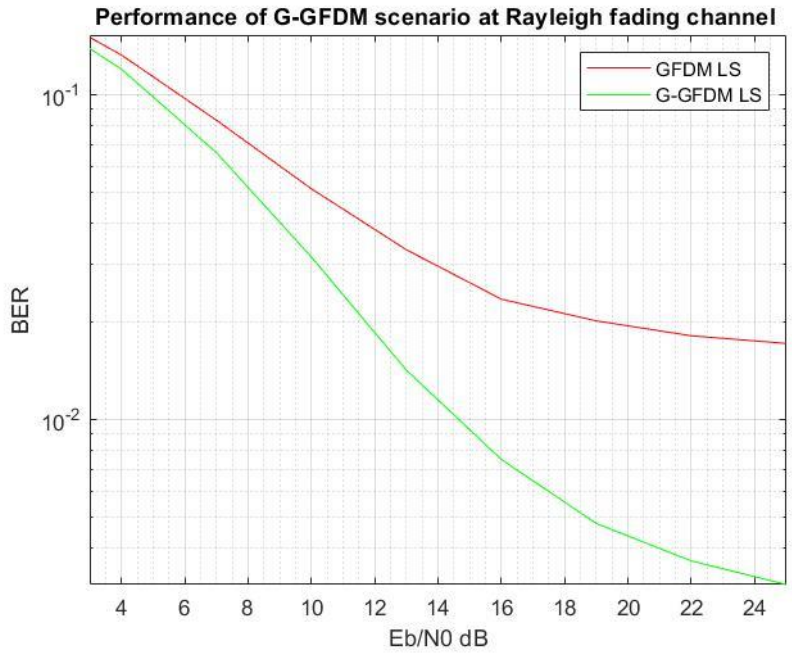

Figure (4.14): The performance of the G-GFDM scenario at the Rayleigh fading channel.

4.9GN-GFDM Scenario Results

This scenario is based on the Genetic Algorithm Artificial Neural Network GFDM (GN-GFDM) and compared with the Genetic Algorithm Least square GFDM (GL-GFDM), which used ANN as channel estimation based on LS with GA to improve the PSF. The system at first performs the estimation-based LS to generate a dataset. This data contains the transmitted and received pilot with channel response. The transmitted and received pilot considered input to train the ANN, while the channel response is desired for the training. The dataset used to train the ANN by three methods: LM, BR, and SCG, with a range of neurons in the hidden layer. Figure (4.15 a) presents the ANN structure with input, output, and hidden layer. Figure (4.15 b) shows the progress of SCG training performance over the epochs and presents the stopping point at best performance training.

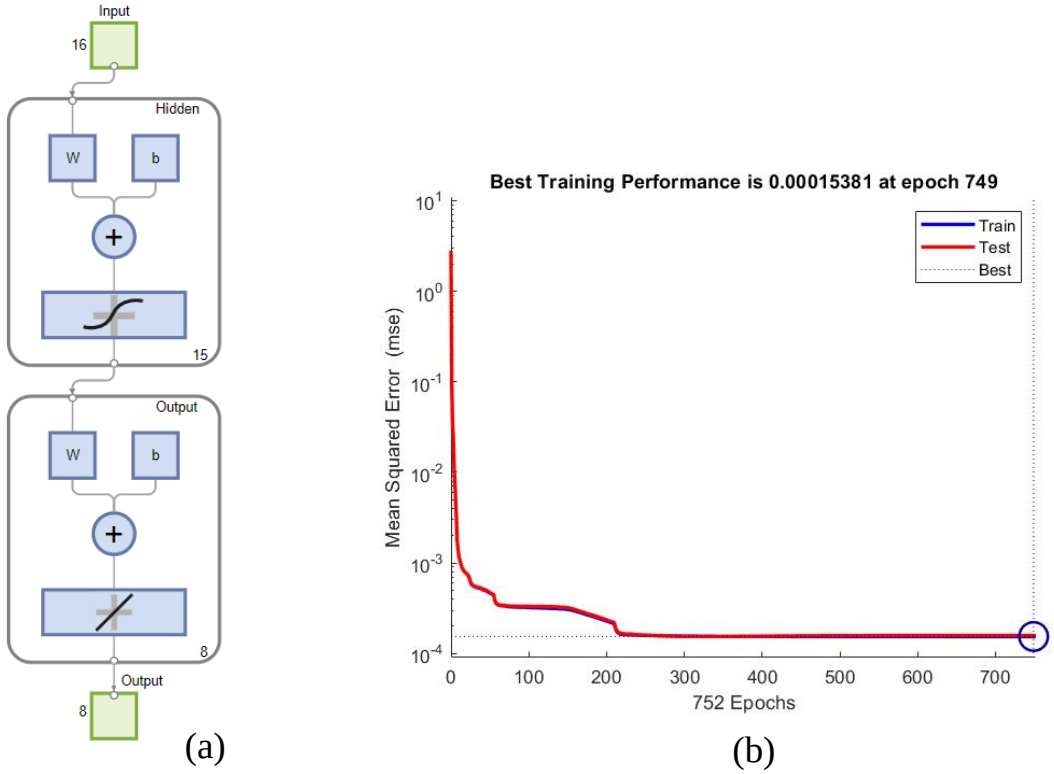

Figure (4.15): (a) ANN structure. (b)Best training results.

Based on the dataset that generated based LS estimation. The dataset was trained with different values of neurons in the hidden layer. Neural network fitting applications are used to train to assign the best performance with the number of neurons and type of training. LM, BR, and SCG are used as training methods. Figure (4.16) shows the performance comparison between GN-GFDM at 13 neurons with G-GFDM and traditional GFDM. This figure presents enhancement of LM method by 0.5dB at BER equal 10^{-2}. The LM and BR give similar performance. The SCG present inability in overcome the standard LS.

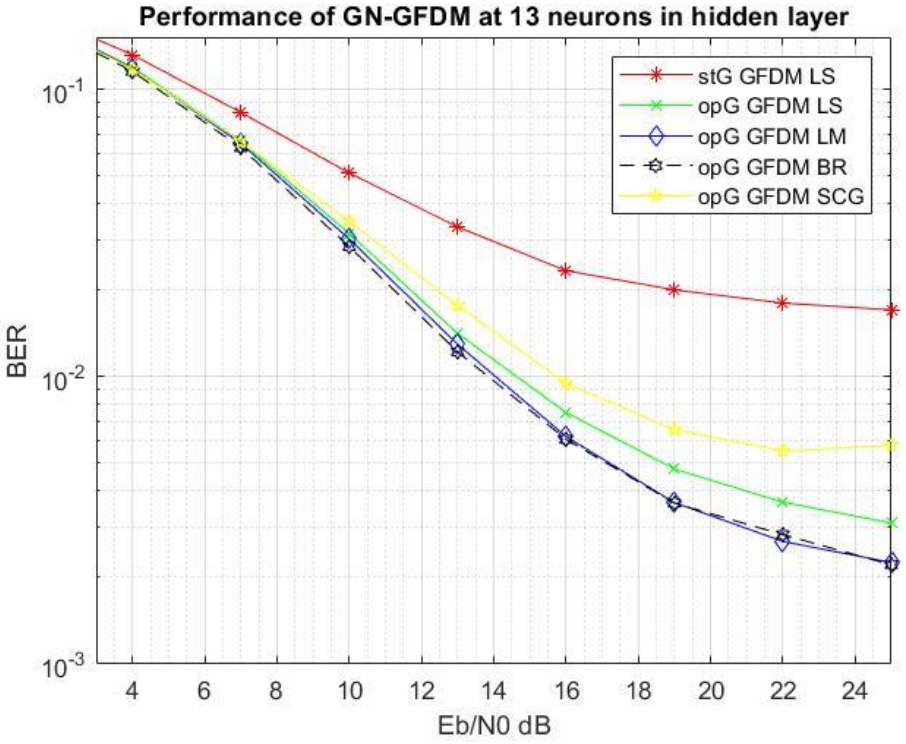

Figure (4.16) GN-GFDM performance at 13 neurons.

Figure (4.17) shows the performance with 14 neurons which the SCG method present enhancement by 1dB at 10^{-2} while the LM present 0.5dB at 10^{-2}. Figure (4.18-20) show the performance with 15-17 neurons which the SCG method present enhancement by 1dB at 10^{-2} while the LM present less than GLP. The enhancement in Figure (4.17) is low and neglect hence the SCG method with 16 neurons is the best performance under GN-GFDM scenario.

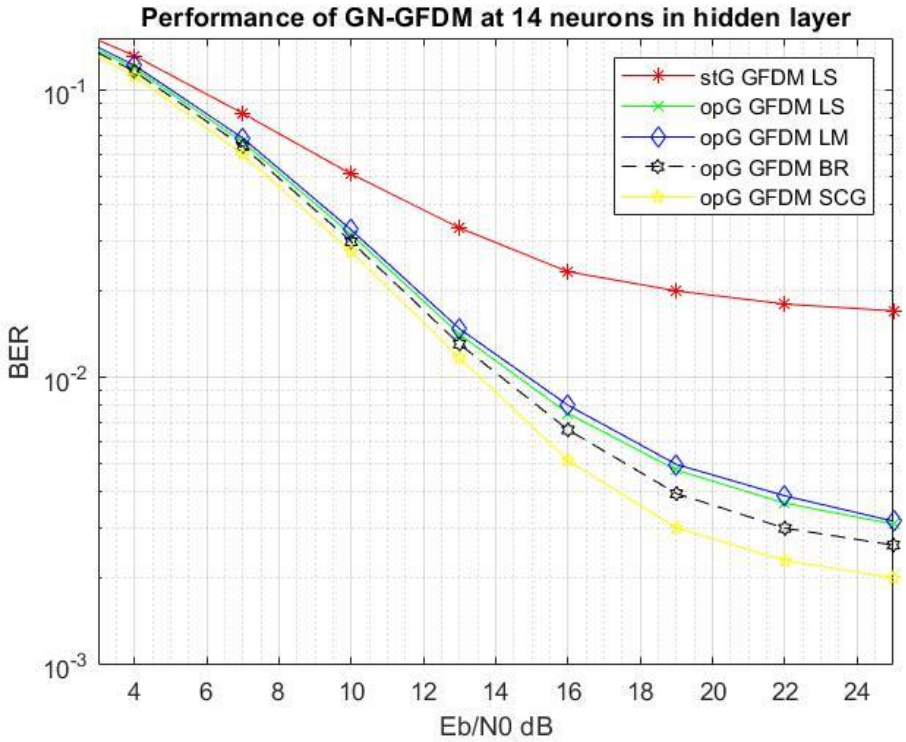

Figure (4.17) GN-GFDM performance at 14 neurons.

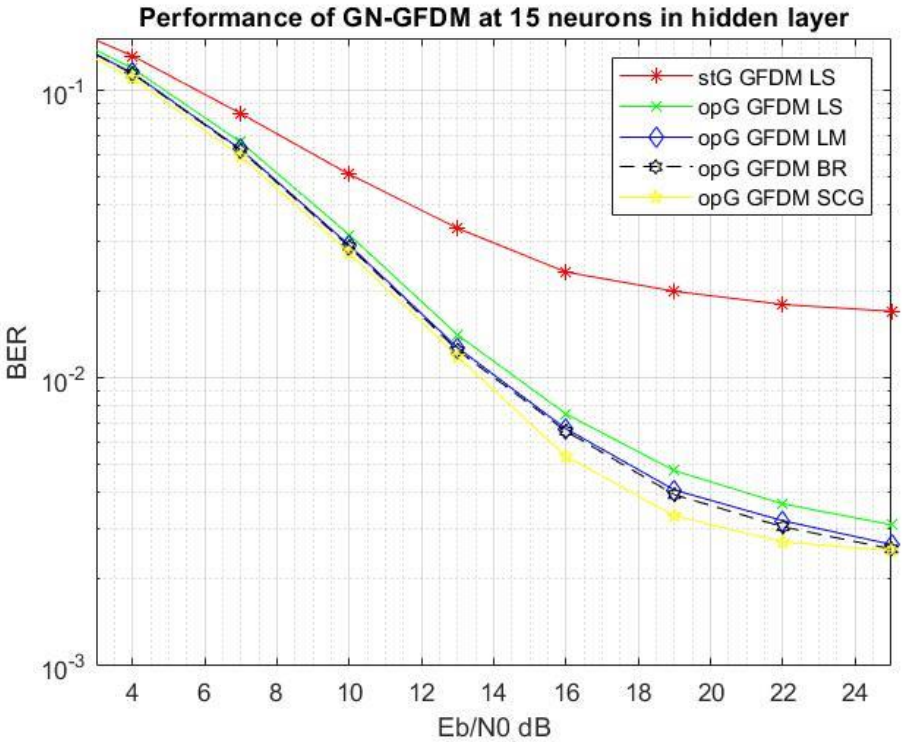

Figure (4.18) GN-GFDM performance at 15 neurons.

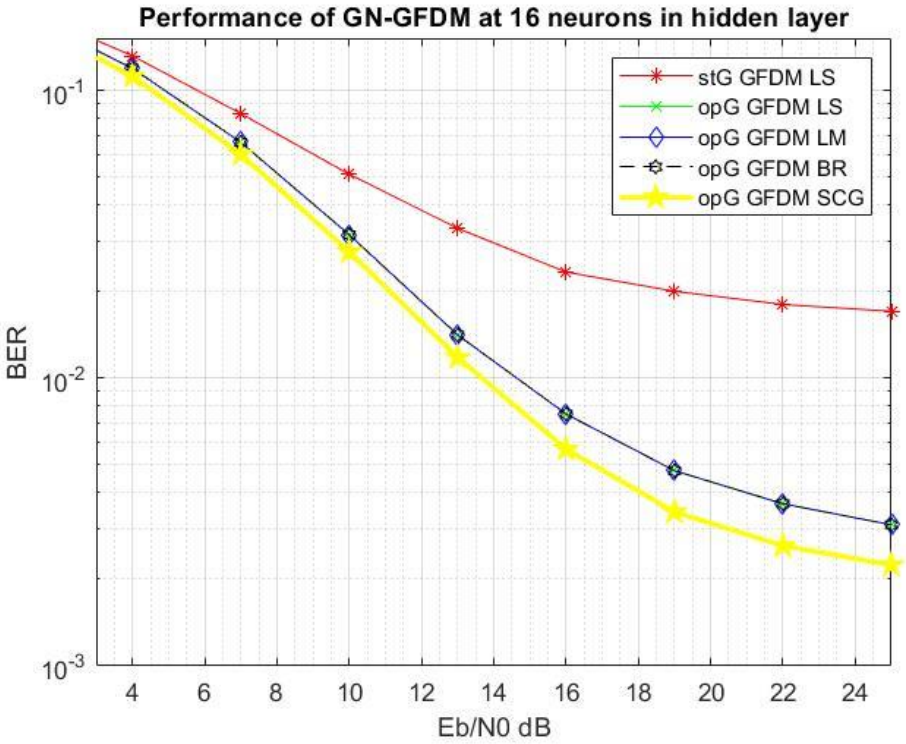

Figure (4.19) GN-GFDM performance at 16 neurons.

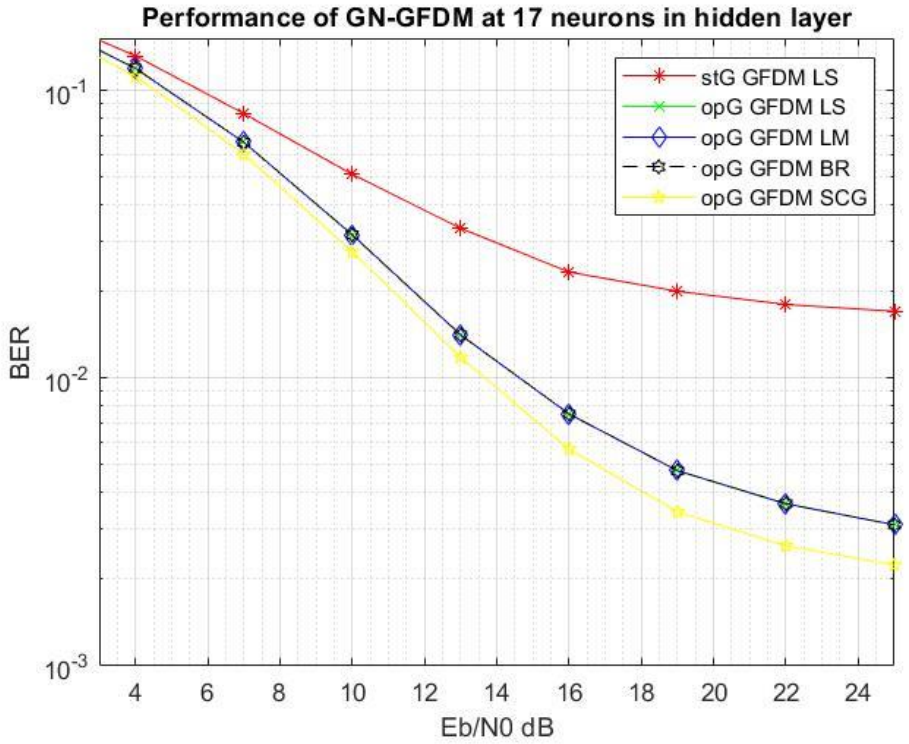

Figure (4.20) GN-GFDM performance at 17 neurons.

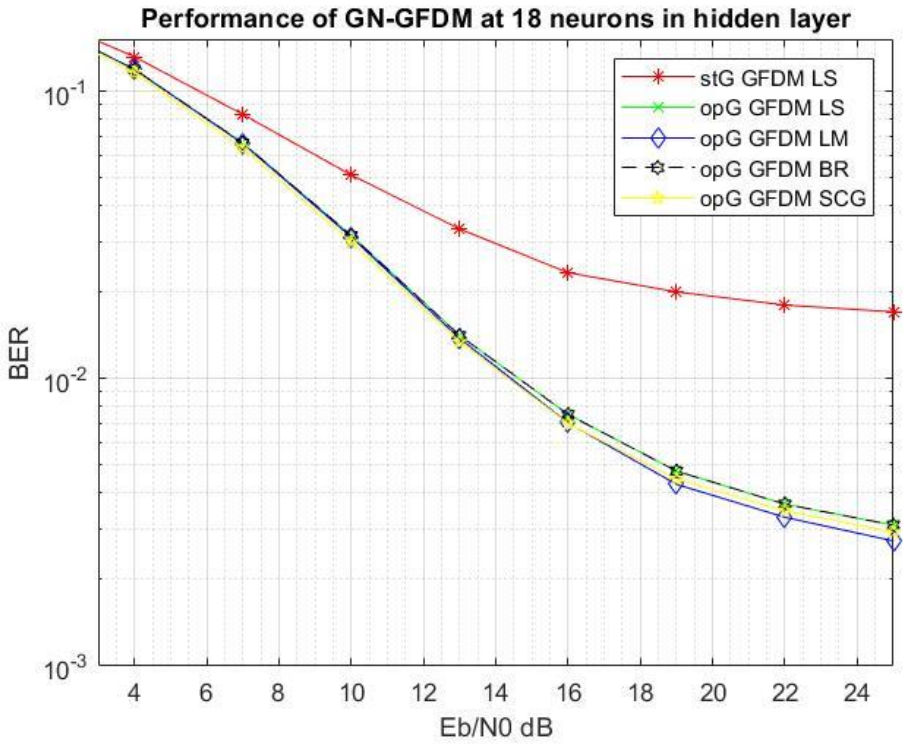

Figure (4.21) GN-GFDM performance at 18 neurons.

4.10 GNP-GFDM Scenario Results

This scenario is presented based on the added PC as a coding system to the GN-GFDM to get the Genetic Algorithm Artificial Neural Network Polar Code-GFDM (GNP-GFDM) scenario and also compare with the Genetic Algorithm Least Square Polar Code-GFDM (GLP-GFDM). The ANN is used as channel estimation. Neural network fitting applications with various numbers of neurons perform the estimation-based LS dataset and compare it with traditional GFDM-LS. The PC added and presented enhancement after 14 dB and degradation before 14dB, as present in the following results. Figures (4.22-24) presents the GNP-GFDM scenario with 12-14 neurons in a hidden layer.

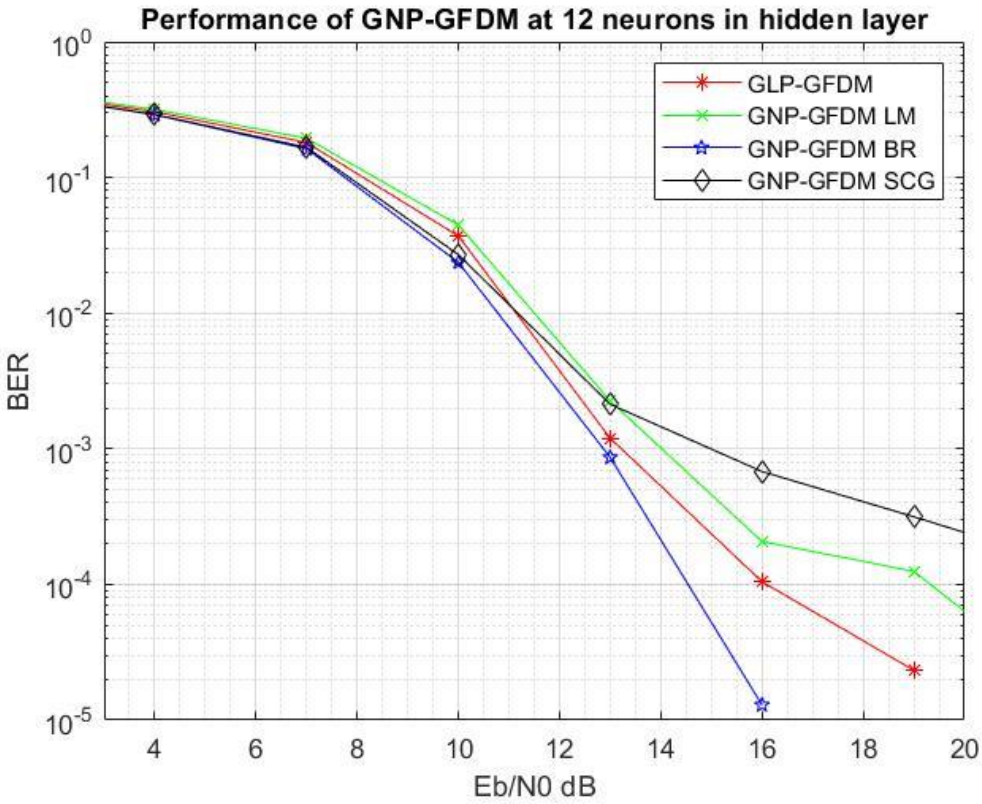

Figure (4.22) GNP-GFDM performance at 12 neurons.

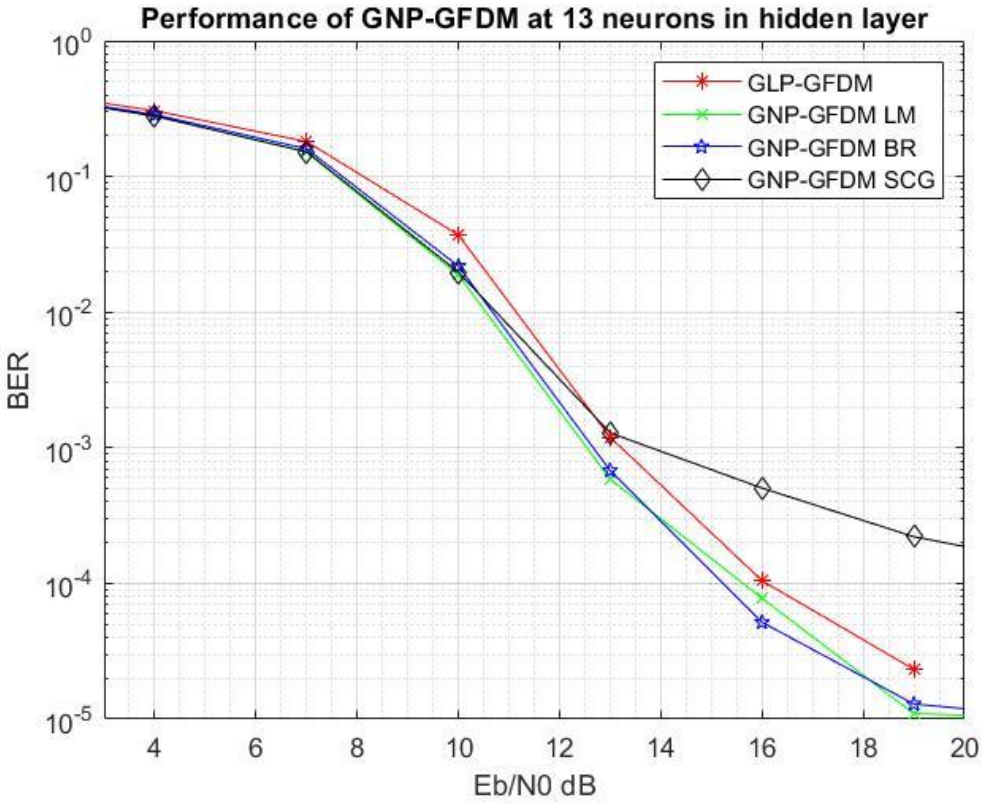

Figure (4.23) GNP-GFDM performance at 13 neurons

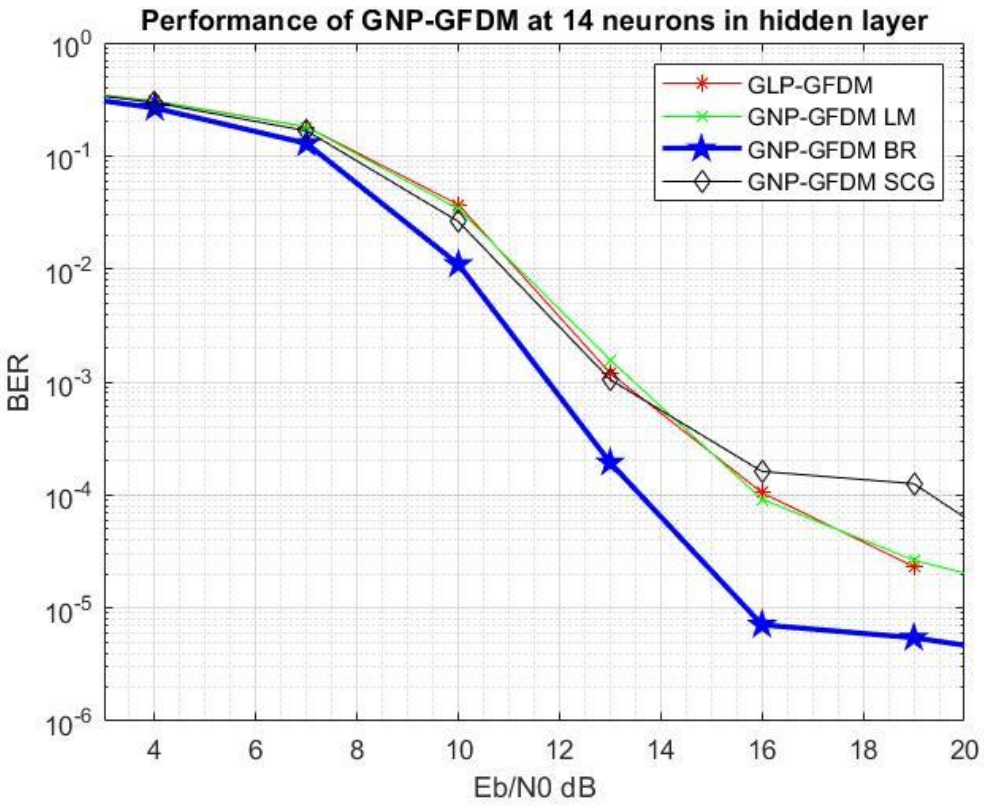

Figure (4.24) GNP-GFDM performance at 14 neurons

In Figure (4.22), the enhancement of BR 0.25dB at BER = 10^{-3}, while the LM and SCG don't present any enhancement. In Figure (4.23), the enhancement of LM and BR are 0.5dB at BER= 10^{-3}, while the SCG don't present any enhancement. In Figure (4.24), the enhancement of BR is 2.5 and 3.5 at BER 10^{-3} and 10^{-4}, while the SCG and LM don't present any enhancement. Hence the BR with 14 neurons present the best performance in GNP-GFDM scenario.

4.11 GNPI-GFDM Scenario Results

This scenario added interleaver to the GNP-GFDM system to get the Genetic Algorithm Artificial Neural Network Polar Code interleaver -GFDM (GNPI-GFDM) and compare it with the Genetic Algorithm Least Square Polar Code interleaver -GFDM (GLPI-GFDM), which presented its enhancement in BER with Eb/No. Random, matrix, and helical interleaves convert burst error to random error. Figure (4.25) presents the performance

of GFDM under LS channel estimation with stG-PSF, opG-GFDM, GLP, GNP and GNPI. Each case presents its own improvement.

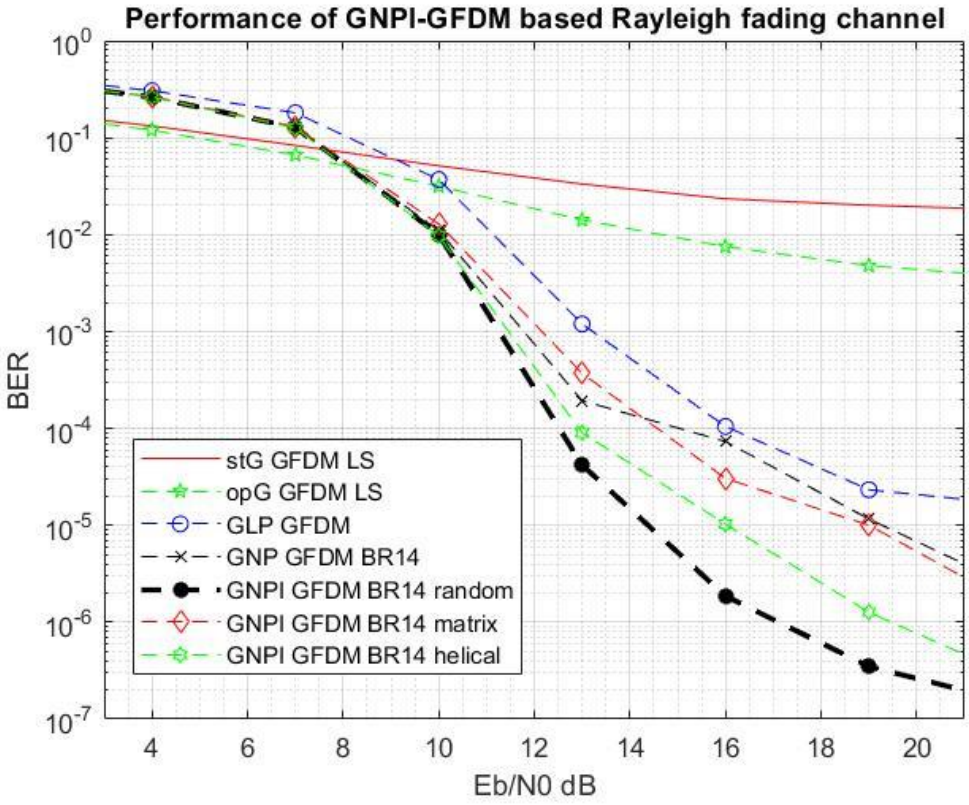

Figure (4.25): GNPI-GFDM performance.

The GNPI based random interleaver present enhancement by 2 dB and 3.5dB in BER equal 10^{-3} and 10^{-4}. While the helical present lower performance approach to 0.5dB.

4.12 Enhancement Comparison

This section presents the comparison between the enhancement scenarios, as well as a comparison with other researchers. The scenarios present cumulative improvement for the proposed scenarios. The enhancement presented is based on two structures (K20, M16, and K16 M15); the first one, tested at AWGN, is considered the best environment than the other structure, presents a PI-GFDM scenario, and is compared

with traditional GFDM. Figure (4.26) present this enhancement-based PI-GFDM scenario with K16 M15. The are 2 dB, 3.5 dB and 5dB at BER equal to 10^{-3}, 10^{-4}, 10^{-5}.

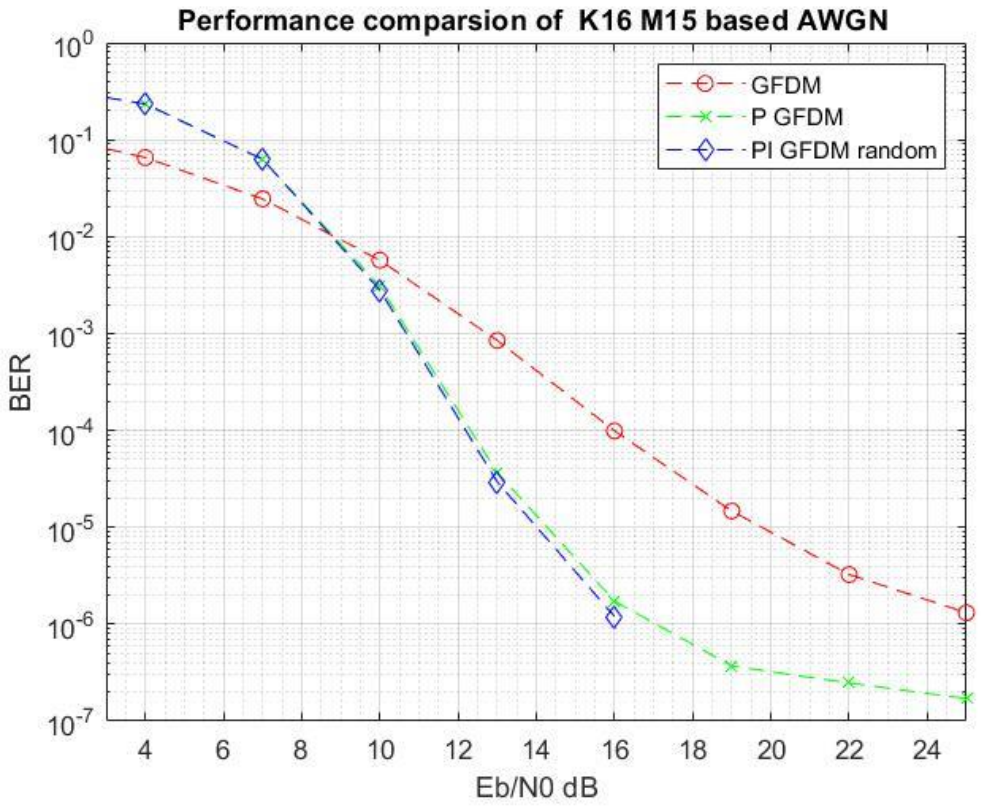

Figure (4.26): Proposed scenario enhancement based on K16 M15.

The second structure (K20, M16) is in an environment-based Rayleigh fading channel. Its environment is worse than the first structure due to PSF behavior. Figure (4.27) present the scenarios enhancement as comparisons with traditional GFDM. This enhancement compares with standard GFDM with LS estimation based on one path of Rayleigh fading channel. The enhancement scenario of G-GFDM, GN-GFDM, GNP-GFDM, and GNPI-GFDM to standard GFDM in Figure (4.27) and Table (4.1) present the numerical comparison.

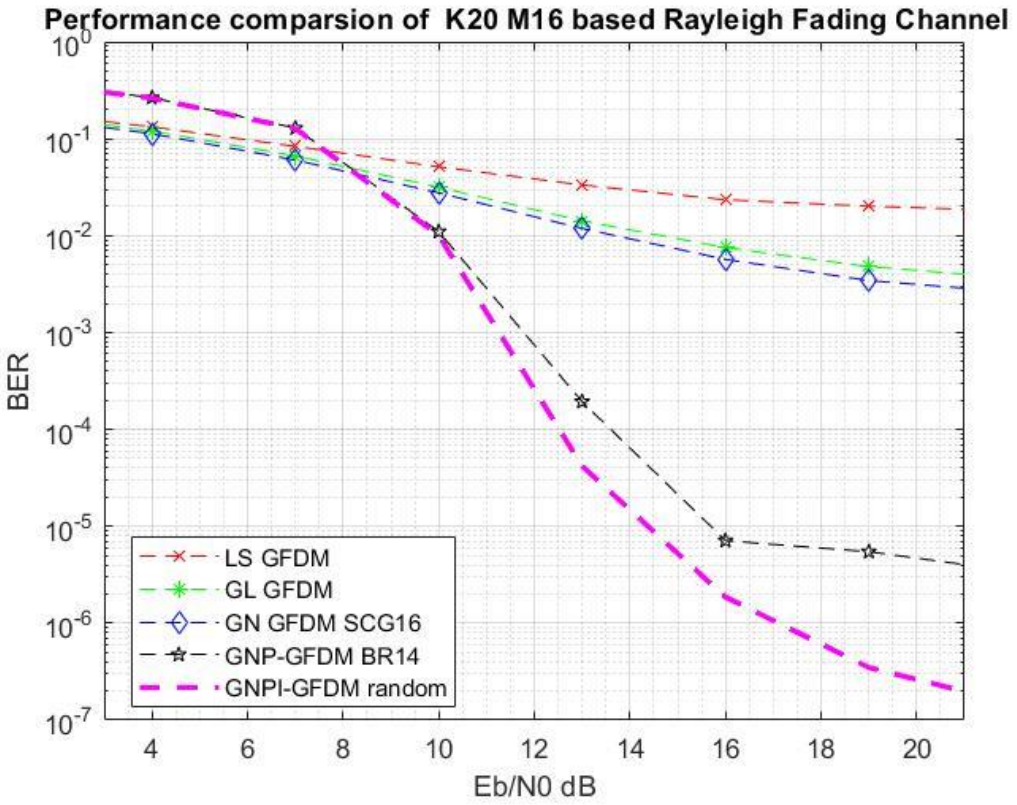

Figure (4.27) Proposed scenarios enhancement based on K20 M16.

Table (4.1): proposes a scenario comparison with standard GFDM-LS (K20, M16).

Scenario	BER Enhancement comparison with GFDM-LS at 13 dB	BER Enhancement comparison with GFDM-LS at 19 dB
G-GFDM	0.0191	0.0153
GN-GFDM	0.0214	0.0167
GNP-GFDM	0.0331	0.0201
GNPI-GFDM	**0.0332**	**0.0201**

The comparison between the proposed scenario and other related work is presented in Table (4.2). It presents the comparison with PI-GFDM under the AWGN channel. The comparison is based on the BER. The structure of PI-GFDM is built with different values of K and M based on the related work. In comparison, similar points were adopted structure (value of K and M), channel and SNR. The comparison is based on the BER value of traditional GFDM with the proposed GFDM of the scenario or related work based on the same SNR or Eb/No.

The related work in [18] and [19] presents its work based on the Rayleigh Fading Channel hence the proposed scenario in the same environment. The Ref [18] applied his enhancement-based Kalman filter under Rayleigh Fading Channel, which the BER of traditional and his proposed are 2×10^{-1} and 2×10^{-2} at 30 dB. At the same time, traditional GFDM and GNPI-GFDM in this dissertation are 0.0160 and 6.459×10^{-6}. Also, Ref [19] presents enhancement-based BIC-PC, which traditional and his proposed are 10^{-1} and 10^{-3} at 19 dB, while in traditional GFDM and GNPI-GFDM scenario in this dissertation are 0.02 and 1.395×10^{-5}.

Structure	K	64	64	256	128	128
	M	48	64	5	24	5
	(dB)	Eb/No=20	Eb/No=13	SNR=12	SNR=21	SNR =15
Proposed system	BER	Traditional GFDM	1.68×10^{-4}	0.0023	0.0037	0.0014	2.4×10^{-4}
		PI GFDM	**1.5×10^{-7}**	**6.3×10^{-7}**	**2.8×10^{-5}**	**2×10^{-7}**	**1×10^{-7}**
literature survey	Ref.		[14]	[15]	[21]	[22]	[23]
	Type		SIC	2-Sided SIC	SIM- CP	CBBO-SLM	JAYA-SLM
	BER	Traditional GFDM	6.5×10^{-4}	3.5×10^{-3}	10^{-4}	10^{-2}	9×10^{-5}
		literature GFDM	1.5×10^{-5}	10^{-5}	0.5×10^{-6}	10^{-5}	10^{-6}

Table (4.2) Performance comparison based on BER enhancement with a literature survey

CHAPTER Five

Conclusion and Suggestion for Future Work

Chapter Five

Conclusion and Suggestion for Future Work

5.1Conclusion

The GFDM is considered a new communication system and has yet to be officially adopted in the generations of wireless communications. Thus, it is within the stage of development and improvement. Traditional GFDM is studied with AWGN and Rayleigh fading channels. This dissertation presents scenarios for developing the BER of the GFDM system. These scenarios present in two structures: the first one presents good performance while the second presents bad performance used to make room for artificial intelligence to do the improvement process. The difference in performance belongs to the PSF behavior. These scenarios give results, as shown in Chapter Four. Based on these results, we conclude the following:

1- The PI-GFDM scenario presents the performance by adding PC to the traditional GFDM over AWGN channel. It's shown that the interleaver does not affect the performance since the errors have random nature over this channel.

2- LP-GFDM scenario presents the enhancement of PC depending on the PR, the performance enhanced when decreased the PR.

3- LPI-GFDM scenario presents the effect of interleaver to convert the burst error to a random error. The interleaver effect appears with the coding system, which its work helps the PC detect and correct the error effectively.

4- G-GFDM scenario presents a method of enhancement of the PSF of GFDM by assigning its parameters-based GA. This method presents high performance with the AWGN channel, but at Rayleigh fading

channels, the enhancement is relatively less due to the randomness values of the tapes in the channel.

5- GN-GFDM scenario combines the enhancement of G-GFDM with using the ANN as channel estimation instead of LS. At the same time, the addition of ANN gives more complexity and thus presents a tradeoff between performance and complexity.

6- GNP-GFDM scenario combines the PC as coding system with the GN-GFDM, increasing the enhancement despite the PR value. However, the amount of improvement remains interesting in the case of higher values of SNR.

7- GNPI-GFDM scenario added the interleaver to the GNP-GFDM to increase the enhancement. This scenario presents the last step in the enhancement of the GFDM system. Hence the GFDM-based PC with random interleaver and the ANN gives low BER to Eb/No.

5.2 Suggestion for Future Work

The following points can be considered general titles in the path of developing the proposed system:

1. Software-Defined Radio (SDR) hardware implementation to the developed GFDM transceiver.
2. Apply the proposed scenarios for Orthogonal-GFDM.
3. Investigate another estimation algorithm, such as (MMSE).

References

References

[1] Ameen, M. J. M., & Hreshee, S. S. (2022). Securing Physical Layer of 5G Wireless Network System over GFDM Using Linear Precoding Algorithm for Massive MIMO and Hyperchaotic QR-Decomposition. International Journal of Intelligent Engineering and Systems, 15(5), 579–591.

[2] Antapurkar, S. K., Pandey, A., & Gupta, K. K. (2016). GFDM performance in terms of BER, PAPR and OOB and comparison to OFDM system. AIP Conference Proceedings, 1715.

[3] Marques da Silva, M., Dinis, R., & Guerreiro, J. (2020). A Low Complexity Channel Estimation and Detection for Massive MIMO Using SC-FDE. Telecom, 1(1), 3–17.

[4] Cheng, H., Xia, Y., Huang, Y., Yang, L., & Mandic, D. P. (2019). Joint Channel Estimation and Tx/Rx I/Q Imbalance Compensation for GFDM Systems. IEEE Transactions on Wireless Communications, 18(2), 1304–1317.

[5] Akai Y., Enjoji Y., Sanada Y., Kimura R., Matsuda H., Kusashima N., Sawai R.(2017).Channel estimation with scattered pilots in GFDM with multiple subcarrier bandwidths. IEEE 28th Annual International Symposium on Personal, Indoor, and Mobile Radio Communications (PIMRC), Montreal, QC, Canada, 1-5,

[6] Ali A. H., Al-Ja’, M. A. M., & Abdulwahed, S. H. (2018). Rheumatoid Arthritis Diagnosis Based on Intelligent System. In Journal of University of Babylon for Pure and Applied Sciences, 26(7),47-53.

[7] Ameer Hussein Mohammed Supervised by Hanan R Akkar, (2015). Design and Implementation of Artificial Neural Network for Mobile Robot based on FPGA in a Partial Fulfillment of the Requirements for the Degree of Master of Science in Electronic Engineering.

[8] Elkelesh, A., Ebada, M., Cammerer, S., & ten Brink, S. (2019). Decoder-Tailored Polar Code Design Using the Genetic Algorithm. IEEE Transactions on Communications, 67(7), 4521–4534.

[9] Ramabadran, S., Madhukumar, A. S., Wee Teck, N., & See, C. M. S. (2017). Parameter Estimation of Convolutional and Helical Interleavers in a Noisy Environment. IEEE Access, 5, 6151–6167.

[10] Wei Xiang, Kan Zheng, Xuemin (Sherman) Shen. (2017). 5G Mobile Communications. Springer.

[11] Erdal Arıkan (2009). Channel polarization: A method for constructing capacity-achieving codes for symmetric binary-input memoryless channels. IEEE Access,5.

[12] Chiu M. (2020). Interleaved Polar (I-Polar) Codes. IEEE TRANSACTIONS ON INFORMATION THEORY, 66(4), 2430-2442.

[13] G. Fettweis, M. Krondorf and S. Bittner. (2009). GFDM - Generalized Frequency Division Multiplexing," VTC Spring - IEEE 69th Vehicular Technology Conference, Barcelona, Spain, 2009, 1-4.

[14] Datta, R., Fettweis, G., Kollár, Z., & Horváth, P. (2011). FBMC and GFDM interference cancellation schemes for flexible digital radio PHY design. Proceedings - 14th Euromicro Conference on Digital System Design: Architectures, Methods and Tools, 335–339.

[15] Datta, R., Michailow, N., Lentmaier, M., & Fettweis, G. (2012). GFDM interference cancellation for flexible cognitive radio phy design. IEEE Vehicular Technology Conference.

[16] F. Li, L. Zhao, K. Zheng and J. Wang. (2016). A Interference-Free Transmission Scheme for GFDM System. IEEE Globecom Workshops (GC Wkshps), Washington, DC, USA. 1-6.

[17] S. P. Valluri and V. V. Mani. (2018). Receiver design for UW-GFDM systems. 21st International Symposium on Wireless Personal Multimedia Communications (WPMC), Chiang Rai, Thailand, 2018, pp. 588-593.

[18] P. Agrawal and K. Appaiah.(2019).Kalman Filter Based Channel Tracking for Precoded GFDM Systems. TENCON - IEEE Region 10 Conference (TENCON), Kochi, India, 817-822.

[19] Li, Y., Niu, K., & Dong, C. (2019). Polar-Coded GFDM Systems. IEEE Access, 7, 149299–149307.

[20] Valluri, S. P., Vejandla, K., & Mani, V. V. (2020). Low complex implementation of GFDM system using USRP. IET Communications, 14(13), 2060–2067.

[21] Kumar, R. A., Prasad, S., Vignan', K., & Satya Prasad, K. (2021). Enhanced Diversity Gain of Subcarrier Index Modulated MIMO-GFDM using Constellation Precoding Technique for 5G.

[22] Selvin Pradeep Kumar, S., Agees Kumar, C., & Jemila Rose, R. (2022). An efficient SLM technique based on chaotic biogeography-based optimization algorithm for PAPR reduction in GFDM waveform. Automatika, 64(1), 93–103.

[23] Bouslam, K. A., Amadid, Jamal, Fatim-Zehra Bennioui, Cherij, D., Iqdour, Radouane, & Zeroual, A. (2023). JAYA algorithm based selective mapping for PAPR reduction in GFDM systems.

[24] da Costa, D. B., & Yang, H.-C. (2020). Grand Challenges in Wireless Communications. Frontiers in Communications and Networks, 1.

[25] Taha, H. J., & Salleh, M. F. M. (2009). Multi-carrier Transmission Techniques for Wireless Communication Systems: A Survey.8(5),

[26] Oustry A., Xu L., Vanier S. H., Cordero J. A., Clausen T. (2022). Optimization in Wireless Networks. Encyclopedia of Optimization, 3nd Edition, Springer, In press, ISBN: 978-0 387-74759-0

[27] Gupta M., Gamad R.S. (2022). 5th Generation of GFDM and Analysis of Ser Using Filter. Mathematical Statistician and Engineering Applications. 71(4). 3534-3552.

[28] Michailow, N., Matthé, M., Simões Gaspar, I., Navarro Caldevilla, A., Mendes, L. L., Festag, A., & Fettweis, G. (n.d.). Generalized Frequency Division Multiplexing for 5th Generation Cellular Networks. In IEEE TRANSACTIONS ON COMMUNICATIONS.62(9), 3045-3061,

[29] AL Hasaani N. A. and Algamluoli A. (2018). Performance of GFDM and OFDM over Fading Channels. International Journal of Multidisciplinary Research and Publications (IJMRAP), 1(7),10-12.

[30] Linsalata, F., & Magarini, M. (2020). On the Performance of Soft LLR-based Decoding in Time-Frequency Interleaved Coded GFDM Systems. IEEE 31st Annual International Symposium on Personal, Indoor and Mobile Radio Communications, London, UK, 1-6,

[31] M. J. M. Ameen and S. S. Hreshee.(2022).Hyperchaotic Based Encrypted Audio Transmission via Massive MIMO - GFDM System using DNA Coding in the Antenna Index of PSM. 5th International

Conference on Engineering Technology and its Applications (IICETA), Al-Najaf, Iraq,19-24.

[32] Ali, A. H., & Saffah Hreshee, S. (2023). GFDM Pulse Shaping Optimization Based Genetic Algorithm,31 (2).

[33] Thirunavukkarasu, G., & Murugesan, G. (2019). A Comprehensive Survey on Air-Interfaces for 5G and beyond. 2019 10th International Conference on Computing, Communication and Networking Technologies, ICCCNT 2019.

[34] Michailow, N., Matthe, M., Gaspar, I. S., Caldevilla, A. N., Mendes, L. L., Festag, A., & Fettweis, G. (2014). Generalized frequency division multiplexing for 5th generation cellular networks. IEEE Transactions on Communications, 62(9), 3045–3061.

[35] Lizeaga, A., Rodríguez, P. M., Val, I., & Mendicute, M. (2017). Evaluation of 5G Modulation Candidates WCP-COQAM, GFDM-OQAM, and FBMC-OQAM in Low-Band Highly Dispersive Wireless Channels. Journal of Computer Networks and Communications, 2017.

[36] Haneesha P., Meerja K. A. (2020). An Optimal Bit Error Rate Improvement Using Generalized Pattern Division Multiple Accesses in Wireless 5G.7(15). Journal Of Critical Reviews.

[37] Shimodaira, H., Kim, J., & Sadri, A. S. (2016). Enhanced next generation millimeter-wave multicarrier system with generalized frequency division multiplexing. International Journal of Antennas and Propagation.

[38] Zhang, D., Festag, A., & Fettweis, G. P. (2017). Performance of Generalized Frequency Division Multiplexing Based Physical Layer in Vehicular Communications. IEEE Transactions on Vehicular Technology, 66(11), 9809–9824.

[39] Datta, R., Michailow, N., Lentmaier, M., & Fettweis, G. (2012). GFDM interference cancellation for flexible cognitive radio phy design. IEEE Vehicular Technology Conference.

[40] Uwaechia, A. N., & Mahyuddin, N. M. (2020). A comprehensive survey on millimeter wave communications for fifth-generation wireless networks: Feasibility and challenges. IEEE Access, 8, 62367–62414.

[41] Habib, A., & Moh, S. (2019). Wireless channel models for over-the-sea communication: A comparative study. In Applied Sciences (Switzerland),9 (3). MDPI AG.

[42] Yong Soo Cho Y. S., Kim Y., Yang W. Y. (2010). MIMO-OFDM WIRELESS COMMUNICATIONS WITH MATLAB. John Wiley & Sons.

[43] Ijiga, O. E., Ogundile, O. O., Familua, A. D., & Versfeld, D. J. J. (2019). Review of channel estimation for candidate waveforms of next generation networks. In Electronics (Switzerland), MDPI AG. 8 (9).

[44] Kumar, S., Gupta, P. K., Singh, G., & Chauhan, D. S. (2013). Performance Analysis of Rayleigh and Rician Fading Channel Models using Matlab Simulation. International Journal of Intelligent Systems and Applications, 5(9), 94–102.

[45] Boas E.C. V., Silva J. D. S., Figueiredo F. A. P. , Luciano L. Mendes L. L. and Souza R. A. A. (2022). Artifcial Intelligence for Channel Estimation in Multicarrier Systems for B5G/6G Communications: A Survey. EURASIP Journal on Wireless Communications and Networking. 2022. 01-63.

[46] Tai C. L., Su B., Jia C.(2020). Interference-Precancelled Pilot Design for LMMSE Channel Estimation of GFDM. IEEE 21st International Workshop on Signal Processing Advances in Wireless Communications (SPAWC), 1-5,

[47] Hu C. , Dai L., Han S. and Wang X.(2021).Two-Timescale Channel Estimation for Reconfigurable Intelligent Surface Aided Wireless Communications. in IEEE Transactions on Communications, 69(11), 7736-7747, Nov.,

[48] Cheng, H., Xia, Y., Huang, Y., Yang, L., & Mandic, D. P. (2019). Joint Channel Estimation and Tx/Rx I/Q Imbalance Compensation for GFDM Systems. IEEE Transactions on Wireless Communications, 18(2), 1304–1317.

[49] Permana A., Hamid E. Y.(2018).DFT-Based Channel Estimation for GFDM on Multipath Channels. 10th International Conference on Information Technology and Electrical Engineering (ICITEE), 31-35,

[50] Prasad, S. R., & Joshi, Y. v. (2016). Unknown System Identification using LMS Algorithm. Journal of Signal Processing. 2(1).

[51] Ghauri S. A., Sohail M. F.(2013). System Identification using LMS, NLMS and RLS. IEEE Student Conference on Research and Development (SCOReD). 65-69.

[52] Rana, M. M., Korea, S., & Kamal Hosain, M. (2010). Adaptive Channel Estimation Techniques for MIMO OFDM Systems. In *IJACSA) International Journal of Advanced Computer Science and Applications. 1* (6).

[53] Migabo E, Djouani K, Kurien A. (2020). An Energy-Efficient and Adaptive Channel Coding Approach for Narrowband Internet of Things (NB-IoT) Systems. Sensors. 20(12).

[54] Bioglio, V., Condo, C., & Land, I. (2021). Design of Polar Codes in 5G New Radio. IEEE Communications Surveys and Tutorials, 23(1), 29–40.

[55] DHUHEIR M. and ÖZTÜRK S. (2018). Polar Codes Analysis of 5G Systems. 6th International Conference on Control Engineering & Information Technology (CEIT), Istanbul, Turkey. 1-6.

[56] Chiu, M.-C., Chen C. -Y. (2020). Interleaved Polar (I-Polar) Codes. IEEE Communications Letters, 24(9).1865-1869.

[57] Mohammed Ameen, M. J., & Hreshee, S. S. (2022). Hyperchaotic Modulo Operator Encryption Technique for Massive Multiple Input Multiple Output Generalized Frequency Division Multiplexing system.

International Journal on Electrical Engineering and Informatics, 14(2), 311–329.

[58] Qammar, N., & Singh, M. (2020). Analysis of Interleaving Schemes in CDMA System Using Simulink. International Journal of Innovative Research in Electrical, Electronics, Instrumentation and Control Engineering, 8(2), 2321–5526.

[59] Vasyl S. & Oleksandr V. (2021). The simplification of computational in error correction coding. Technology audit and production reserves. 3. 24-28.

[60] Chavan, P. N., & Jadhav, H. M. (2014). Survey on Interleavers in IDMA System. In International Journal of Science and Research.3(12).

[61] Raje, B., & Markam, K. (2018). Review paper on study of various Interleavers and their significance. International Research Journal of Engineering and Technology, 5(10).430-434.

[62] Kaur M., and Kaur H. (2016). Evaluation of Turbo Codes Varying Various Parameters Using BCJR Algorithm. International Journal of Advanced Research in Electrical, Electronics and Instrumentation Engineering,5(6).

[63] Ameen M. J. M., Kadhim H. J. (2020). The efficient interleaving of DVB-S2 system. TELKOMNIKA Telecommunication, Computing, Electronics and Control.18(5). 2362-2370.

[64] Ameen, M. J. M., & Kadhim, H. J. (2020). The efficient interleaving of digital-video-broadcasting-satellite 2nd generations system. Telkomnika (Telecommunication Computing Electronics and Control), 18(5), 2362–2370.

[65] Alrubei M. A., Ali A. H., Nukhailawi Y. J. K., Al-Ja'afari M. A. M. , Abdulwahed S. H.(2020).Ulcerative Colitis Diagnosis Based on Artificial Intelligence System. Journal of University of Babylon,28(2).

[66] A Oliveira, E. C., Castro, V. F., L Reis, P. A., Pereira, C., (2019). Artificial neural networks for spatial distribution of fuel assemblies in reload of PWR reactors. BRAZILIAN JOURNAL OF RADIATION SCIENCES.

[67] Sufian, M. D. I. M., Salim, N. A., Mohamad, H., & Yasin, Z. M. (2022). Implementation of artificial intelligence for prediction performance of solar thermal system. International Journal of Power Electronics and Drive Systems, 13(3), 1751–1760.

[68] Bakhshaei, M., Ahmadi, H., Motamedvaziri, B., & Najafi, P. (2020). RUNOFF ESTIMATION IN URBAN CATCHMENT USING ARTIFICIAL NEURAL NETWORK MODELS. S&G JOURNAL, 15(2), 170–180.

[69] Zurada, J. M., & Paul New York Los Angeles San Francisco, S. (1992). Introduction to Artificial Neural Systems.

[70] Singh J. and Banerjee R.(2019).A Study on Single and Multi-layer Perceptron Neural Network. 3rd International Conference on Computing

Methodologies and Communication (ICCMC), Erode, India, 35-40,

[71] Chen, L.-S., Chung, W.-H., Chen, I.-Y., & Kuo, S.-Y. (2020). AMC With a BP-ANN Scheme for 5G Enhanced Mobile Broadband. IEEE Access, 1–1.

[72] Priddy K. L. and Keller. P. E. (2005). Artificial Neural Networks. SPIE.

[73] Guillod, T., Papamanolis, P., & Kolar, J. W. (2020). Artificial neural network (ann) based fast and accurate inductor modeling and design. IEEE Open Journal of Power Electronics, 1, 284–299.

[74] Shukla, R. G., Kumar, P. G., Kumar Vishwakarma, D. G., Ali, R., Kumar, R., & Kuriqi, A. (2021). Modeling of Stage-Discharge Using Back Propagation ANN, ANFIS, and WANN-based Computing Technique.

[75] Iftikhar, A., Alam, M., Ahmed, R., Musa, S., & Su'Ud, M. M. (2021). Risk Prediction by Using Artificial Neural Network in Global Software Development. Computational Intelligence and Neuroscience.

[76] Rautela, K. S., Kumar, D., Gandhi, B. G. R., Kumar, A., & Dubey, A. K. (2022). Application of ANNs for the modeling of streamflow, sediment transport, and erosion rate of a high-altitude river system in Western Himalaya, Uttarakhand. Revista Brasileira de Recursos Hidricos, 27.

[77] Parmar, R., Shah, M., & Shah, M. G. (2017). A Comparative study on Different ANN Techniques in Wind Speed Forecasting for Generation of Electricity. IOSR Journal of Electrical and Electronics Engineering, 12(01), 19–26.

[78] Gouravaraju, S., Narayan, J., Sauer, R. A., & Gautam, S. S. (2020). A Bayesian regularization-backpropagation neural network model for peeling computations.

[79] Agnihotri A. and Gupta I. K. (2018). A hybrid PSO-GA algorithm for routing in wireless sensor network, 4th International Conference on Recent Advances in Information Technology (RAIT), Dhanbad, India, 2018, 1-6,

[80] Khoumbati K. u. R., Solangi S. A., Bhatti Z. and Hakro D. N.(2020). Optimal Route Planning by Genetic Algorithm for Wireless Sensor Networks. International Conference on Information Science and Communication Technology (ICISCT), Karachi, Pakistan, 1-4,

[81] Xu C., Wu T. K., Cheng R. -H. and Yu C. W. (2018). A Genetic Algorithm for Multiple Charging Car Scheduling Problem in Wireless Rechargeable Sensor Networks. IEEE Asia-Pacific Conference on Antennas and Propagation (APCAP), Auckland, New Zealand, 136-138,

[82] Ba M., Hu Y., Xu C. and Zhong Y. (2019). A Course Scheduling Algorithm in Secondary Vocational School Based on Genetic Algorithm. 6th International Conference on Systems and Informatics (ICSAI), Shanghai, China, 1543-1547,

[83] Elkelesh, A., Ebada, M., Cammerer, S., & ten Brink, S. (2019). Decoder-Tailored Polar Code Design Using the Genetic Algorithm. IEEE Transactions on Communications, 67(7), 4521–4534.

[84] Pal, V., Yogita, Singh, G., & Yadav, R. P. (2015). Cluster Head Selection Optimization Based on Genetic Algorithm to Prolong Lifetime of Wireless Sensor Networks. Procedia Computer Science, 57, 1417–1423.

[85] Abo-Zahhad, M., Ahmed, S. M., Sabor, N., & Sasaki, S. (2014). A New Energy-Efficient Adaptive Clustering Protocol Based on Genetic Algorithm for Improving the Lifetime and the Stable Period of Wireless Sensor Networks. International Journal of Energy, Information and Communications, 5(3), 47–72.

الخلاصة

نظرًا للتطور الهائل في مجال الاتصالات اللاسلكية والمتطلبات الواسعة للأجيال الحالية، مثل معدلات البيانات العالية، واستهلاك الطاقة المنخفض للغاية، والأداء العالي، ونظرا للقيود التي فرضتها الأنظمة السابقة، كان من الضروري المضي قدما في عمليات التحسين. كان إدخال تقنية تعدد الإرسال بتقسيم التردد العمومي (GFDM) إحدى الطرق المقترحة؛ إنه أحد المخططات المرشحة للأجيال الحالية وما بعدها. مخطط تشكيلها متعدد الموجات وهيكلها عبارة عن مجموعات مستقلة، وتحتوي كل مجموعه على موجات حاملة فرعية (K) ورموز فرعية (M)؛ يتم ترشيح K بنموذج أولي لمرشح تشكيل النبض (PSF) يتحول حسب الوقت ومجال التردد تم تقديم GFDM كطريقة محسنة مقارنة بتقنية تعدد الإرسال الأخرى، حيث قدمت تحسينًا في مجال خارج النطاق (OOB) ونسبة القدرة القصوى (PAPR). ومع ذلك، فقد قدم في نفس الوقت أداءً أقل في BER بنسبة SNR. في هذه الاطروحة تم تقديم عدة سيناريوهات لتحسين أداء نظام GFDM حيث تم تقديم هيكلين K16 M15 و K20 M16 حيث كان الهيكل الأول يتمتع بأداء أفضل حيث تم تحسينه بإضافة نظام تشفير يعتمد على الترميز القطبي (PC) والتشذير باستخدام ثلاثة أنواع، عشوائية، مصفوفة وحلزونية. في المقابل، أعطت البنية الثانية أداءً اسوء لإفساح المجال لطرق التحسين القائمة على الذكاء الاصطناعي.

تم تقديم طريقة جديدة لتحسين أداء GFDM باستخدام الخوارزمية الجينية (GA) لتحسين أداء PSF في GFDM. تم إجراء تقدير القناة بناءً على طريقة LS، ومن ثم تم استخدام الشبكة العصبية للانتشار العكسي المستندة إلى الشبكة العصبية الاصطناعية (ANN) لتعزيز عملية التقدير. تم تقديم السيناريوهات PC Interleaver GFDM (PI-GFDM) و Least Square PC GFDM (LP-GFDM) و(Least Square PC Interleaver GFDM (LPI-GFDM و GA-GFDM (G-GFDM) و GA ANN GFDM (GN-GFDM) و ANN PC GFDM (GNP-GFDM) و GA ANN PC Interleaver GFDM (GNPI-GFDM). تم إجراء مقارنة بين أنواع السيناريوهات المقترحة من حيث مقدار التحسين. يقدم GNPI-GFDM المقترح تحسينًا مع الGFDM التقليدي حوالي 3.5 ديسيبل عند $BER = 10^{-4}$ في قناة ريلي المتلاشية ويقدم PI-GFDM تحسينًا مع الGFDM التقليدي يبلغ حوالي 5 ديسيبل عند $BER = 10^{-5}$ في قناة AWGN.

جمهورية العراق
وزارة التعليم العالي والبحث العلمي
جامعة بابل
كلية الهندسة
قسم الهندسة الكهربائية

تقييم أداء تعدد الإرسال بتقسيم التردد العمومي القطبي المرمز باستخدام تقنيات الذكاء الاصطناعي

اطروحة
مقدمة إلى كلية الهندسة في جامعة بابل
وهي جزء من متطلبات الحصول على درجة الدكتوراة
فلسفة في هندسة الالكترونيك والاتصالات

من قبل

امير حسين محمد علي

بإشراف
الاستاذ الدكتور

سعد سفاح حسون حريشي

٢٠٢٣م ١٤٤٥ هـ